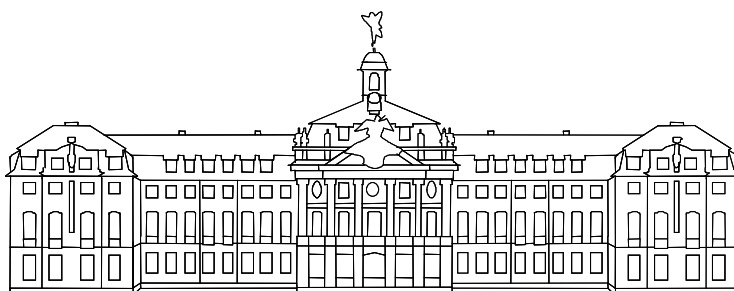


Saroj Kumar Panda

**Liquid Chromatography and High Resolution Mass
Spectrometry for the Speciation of High Molecular
Weight Sulfur Aromatics in Fossil Fuels**



**NRW Graduate School of Chemistry
University of Münster
Germany**

-2006-

Analytische Chemie

**Liquid Chromatography and High Resolution Mass
Spectrometry for the Speciation of High Molecular Weight
Sulfur Aromatics in Fossil Fuels**

Inaugural-Dissertation
zur Erlangung des Doktorgrades
der Naturwissenschaften in der NRW Graduate School of Chemistry
im Fachbereich Chemie und Pharmazie
der Mathematisch-Naturwissenschaftlichen Fakultät
der Westfälischen Wilhelms-Universität Münster

vorgelegt von
Saroj Kumar Panda
aus Orissa, Indien

-2006-

Dekan	:	Prof. Dr. F. E. Hahn
Erster Gutachter	:	Prof. Dr. Jan T. Andersson
Zweiter Gutachter	:	Prof. Dr. Uwe Karst
Tag der mündlichen Prüfungen	:
Tag der Promotion	:

To my family

Table of Contents

1. Introduction.....	1
1.1 Energy Sources.....	1
1.2 Crude Oil and Sulfur	2
1.3 Sulfur Limits in Transportation Fuels	3
1.4 Introduction of Sulfur in Crude Oil	4
1.5 The Refining Process.....	7
1.6 Desulfurization	10
1.6.1 Hydrodesulfurization.....	10
1.6.2 Other Methods of Desulfurization.....	13
1.7 Summary	14
2. Analytical Techniques for Heavy Petroleum Fractions	15
2.1 Liquid Chromatography	15
2.1.1 Group Separation into Saturates, Aromatics, Resins and Asphaltenes	15
2.1.2 High Performance Liquid Chromatography	16
2.1.3 Thin-Layer Chromatography.....	17
2.1.4 Size Exclusion Chromatography	17
2.2 Spectroscopic Techniques	17
2.2.1 Ultraviolet/Visible and Fluorescence Spectroscopy.....	17
2.2.2 Infrared Spectroscopy.....	17
2.2.3 Nuclear Magnetic Resonance Spectroscopy	18
2.2.4 X-ray Scattering	18
2.3 Mass Spectrometry	18
2.3.1 FT-ICR MS of High-Boiling Petroleum Fractions.....	19
2.4 Chemical Methods.....	20
3. Objectives.....	21
4. Ultra-High Resolution Mass Spectrometry	22
4.1 Ionization Techniques	22
4.1.1 Electrospray Ionization.....	22
4.1.2 Matrix Assisted Laser Desorption Ionization.....	23
4.1.3 Field Ionization/Field Desorption	23
4.1.4 Atmospheric Pressure Chemical Ionization	24
4.1.5 Atmospheric Pressure Photo Ionization	24
4.2 Mass Analyzers	25
4.2.1 Definitions	25
4.2.1.1 Mass Resolution	25
4.2.1.2 Mass Resolving Power	25
4.2.1.3 Mass Accuracy	26
4.2.2 Types of Mass Spectrometers.....	26
4.2.2.1 Sector Field.....	26
4.2.2.2 Quadrupoles.....	27
4.2.2.3 Ion Trap	28
4.2.2.4 Time of Flight.....	29
4.2.2.5 Fourier Transform Ion Cyclotron Resonance.....	30
4.3 ESI FT-ICR Mass Spectrometer	31
4.4 Data Interpretation.....	32
4.4.1 Nominal Mass Series.....	33

4.4.2 Kendrick Mass Defect	33
4.4.3 Multiple Sorting	35
4.5 Limitations of MALDI and ESI	37
4.6 Methylation of Sulfur Compounds.....	37
4.7 Phenylation of Sulfur Compounds	38
4.8 MALDI FT-ICR MS of Derivatized Sulfur Compounds	39
4.9 Generation of Pseudograms.....	40
4.10 ESI FT-ICR MS of Derivatized Sulfur Compounds	41
4.11 Summary	42
5. Pattern of Sulfur Heterocycles in Vacuum Gas Oils	43
5.1 Experimental Section	44
5.1.1 Sample	44
5.1.2 Ligand Exchange Chromatography	45
5.1.3 Sulfur Selective Methylation.....	46
5.1.4 High-Resolution Mass Spectrometry	46
5.1.5 Data Analysis	46
5.2 Results and Discussion.....	47
5.2.1 Low-Boiling Range VGO	49
5.2.2 Middle-Boiling Range VGO	51
5.2.3 High-Boiling Range VGO.....	53
5.3 Summary	56
6. Distribution of Sulfur Heterocycles in Crude Oils.....	57
6.1 Experimental Section	57
6.1.1 Sample	57
6.1.2 Ligand Exchange Chromatography	57
6.1.3 Sulfur Selective Methylation.....	58
6.1.4 High-Resolution Mass Spectrometry	58
6.1.5 Data Analysis	58
6.2 Results and Discussion.....	58
6.2.1 Identification of Sulfur Heterocycles with FT-ICR MS.....	59
6.2.2 Arabian Heavy.....	63
6.2.3 Arabian Medium.....	66
6.2.4 Arabian Light	67
6.2.5 Comparison with the GC Techniques	68
6.2.6 Limitations of FT-ICR MS.....	70
6.3 Summary	71
7. Recalcitrant Sulfur Aromatics in Desulfurized Vacuum Gas Oils.....	72
7.1 Experimental Section	72
7.1.1 Sample	72
7.1.2 Sulfur Mass Fraction in Vacuum Gas Oils.....	73
7.1.3 Ligand Exchange Chromatography	73
7.1.4 Sulfur Selective Methylation.....	73
7.1.5 High-Resolution Mass Spectrometry	73
7.1.6 Data Analysis	73
7.2 Results and Discussion.....	74
7.3 Summary	81

8. Liquid Chromatography of Sulfur Heterocycles	82
8.1. Experimental Section	83
8.1.1 Sample	83
8.1.2 Chemicals and Standard Compounds	83
8.1.3 Ligand Exchange Chromatography	84
8.1.4 Comparison of Three Stationary Phases	84
8.1.5 Sulfur Selective Methylation	85
8.1.6 High-Resolution Mass Spectrometry	85
8.1.7 Data Analysis	85
8.2 Results and Discussion	85
8.2.1 Selection of a Stationary Phase	86
8.2.2 Identification of PASHs with FT-ICR MS	92
8.2.3 Fraction 1	94
8.2.4 Fraction 2	96
8.2.5 Fraction 3	97
8.3 Summary	99
9. Summary	100
10. Zusammenfassung	104
11. Appendix	108
11.1 Synthesis of Pd(II)-ACDA Silica Gel	108
11.1.1 Synthesis of 2-Amino-1-cyclopentene-dithiocarboxylic Acid	108
11.1.2 Synthesis of Aminopropano Silica Gel	109
11.1.3 Synthesis of ACDA-functionalized Silica Gel	109
11.2 Synthesis of Pd(II)-Mercaptopropano Silica Gel	110
11.3 Synthesis of Tetrachlorophthalimide Silica Gel	110
11.3.1 Synthesis of Tetrachlorophthalicmonoallylamide-allylammonium Salt	110
11.3.2 Synthesis of Tetrachlorophthalicallylimide	110
11.3.3 Synthesis of Tetrachlorophthalimidopropanodimethylchlorosilane	111
11.3.4 Synthesis of Tetrachlorophthalimidopropanosilica	111
11.4 Synthesis of Model Thiophenic Compounds	112
11.4.1 Synthesis of 3-[(4-Butylphenyl)ethano]benzo[<i>b</i>]thiophene	112
11.4.2 Synthesis of 2-(1-Naphthylethano)thiophene	113
11.4.3 Synthesis of Dodecylbenzothiophene	114
11.4.4 Synthesis of 2-(3,7-Dimethyloctyl)benzothiophene	114
11.5 Instrumental Parameters	115
11.5.1 HPLC Instrumentation	115
11.5.2 Gas Chromatographs	116
11.5.3 FT-ICR MS	117
11.5.4 Elemental Analyses or CHNS Analyses	117
11.6 Materials	118
11.7 Abbreviations	120
12. References	122

1. Introduction

1.1 Energy Sources

Energy is one of the fundamental requirements in a civilized society to maintain the pace of modernization with respect to time. However, the sources of energy, essential for various processes in day-to-day life, have been continually changing in the last centuries (Figure 1.1). In the present scenario, fossil fuels (coal, oil and natural gas) provide about 60 % of total energy. Among them, oil is economically the most viable source. In the USA, 40 % of total energy and 99 % of transportation fuels are obtained from oil [1]. Although other alternatives like hydrogen- and nuclear-based energy sources are expected to fill the gap of energy formed due to diminishing supply of crude oils, the serious technical challenges associated with former sources cannot be ignored.

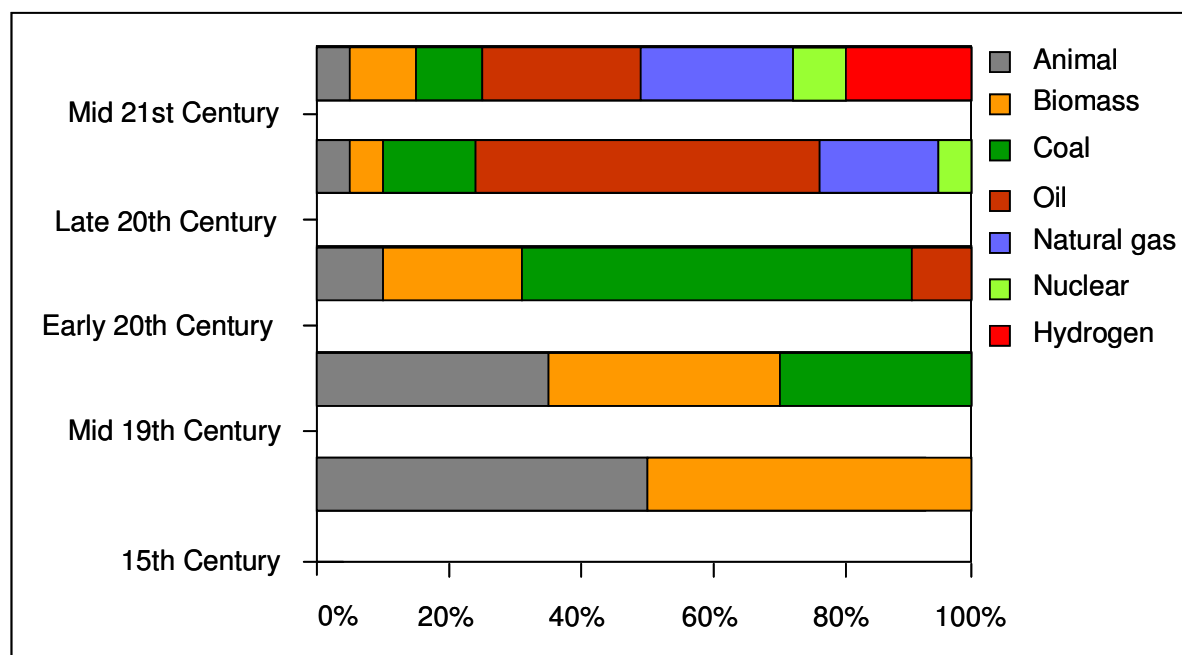


Figure 1.1. Evolution of energy sources.¹

There is therefore a strong demand in exhaustive use of petroleum as a source of energy. In order to sustain the supply of energy from petroleum sources, high-boiling petroleum fractions like vacuum gas oils and vacuum residues including heavy oils are

¹ <http://people.hofstra.edu/geotrans/eng/ch8en/conc8en/evolenergy.html>

increasingly used though these sources need multiple secondary refinery processes before being used as sources of energy.

1.2 Crude Oil and Sulfur

Petroleum is one of the most complex mixtures known with respect to the number of individual species, which probably ranges from 10,000 to 100,000 [2]. The composition of crude oil can vary greatly from source to source. However, all crude oils are mainly composed of carbon and hydrogen in the form of alkanes, naphthenes and aromatics, i.e. hydrocarbons. In addition, minor amount of sulfur-, oxygen- and nitrogen-containing heterocycles, and trace amount of metals like vanadium and nickel are also found. The abundance of heteroatoms rises with increase in average molecular weight of the sample, which in turn is related to boiling point of distillation.

Although heterocycles containing S, O and N represent a minor portion in most crude oils, they are of crucial importance for exploration, production and refining of petroleum. Sulfur being the third most abundant element next to carbon and hydrogen poses a serious threat in view of both economy and environment. Generally, sulfur content in crude oils varies from 0.05 to 13.95 wt % [3]. Oils containing, however, more than 1 wt % are considered as sulfur rich oils. Although light, sweet crude serves best to provide low-sulfur fuels, the heavy, sour crude cannot be ignored simultaneously. Viscosity (measured in API gravity unit²), in addition to sulfur content, also plays an important role for the economic value of crude oil. The heavier and more sour (high sulfur) the crude, the more difficult and expensive it is to turn it into usable refined products. There is therefore a great demand for light sweet (low sulfur) crude oils in order to provide low-priced fuels. However, at the present scenario, the decrease in supply of light, sweet crude enhances the price of crude oil. The graph shown in Figure 1.2 shows that every year over the last five years, the average API gravity of non-OPEC (Organization of the Petroleum Exporting Countries) oils has decreased (produced crude is increasingly "heavy") and the sulfur content has increased (crude is increasingly "sour"). In addition, SO_x, a major air pollutant causing acid rain, from petroleum-derived fuels also poses a serious threat to the environment. Sulfur compounds also affect the emission of NO_x and hydrocarbons from automobile engines by reducing the activity of catalytic converters. Moreover, sulfur oxides have detrimental effects on human

² API gravity = (141.5/Specific gravity at 60 °F) - 131.5

health, wildlife and agricultural productivity. Therefore, most countries have defined the limits on sulfur in transportation fuels, being the major source of SO_x , in order to protect the environment.

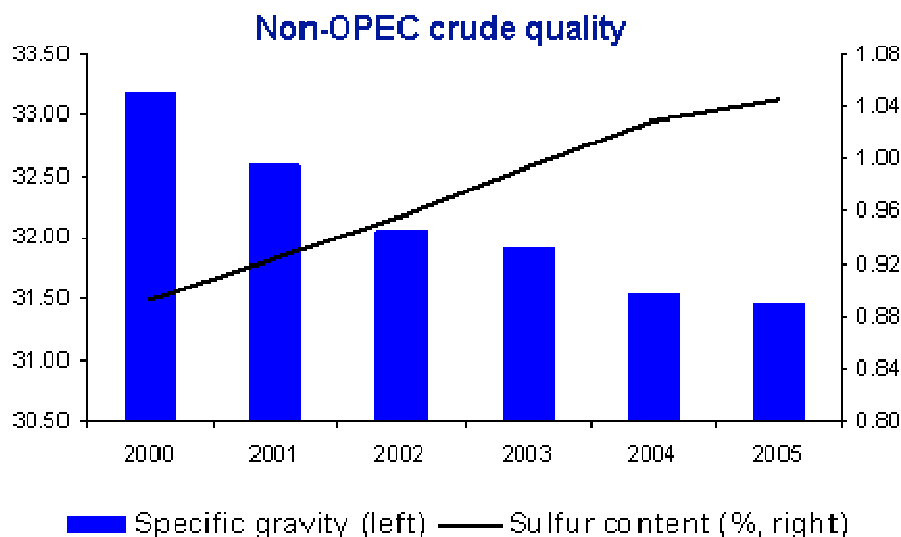


Figure 1.2. Shifting trend towards heavy and sour crude oil in recent years.³

1.3 Sulfur Limits in Transportation Fuels

The trend for limits on sulfur content in transportation fuels, due to environmental pollution, is gradually declining. In 1998, the European directive on transportation fuels put limits on sulfur in gasoline and diesel fuel to 150 ppm and 350 ppm, respectively. In 2005, the limit for sulfur in transportation fuels was lowered to 50 ppm. Germany introduced strict legislation alone by rising taxes 1.53 cents per litre of gasoline exceeding 10 ppm sulfur. Similarly, the USA also limited the sulfur content in diesel fuels to 50 ppm through the Clean Air Act in 1994 and by June 2006 a 15 ppm sulfur limit for at least 80 % of the highway diesel fuel produced will be in effect. Refiners must meet a 500 ppm cap on all off-road diesels produced by June 2007 and for all diesels to be at the 15 ppm ultra-low sulfur level by 2010⁴. Locomotive and marine diesel would remain at the 500 ppm sulfur cap until 2010. In a similar fashion, Japan also started to reduce the sulfur content in diesel by lowering the allowable limit from 2000 ppm (1994), 500 ppm (1997), 50 ppm (2005) to 10 ppm in 2007⁵.

³ http://www.econbrowser.com/archives/2005/08/sweet_and_sour.html

⁴ http://www.npra.org/issues/fuels/diesel_sulfur.cfm

⁵ <http://www.dieselnets.com/standards/jp/fuel.html>

The transportation fuels meeting the limits of sulfur content set by different countries can be obtained from light, sweet crude oils by present technology. However, diminishing supplies of light, sweet crude sources have shifted attention to heavy, sour crude oils for the production of low-sulfur petroleum products. This conversion cannot be achieved without implementation of modern technologies, which is a multi-year, multi-billion-euro project. Therefore, most refiners prefer to refine only light, sweet crude oils to produce low-sulfur products. But, in future, there will be a great demand for heavy oils with more sulfur as statistics shows the production of light, sweet crude oil has already declined during 2000-2004. This gap can be filled through upgrading of low-quality oils, containing high sulfur, available at low prices. In the near future, increase in restrictions for low-sulfur transportation fuels and decrease in supply of light, sweet crude oil will promote the upgrading of present refineries with adoption of modern desulfurization processes used for removal of sulfur from oil. Thus, the efficiency of the desulfurization process will be a key factor to decide the fate of oil used as a source of energy.

1.4 Introduction of Sulfur in Crude Oil

The price of crude oil, the major backbone of a developed economy, is largely decided by the amount of sulfur in it. Moreover, sulfur being the most abundant hetero element in crude oil is of more concern than other heteroatoms. However, the source of such high amount of sulfur in fossil fuels still remains a mystery. The origin of sulfur cannot be explained completely by sulfur from biota as this amount is not present in living organisms. Thus, the origin of sulfur from inorganic sources like sulfates from sea water can be considered as a major source. The sulfur cycle in the sea involves a continuous oxidation and reduction by microorganisms. Microorganisms like *Desulfovibrio* and *Desulfobacter* reduce sulfate to sulfide and the reduced sulfur is further oxidized to elemental sulfur by microbes like *Thiobacillus*. The elemental sulfur produced undergoes anaerobic incorporation into plant and/or animal derived organic material [4]. The aliphatic sulfur compounds are further converted to complex aromatic systems by cyclization and aromatization, in dependence of time, temperature and many geological parameters. Therefore, sulfur exists both in aliphatic and aromatic form in crude oil. All are collectively termed organic sulfur compounds (OSC). A few typical structures of both aliphatic and aromatic OSC are presented in Figure 1.3.

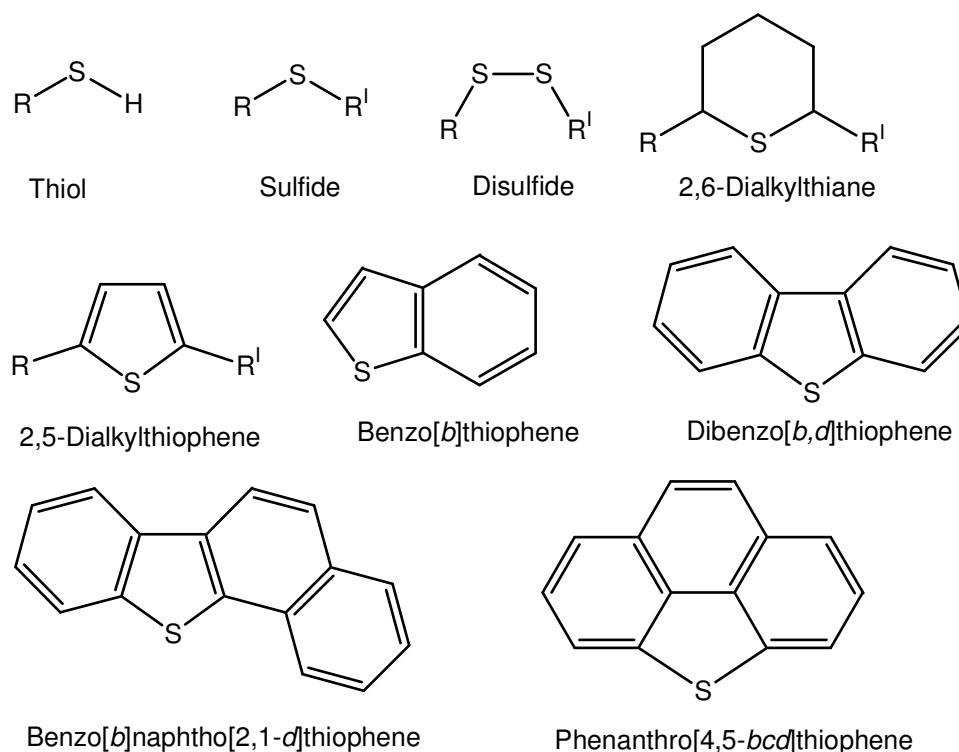


Figure 1.3. Typical organic sulfur compounds found in crude oils.

However, the incorporation of sulfur into crude oil has not been clearly understood until now, although many hypotheses have been proposed with respect to the interaction of sulfur and carbon in the geosphere. These hypotheses are based on geologically occurring hydrocarbons and their biochemical precursors. Out of them, biosynthesis, formation during early diagenesis and formation by reaction of elemental sulfur and hydrocarbons are considered to be major routes in the formation of OSC.

Biosynthesis. Cyr *et al.* proposed a biosynthetic origin for the bicyclic, tetracyclic and hopane sulfides present in petroleum [5]. This was based on the structural similarity of bicyclic and tetracyclic terpenoid sulfides reported in different petroleum sources [6,7]. In all cases, the sulfur atom is attached to the second carbon atom of the alkyl side chain of the hydrocarbon analogues (shown in Figure 1.4). This common structural feature can be explained by the site specificity of the biosynthetic pathway for sulfur incorporation into a hydrocarbon framework. However, neither of the reported OSC nor their functionalized precursors have been reported to occur in biota.

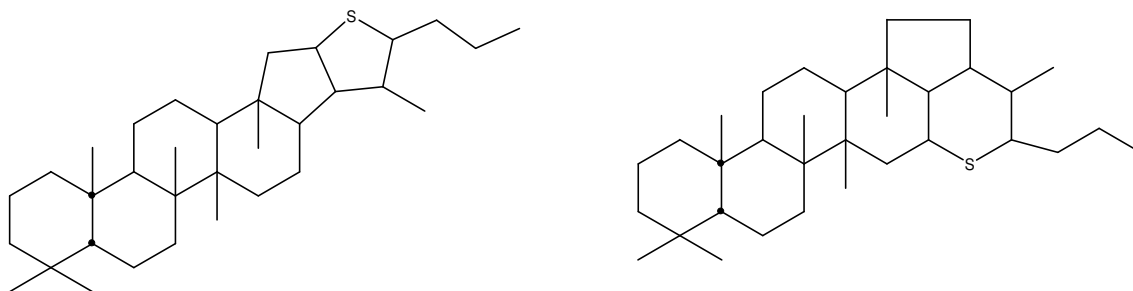


Figure 1.4. S-hopanes present in crude oil.

Formation during early diagenesis. *Brassell et al.* identified one of the alkyl thiophenes, which are formed widely in both recent and ancient deep-sea sediments, occurring as a limited number of the possible stereoisomers [8]. This thiophene is assumed to be originated from the incorporation of sulfur into chlorophyll-derived phytol, or archaeobacterial phytenes or their diagenetic products. Sulfur from H_2S or polysulfides may be involved in this process although the precise mechanism is not clear. *Sinninghe Damste et al.* further corroborated the idea of early sulfur incorporation with the experience from extensive studies [9-11].

Formation by reaction of elemental sulfur and hydrocarbons. *Schmid et al.* reported the identification and geochemical significance of long-chain 2,5-di-*n*-alkylthiolanes and also suggested that this type of compounds might originate from reactions of the *n*-alkanes present in the oil with elemental sulfur during early maturation [12]. This hypothesis was partly supported by the simulation experiment in which *n*-octadecane was heated in the presence of sulfur at 200-250 °C for ~65 h. This experiment produced a randomized mixture of C_{18} 2,5-di-*n*-alkylthiophenes although the C_{18} 2,5-di-*n*-alkylthiolanes were not present. In a further extended work by *Schmid*⁶, a mixture of isoprenoid C_{19} -thiophenes, bithiophenes and trithiophenes was obtained from heating pristane with elemental sulfur under the same experimental conditions. The structures of the latter compounds are comparable with those possessing the phytane framework present in Rozel Point Oil [10,13].

Sinninghe Damste et al. further evaluated this hypothesis by comparing the distribution pattern of hydrocarbons obtained after desulfurization of OSC and originally present hydrocarbons in nine oil samples. This comparison ruled out the possibility of sulfur

⁶ Schmid J. C., Ph.D. dissertation (1986), University of Strasbourg

incorporation by reaction between elemental sulfur and hydrocarbons as the major source [14]. All these assumptions made on experimental basis provide basic information regarding sulfur incorporation into organic matter, although none of them is able to explain the observed compounds with absolute certainty.

1.5 The Refining Process

Crude oil needs to be refined before its use as a source of energy. Therefore, the refining process is of utmost importance for the quality of petroleum products. This process involves quite complex steps. Below an attempt is made to explain the central concepts of the process.

Distillation. A Liquid or vapor mixture of two or more substances is separated into its component fractions of desired purity, by the application and removal of heat. During the distillation of crude oil, the lightest materials, like propane and butane, vaporize and rise to the top of the column maintained at atmospheric pressure. Medium weight materials, including gasoline, jet and diesel fuels, condense in the middle. Heavy materials, called gas oils, condense in the lower portion of the atmospheric column. The heaviest tar-like material, called atmospheric residue, is found in the bottom of the column. The residue obtained from the atmospheric column is further distilled in a column operated below atmospheric pressure so called vacuum distillation. This procedure lowers the boiling point of hydrocarbon mixtures, which helps to minimize the decomposition of high molecular weight components present in crude oil.

Cracking. The heavier ends like gas oils, middle distillates and residues obtained during distillation cannot be directly used as fuels. Therefore, the high molecular weight hydrocarbons present in these fractions are broken down into low molecular weight compounds in the range of gasoline, jet and diesel fuels. The cracking process is divided into three categories, namely fluid catalytic cracking (FCC), hydrocracking and coking. FCC is carried out with heat and catalysts to convert gas oils into mostly gasoline whereas hydrocracking is carried out with catalysts, heat and hydrogen under high pressure to make both jet fuel and gasoline from gas oils. Coking is generally used for the cracking of low-value residue to high-value light products under high temperature.

Treating. The concern of environmental pollution due to N- and S-containing compounds in transportation fuels makes a treating process of utmost importance. It is the process used to remove natural impurities such as sulfur and nitrogen from the crude and other processing streams. This process is indispensable for heavier oils, which contain higher amounts of sulfur and nitrogen. In this process, sulfur is converted to hydrogen sulfide and sent to the sulfur unit where it is converted into elemental sulfur, and nitrogen is transformed into ammonia, which is removed from the process by water-washing. Later, the water is treated to recover the ammonia as a pure product for use in the production of fertilizer.

Reforming. The octane number⁷ is the key parameter in the specification of fuel quality. This parameter gives an indication of how well gasoline performs in an automobile engine. In the reforming process, hydrocarbon molecules are “reformed” into high octane gasoline components. For instance, methyl cyclohexane is reformed into toluene.

Although these are the major steps in the refining process, some other steps like combining and blending cannot be overlooked with respect to the economic point of view. Combining is the process used to combine the molecules lighter than the gasoline range from cracking units in the presence of a sulfuric acid catalyst to obtain high octane gasoline. Blending is the final and critical step in the petroleum industry. Gasoline, for example, is blended from treated components made in several processing units to get the right octane level, vapor pressure rating and other important specifications. A detailed schematic diagram explaining all the processes involved in refinery unit is presented in Figure 1.5.

⁷ A value used to indicate the resistance of a motor fuel to knocking. Octane numbers are based on a scale on which isooctane (2,2,4-trimethylpentane) is 100 (minimal knock) and heptane is 0 (bad knock).

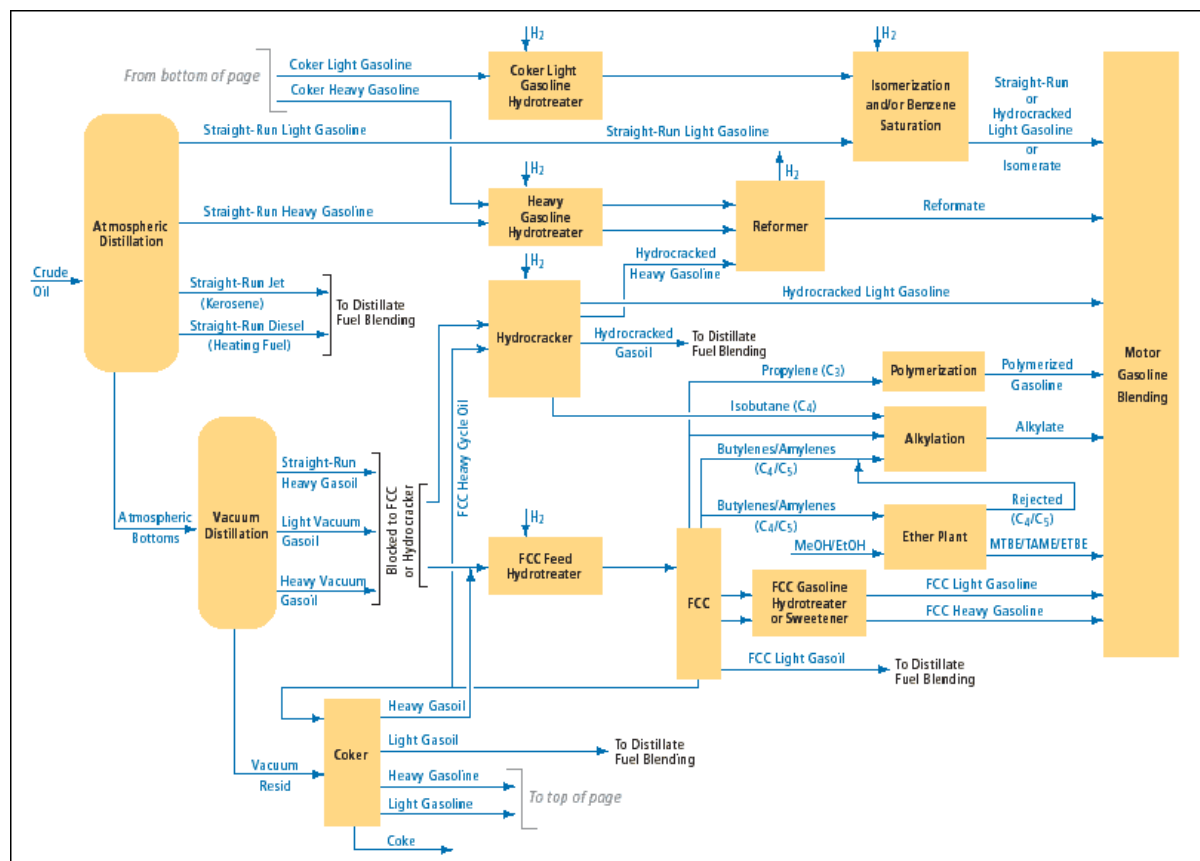


Figure 1.5. Schematic diagram of the refining process [15].

As mentioned in the earlier section, crude oil can be used only after collection of different fractions from distillation unit and not in the form of whole crude oil. Therefore, it is essential to know the utility of each fraction, which is associated with molecular weight and number of carbon atoms. This knowledge in turn helps to understand the mechanism and to improve the efficiency of processes involved in upgrading the product quality obtained from different cuts. The fractions obtained from a distillation unit with respect to boiling ranges are presented in Table 1.1. The amount of distillation residues ranges from 14 to ~55 wt % of the crude oil feedstock [16]. The residue obtained is further distilled under reduced pressure (vacuum distillation) to obtain vacuum gas oils (VGO), and the residue obtained from this unit is called vacuum residue. These fractions cannot be directly used as sources of energy without prior treatment. Generally, these fractions are converted into lighter fractions by different cracking procedures. The presence of heteroatoms, however, causes inhibition to catalyst-regulated cracking processes. Therefore, the removal of heteroatoms, in particular sulfur, will be discussed in the desulfurization section below.

Table 1.1 Classification of refinery cuts according to boiling ranges.⁸

	Boiling Range (Degrees Celsius)	Carbon numbers	Utilities
Petroleum gas	< 40	1-4	Heating, cooking
Naphtha	60-100	5-9	Intermediate of gasoline
Gasoline	40-205	5-12	Motor fuel
Kerosene	175-325	10-18	Fuel for jet and tractor engines
Gas oil	250-350	> 12	Diesel fuel, heating oil
Lubricating oil	300-370	20-50	Motor oil, grease
Heavy gas oil	370-550	20-70	Industrial fuel
Residuals	> 550	> 70	Coke, tar, wax

1.6 Desulfurization

The limit of sulfur content in transport fuels set by the USA, Europe, Japan and other countries is gradually lowered in order to protect the environment from emissions of sulfur oxides that cause acid rain. Therefore, removal of sulfur from the feedstock of gasoline, diesel and other petroleum-derived fuels is highly desirable. In this regard, there are several approaches that have been attempted including photochemical and biodesulfurization methods. Still, for more than 50 years, hydrodesulfurization (HDS) is the dominating one used for the removal of sulfur in petroleum fractions.

1.6.1 Hydrodesulfurization

HDS is the process by which sulfur is removed from sulfur containing compounds by reaction with hydrogen, thereby forming hydrogen sulfide. It is a catalyzed reaction usually involving a metal sulfide catalyst, in particular sulfided Co/Mo/Al₂O₃ or sulfided Ni/Mo/Al₂O₃. The HDS reaction is usually operated at moderately high temperature and pressure; typical conditions are 300-350 °C and 50-100 atm [17,18]. Although HDS serves the best for removal of sulfur, the process is most effective only for a range of sulfur-containing compounds like thiols, sulfides and disulfides. This process is highly dependent on the local environment of the sulfur atom in the molecule, and the overall shape of the

⁸ <http://science.howstuffworks.com/oil-refining2.htm>

molecule. *Nag et al.* showed the order of reactivity among sulfur-containing aromatic compounds as follows: thiophene > benzothiophene > benzonaphthothiophene > tetrahydrobenzonaphthothiophene > dibenzothiophene [19]. Recently, *Choudhary et al.* further extended the investigations including further types of sulfur compounds starting from nonaromatic sulfides to phenanthrothiophenes, which is the least reactive class of compounds towards HDS [20]: Nonaromatic sulfides > thiophenes \approx benzothiophenes » extended five-ring thiophenes (Cata-condensed) \approx six-ring thiophenes > benzonaphthothiophenes \approx compact five-ring thiophenes (Peri-condensed) > C₀/C₁ dibenzothiophenes » C₂₊ dibenzothiophenes > phenanthrothiophenes. The reaction pathways for desulfurization of thiophenes, benzothiophenes and dibenzothiophenes are presented in the following sections.

Reaction pathways for thiophenes. The HDS process for thiophenes proceeds via two parallel pathways as shown in Figure 1.6. In the first of the parallel pathways, the thiophene ring is hydrogenated prior to desulfurization; this is known as the hydrogenation pathway. In the second pathway the thiophene ring can be split due to attack by surface adsorbed hydrogen at the sulfur atom. Sulfur is removed in the form of H₂S, leaving butadiene as the other product; this pathway is known as the hydrogenolysis pathway. However, the reactivity of thiophenes is significantly affected by the degree of substitution of the thiophenic ring. It is observed that the reactivity of alkylated thiophenes varies in the following order: Thiophene > 2-methylthiophene > 2,5-dimethylthiophene [21]. Surprisingly, in another study it was found that substitution at the third position enhances the rate of HDS reaction, and so reactivity is not a simple function of ring substitution [22].

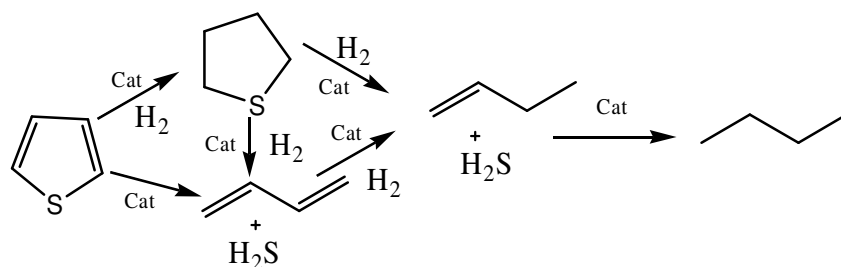


Figure 1.6. Most probable desulfurization pathways for thiophene.

Reaction pathways for benzothiophenes. *Kilanowski and Gates* have observed that the only product from HDS of benzothiophene is ethylbenzene [23]. The HDS of benzothiophenes was further studied by *Van Parijs et al.* [24,25]. They suggested a parallel

pathway similar to that for thiophenes and, again, proposed that hydrogenation and hydrogenolysis occur at different sites as shown in Figure 1.7. *Geneste et al.* observed that methyl substitution of benzothiophene reduced its rate of partial hydrogenation, making the hydrogenolysis route more favorable [26]. The order of reactivity for hydrogenation of the following compounds is as follows. Benzothiophene > 2-methylbenzothiophene > 3-methylbenzothiophene > 2,3-dimethylbenzothiophene. The effect of this substitution, however, is proposed to be due to electronic factors and not steric constraints.

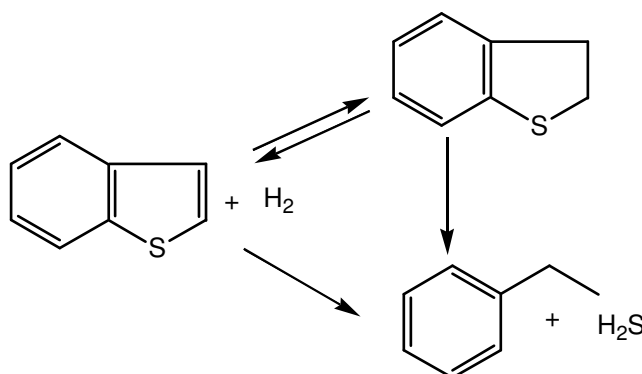


Figure 1.7. Most probable desulfurization pathways for benzothiophene [25].

Reaction pathways for dibenzothiophene. The HDS process is not highly efficient for dibenzothiophene and alkylation at certain positions makes the desulfurization more difficult. Therefore, desulfurization of hindered dibenzothiophenes remains a challenging task till date. *Shafi and Hutchings* reviewed the detailed mechanism involved in the HDS process for dibenzothiophenes [18]. The proposed reaction pathways are given in Figure 1.8.

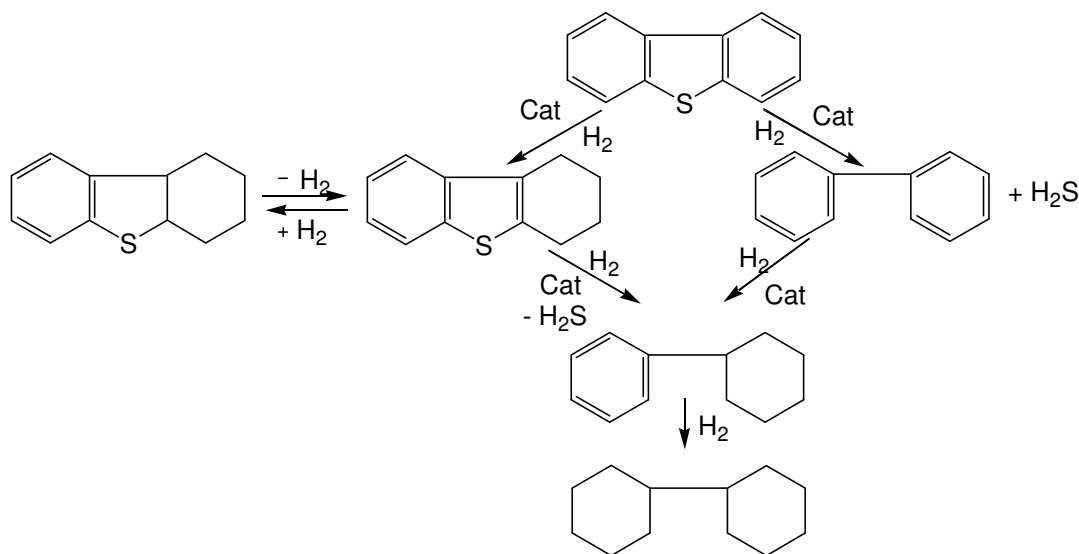


Figure 1.8. Proposed reaction pathways for dibenzothiophene.

The order of reactivity towards HDS reaction in dibenzothiophenes: Dibenzothiophene > 4-methyldibenzothiophene > 4,6-dimethyldibenzothiophene. As shown in Figure 1.9, 4,6-dimethyldibenzothiophene (4,6-DMDBT) was found to be the most recalcitrant species towards the HDS process. The reason is due to the presence of the sulfur atom at a sterically hindered position. Therefore, the abundance of 4,6-DMDBT is quite high in low-sulfur diesels [27,28]. The limitations of present catalysts drive scientists to develop better catalysts.

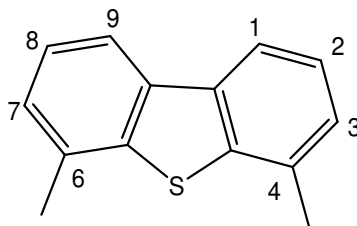


Figure 1.9. Position numbering of alkylated dibenzothiophene.

Except for the direct desulfurization, all other pathways mainly center on removing the steric hindrance of the methyl groups present at the 4 and 6 positions. Recently, *Bej et al.* have presented studies on finding an efficient 4,6-DMDBT hydrodesulfurization catalyst [29]. Although a lot of investigations are carried out with 4,6-DMDBT because of its being considered the most recalcitrant species, *Schade and Andersson* reported for the first time that a methyl group in the 1 position of dibenzothiophene can also lead to a lower reactivity under HDS conditions [30]. Here, non-planarity of the aromatic system may play a significant role in reducing the catalytic activity of HDS reactions.

1.6.2 Other Methods of Desulfurization

Photochemical methods have been applied for the desulfurization of sulfur compounds. *Moza et al.* have studied the photodegradation of aromatic sulfur compounds in a thin liquid film on water using irradiation with a mercury lamp [31]. *Hirai et al.* further applied this technique to hindered dibenzothiophenes [32] as it demonstrated several advantages over catalytic techniques, e.g.

- (a) ambient temperature operation,
- (b) no hydrogen is required,
- (c) relatively easy to operate and

(d) all hindered dibenzothiophenes can be desulfurized efficiently. Here, the order of reactivity was reverse compared to that of the HDS process, i.e. DBT < 4-MDBT <

4,6-DMDBT [33]. The reversal of the reactivity order was explained in terms of the expanded electron cloud of 4-MDBT and 4,6-DMDBT facilitating the excitation of DBTs. Although this process was satisfactory for standard compounds, it resulted in low yields for pre-distilled crude oil. This result was explained as being caused by a shielding effect due to the presence of various unsaturated compounds in the crude oil. Therefore, this process cannot compete with the HDS in an industrial process.

Also, many studies have been performed utilizing microbial degradation of sulfur compounds with emphasis on dibenzothiophenes [33,34]. However, no studies have been reported on microbial degradation of hindered DBT (e.g. 4,6-DMDBT).

1.7 Summary

With the present HDS technique, it is possible to obtain nearly sulfur-free fuels in the lower boiling ranges of petroleum fractions. However, the removal of sulfur from heavy fractions (starting with atmospheric gas oil and higher fractions) to the desired level is quite difficult with the present industrial procedures [17]. In order to meet the sulfur limit in heavy oils, multi-billion euros are expected to be spent on upgrading the present techniques employed for HDS. Therefore, information on molecular-level structure-reactivity relationships of different groups of sulfur-compounds towards HDS processes is highly desirable for the effective development of modern techniques. Till date, there is a lack of fundamental understanding of sulfur removal chemistry of heavy oil fractions. This limitation can be overcome through the development of new analytical methodologies suitable for heavy oils, including high-boiling fractions, coupled with the basic knowledge of sulfur chemistry from low-boiling fractions.

2. Analytical Techniques for Heavy Petroleum Fractions

Fossil fuel remains the major source of energy although the environmental pollution associated with it has been increasing concern in recent years. Therefore, the analysis of components causing pollution is of high priority in the oil industry. Out of all, sulfur poses the major threat towards the environment, causing acid rain, and it plays a crucial role in the oil economy reducing the efficiency of refining processes. Both environmental and economical concerns have driven the development of analytical methods for sulfur compounds. In addition, the knowledge of high molecular weight compounds, including sulfur-containing compounds, is of utmost importance for refineries as they are moving to operate at higher efficiencies with heavy crude sources. Here, a short overview of analytical techniques, employed in the research of heavy oils and high-boiling petroleum fractions, is given. Gas chromatography technique is ruled out for analysis of heavier fractions due to its limitation with respect to the volatility of the components.

2.1 Liquid Chromatography

The complexity of petroleum sample further limits the group type analysis of compound classes. Therefore, in order to reduce the complexity of a sample, a variety of chromatographic techniques is utilized successively before characterization by any spectroscopic method. The most relevant and widely used chromatographic systems in petroleum analysis will be provided in the following sections.

2.1.1 Group Separation into Saturates, Aromatics, Resins and Asphaltenes (SARA)

The first approach in the analysis is the group separation of petroleum fractions into saturate, aromatic, resin and asphaltene. Asphaltenes, highest molecular weight matter and insoluble in the lower n-alkanes, are removed by precipitation. Then saturate, aromatic, and resin (polar compounds) fractions are eluted from chromatographic columns packed with silica and/or alumina by eluents of increasing polarity.

2.1.2 High Performance Liquid Chromatography (HPLC)

After the successful separation by the SARA method, HPLC methods are applied to further narrow down the complexity of the sample according to well-defined criteria. For our work, the aromatic fraction from SARA is further separated into fractions according to the number of condensed aromatic rings in the normal-phase mode, which helps to identify the exact carbon skeleton of aromatic compounds. Liquid chromatographic separation of polynuclear aromatic compounds from petroleum samples according to the number of aromatic double bonds on aminopropano silica stationary phase has been frequently reported [35,36]. This phase has previously been used in studies of polycyclic aromatic sulfur heterocycles in crude oil [37]. A different separation mechanism, namely a charge-transfer interaction, is found for the many stationary phases that have been used for the separation of polycyclic aromatic compounds (PAC) in coal liquefaction products and pitches [38-43]. This mode of separation, however, is influenced by the presence of heteroatoms and alkyl substituents. Details about the separation of PAC according to the number of condensed rings and the introduction of new stationary phase in this regard will be further depicted in the Chapter 8.

In the reversed-phase mode, the shape selectivity of bonded alkyl stationary phases has been discussed for PAC analysis [44,45]. Here, the length to breadth ratio, planarity and alkyl substitution of aromatic compounds mostly influence the interactions with the stationary phase and allows the separation of isomers that co-elute in the normal-phase mode. By the reversed-phase HPLC, it was possible to isolate an eight-ring polycyclic aromatic hydrocarbon, produced during catalytic hydrocracking of petroleum-derived oils [46]. Moreover, ligand exchange chromatography (LEC) also plays a significant role in the isolation of sulfur aromatics from petroleum fractions in the presence of large number of hydrocarbons. The LEC employed, using a Pd(II)-bonded stationary phase, for the separation of polycyclic aromatic sulfur heterocycles (PASHs) from polycyclic aromatic hydrocarbons (PAHs), was found to be quite efficient for diesel samples [28,30]. In this way, it rules out the probability of interference from PAHs in the characterization of PASHs.

2.1.3 Thin-Layer Chromatography (TLC)

TLC using quartz rods coated with sintered silica particles and flame ionization detection (TLC/FID) was applied for group-type analysis of petroleum heavy distillates and petroleum hydroconversion products [47,48]. A TLC/FID procedure was presented by which hydrocarbon classes (saturates, aromatics, polars) can be well separated and accurately determined [47]. This unique technique was also shown to be effective in providing rapid determination of saturates, aromatic hydrocarbons, polar compounds, and an uneluted fraction of a deasphalted heavy oil and its hydrocracking products [47,48].

2.1.4 Size Exclusion Chromatography (SEC)

Molecular weight distribution of several vacuum residues has been determined by SEC in combination with mass spectrometry [49,50]. However, the choice of mobile phase in SEC plays a significant role in accuracy of measurements. In most cases, 1-methyl-2-pyrrolidinone was used as mobile phase instead of tetrahydrofuran, which was found to lead to partial loss of sample due primarily to solubility limitations [51]. All these investigations were focused on either whole residue or the asphaltenes until it was reported specifically for the aromatic fraction of vacuum residues [52].

2.2 Spectroscopic Techniques

2.2.1 Ultraviolet/Visible and Fluorescence Spectroscopy

The aromatic ring systems in petroleum fractions were examined with emphasis on the presence of one- to three-ring moieties by fluorescence emission spectroscopy [53]. A progressive shift of UV/fluorescence spectral intensity and high molecular mass with decreasing mobility of the fractions on the TLC plate, indicated the presence of increasingly larger PAHs in the less displaced fractions.

2.2.2 Infrared Spectroscopy (IR)

IR was applied to obtain the concentration of several functionalities of fossil fuels [54]. Diffuse reflectance IR spectroscopy (DRIFT) was applied for monitoring and semi quantitative evaluation of structural changes associated with mesophase formation in pitches

[55]. Fourier transform-IR in combination with thermogravimetry was used to evaluate the behavior of sulfur compounds during coal pyrolysis [56].

2.2.3 Nuclear Magnetic Resonance Spectroscopy (NMR)

Since NMR techniques are capable of providing structural differences due to carbon, hydrogen, and heteroatom environments, they have been found to be useful for unraveling complex structures and compositions of many heavy petroleum and coal products. ^1H NMR was applied to determine hydrogen content in coal derived heavy distillates, and the data were found to be consistent with those obtained by combustion method [57]. ^1H NMR was able to provide information on structural changes during hydrogenation upgrading of vacuum residue and its mixture with coal and coal tars [58]. In addition, ^1H NMR was also able to differentiate between α -methyl and α -methylene protons in heavy petroleum fractions [59]. ^{13}C NMR provided protonated and nonprotonated carbons in heavy oils derived from coal liquefaction, and the data were used to estimate average aromatic structures and alkyl groups [60]. A number of reports using both one- and two-dimensional NMR in the characterization of fossil fuels were presented in a review article [61].

2.2.4 X-ray Scattering

The organic sulfur compounds in petroleum samples were determined and quantified by spectroscopic techniques like X-ray absorption near edge structure (XANES) and X-ray photoelectron spectroscopy (XPS) [62-64]. The application of XANES spectroscopy for sulfur and nitrogen molecular structures in asphaltenes and related materials was detailed in a review article [65].

2.3 Mass Spectrometry (MS)

A number of investigations with mass spectrometry have been carried out to identify unknown components present in the complex mixtures of petroleum fractions. The limiting factor in analyzing heavy fractions remains in the ionization efficiency of large molecules with different ionization sources. Therefore, several methods have been developed to identify whole ranges of compounds (polar and non polar) with a mass range from 200-1000 Da.

Boduszynski characterized heavy petroleum fractions with field ionization-MS [66]. However, reliance on thermal introduction discriminates among compounds of varying boiling temperatures. The analysis of non-volatile residue components with field desorption ionization (FD-MS) has been carried out by *Larsen* [67], but the sample loading procedure on a fragile emitter was impractical to use on routine basis. Also, thermospray ionization has been interfaced to MS for analysis of high-boiling polycyclic aromatic compounds as reported by *Hsu* [68]. However, the limitations in sensitivity and the inefficiency to more polar compounds do not allow for universal application. Particle beam ionization (PB) is another option for ionizing heavy aromatic compounds [69], but present PB interface design suffers from sensitivity and linearity limitations [70]. In this regards, matrix assisted laser desorption ionization (MALDI) is extensively used for molecular weight distribution determination of heavy petroleum fractions [52]. Atmospheric pressure chemical ionization (APCI) has also been applied for identification of high molecular weight polycyclic aromatic hydrocarbons [71]. The drawback of APCI-MS spectra is that one analyte gives rise to several possible ions depending on the structure and size of the analyte. Therefore, this ionization mode results in even more complex spectra in an already complex petroleum sample. The most widely used electrospray ionization (ESI) technique can also be applied for this regard. However, direct ionization of aromatic compounds is not quite efficient so that a pre-derivatized technique is highly desirable in order to produce ions before introduction in the ion source. There are some instances that have been reported for ESI with addition of a reagent in order to enhance the ionization of non polar components. In this regard, silver nitrate for aromatic hydrocarbons in heavy petroleum fraction [72], trifluoroacetic acid, 2,3-dichloro-5,6-dicyano-1,4-benzoquinone, and antimony pentafluoride as chemical electron-transfer reagents for the neutral PAC [73] and palladium(II) as sensitive enhancing reagent for polycyclic aromatic sulfur heterocycles have been used [74].

2.3.1 FT-ICR MS of High-Boiling Petroleum Fractions

The application of Fourier transform ion cyclotron resonance mass spectrometry [75] (FT-ICR MS) in petroleum characterization has opened up the new field of petroleomics [2]. Ultra-high mass resolving power and mass accuracy afforded by FT-ICR MS allows for elemental composition assignment of all resolved species and is especially suited for analysis of unknown complex mixtures [76]. Various soft ionization methods, including low-voltage electron ionization (EI) [77], field desorption ionization [78,79], atmospheric pressure photo

ionization (APPI) [80], and electrospray ionization [81-83] have been interfaced with FT-ICR MS for analysis of petroleum fractions. However, only one ionization method is not sufficient for production of ions from both polar and non-polar components present in fossil fuels. Low-voltage electron ionization is suitable for volatile aromatic components. In case of APPI, production of protonated, deprotonated and molecular ions from a single analyte makes data more complicated although it is quite suitable for non-polar components. ESI is quite efficient for polar molecules whereas it is not able to ionize non-polar molecules efficiently. Field desorption ionization is highly attractive because the absence of a matrix and ion formation in vacuum ensure that the resultant spectra are not only free of fragments but also free from interfering species that result from reactions of gas-phase ions with matrix molecules. This technique also ionizes both saturated and aromatic compounds including a variety of non-polar compounds. However, the lack of commercial availability of FD ionization interfaced with FT-ICR mass spectrometer makes less access to chemists involved in petroleum research.

2.4 Chemical Methods

Chemical methods are applied either to make simpler forms of complex molecules or to modify the parent molecule to enhance the sensitivity and/or selectivity of specific compounds. Oxidative degradation of sulfur rich kerogenes by sodium dichromate in glacial acetic acid cleaves off alkyl substituents from the aromatic system at the benzylic positions, leaving aromatic carboxylic acids for assigning the positions of alkyl substituents [84,85]. Ruthenium tetroxide degrades aromatic rings to carboxylic acid function [86,87], leaving alkyl substituents intact. Such a study provides information on the length of alkyl chains. These reactions have been widely used for the study of alkylated compounds in petroleum samples [88,89].

3. Objectives

The concern of sulfur in petroleum fractions, described in detail in the introduction section, has opened ample avenues for analytical chemists. The objective of this work is to develop analytical methods for the speciation of high molecular weight sulfur aromatics in petroleum fractions.

In this regard, chromatographic stationary phases will be developed and tested for their suitability to separate PASHs according to different principles. The fractions obtained will be characterized by FT-ICR MS and UV spectroscopy. The characterization by MS will give an idea of the size of molecules including the distribution of alkyl carbons, and UV spectroscopy will provide information on the size of aromatic rings in the molecules.

The applicability of the developed method will be demonstrated on the high-boiling fractions, namely vacuum gas oils, and whole crude oil. In addition, vacuum gas oil samples, before and after HDS, will be included in this study to investigate the fate of high molecular weight sulfur aromatics during the course of the hydrodesulfurization.

4. Ultra-High Resolution Mass Spectrometry

Generally, high-resolution work is the domain of double-focusing magnetic sector instruments. Later, time of flight (TOF) and to a certain degree triple quadrupole instruments are also capable of resolutions up to about 20,000, which is defined as high-resolution mass spectrometry. However, the rapid development of Fourier transform ion cyclotron resonance (FT-ICR) instruments in recent years has offered ultra-high resolution ($> 250,000$) and highest mass accuracy (50 ppb) required for unambiguous assignment of closely spaced components (1.1 mDa) present in a complex mixture like crude oil [90]. Ultra-high resolution in combination with a soft ionization method such as ESI, MALDI, FDI, APCI or APPI provides the ultimate way to characterize enormous number of intact molecular species contained in a complex mixture.

4.1 Ionization Techniques

4.1.1 Electrospray Ionization

The electrospray process involves the creation of a fine aerosol of highly charged micro droplets in a strong electric field. Electrospray as an ionization technique for mass spectrometry was developed by *Dole et al.* [91] in the late 1960s and considerably improved upon by *Yamashita and Fenn* who in 1984 coupled an electrospray source to a quadrupole mass analyzer [92,93]. A continuous flow of solution containing the analyte from a highly charged (2-5 kV) capillary generates an electrospray. The solution elutes from the capillary into a chamber at atmospheric pressure, producing a fine spray of highly charged droplets due to the presence of electric field, a process called nebulization. Solution flow rate can range from less than a microliter per minute to several milliliters per minute. A combination of thermal and pneumatic means is used to desolvate the ions as they enter the ion source. The solvent contained in the droplets is evaporated by a warm counter-flow of nitrogen gas until the charge density increases to a point at which the repulsion becomes of the same order as the surface tension. The droplet then fragments, called Coulomb explosion, producing many daughter droplets that undergo the same process, ultimately producing bare analyte ions. This technique has tremendous potential for charged, polar compounds.

4.1.2 Matrix Assisted Laser Desorption Ionization

Laser desorption ionization (LDI) was first introduced in the 1960s, but it was not much used until the development of matrix-assisted LDI (MALDI) in the mid 1980s. *Tanaka et al.* first demonstrated the analysis of high molecular weight biomolecules using a matrix [94]. Also, in the same year *Karas, Hillenkamp and co-workers* reported the first of many papers on the use of organic matrixes in MALDI [95]. Laser desorption methods ablate material from a surface using a pulsed laser, typically nitrogen lasers (337 nm) or frequency-tripled Nd:YAG lasers (355 nm), with a pulse width of 5 ns or less. Pulsed lasers can deliver a large density of energy into a small space in a very short period of time, of the order of 10^6 - 10^8 W cm⁻². The energy density is much higher than can be achieved with a continuous laser and is sufficient to desorb and ionize molecules from a solid surface. LDI is good for low- to medium-molecular weight compounds and surface analysis. However, the method improved to its maximum mass range with the introduction of matrix-assisted laser desorption ionization. This involves the use of a solid matrix that is co-crystallized along the sample. A dense gas cloud is formed upon irradiation, which expands supersonically into the vacuum. It is believed that analyte ionization occurs through interactions between neutral analytes, excited matrix radicals/ions and protons and cations such as sodium and silver. The matrixes used for this technique should fulfill the following criteria: (i) absorb light at the laser wavelength; (ii) promote ionization of the analyte; (iii) be soluble in a solvent common to the analyte; and (iv) co-crystallize with the sample. Most matrixes, for instance sinapinic acid, 2,5-dihydroxybenzoic acid and nicotinic acid, are organic acids that have a strong UV chromophore, typically an aromatic ring. The accessible mass range is beyond 500,000 Da.

4.1.3 Field Ionization/Field Desorption

Application of a high positive electric potential to an electrode that shrinks to a sharp point results in a very high potential gradient (10^8 - 10^{10} V cm⁻¹) around the regions of high curvature at the tip. A molecule encountering this field has its molecular orbitals distorted and quantum tunneling of an electron can occur from the molecule to the positively charged anode. This process is called field ionization (FI). The positive ion so formed is repelled by the anode or emitter and flies off into the mass spectrometer. This technique is limited to volatile analytes. This limitation was overcome with the introduction of field desorption (FD), because FD circumvents the evaporation of analyte prior to ionization. Instead, the

processes of ionization and subsequent desorption of the ions formed are united on the surface of the field emitter. The specific interest in FI and FD in particular arises from their extraordinary softness of ionization yielding solely intact molecular ions in most cases, and from the capability of FD to handle neutral as well as ionic analytes. The mass range is typically less than about 2000 to 3000 Da for FD and less than 1000 Da for FI.

4.1.4 Atmospheric Pressure Chemical Ionization

Atmospheric pressure chemical ionization (APCI) represents a high-pressure version of conventional chemical ionization (CI). Here, ion-molecule interactions at atmospheric pressure are employed to generate ions. The plasma is maintained by a corona discharge between a needle and the spray chamber serving as the counter electrode. The ions are transferred into the mass analyzer by use of the same type of vacuum interface as employed in ESI. The nature of the APCI plasma varies widely as both solvent and nebulizing gas contribute to the composition of CI plasma. The great advantage of this technique is that it is able to ionize non-polar molecules, thus making this technique more accessible towards aromatic hydrocarbons.

4.1.5 Atmospheric Pressure Photo Ionization

Atmospheric pressure photo ionization (APPI) involves the use of a discharge lamp (e.g. hydrogen discharge lamp at 10.2 eV) that generates vacuum ultraviolet photons. Most organic molecules have ionization potentials in the range of 7-10 eV [96]. Therefore, the photons produced from a discharge lamp of 10 eV or more can produce molecular ions from most organic molecules. The relative abundance of ions in an APPI spectrum depends on the reactions that the original photoions undergo prior to mass analysis. In the APPI method, the high collision frequency ensures that species with high proton affinities and/or low ionization potential tend to dominate the positive ion spectra. However, the increase in sensitivity of neutral species can be enhanced with the addition of a suitable dopant. This dopant should be selected in such a way that its photoions have a relatively high recombination energy, or a low proton affinity, then the dopant photoions may react by charge exchange or proton transfer with species present in the ionization region. In a study, both acetone (IP = 9.7 eV) and toluene (IP = 8.83 eV) were used as dopants for both basic and neutral compounds. Addition of toluene as a dopant increases the sensitivity of both high and low proton affinity species as a whole although the increase in sensitivity for high proton

affinity compounds is higher, whereas acetone as a dopant is effective only for high proton affinity compounds. Therefore, the choice of dopant remains a key factor affecting the sensitivity and selectivity of APPI [96].

4.2 Mass Analyzers

After the successful creation of charged compounds from neutral analytes in the ionization source, ions are to be separated according to their mass-to-charge ratio. This job is carried out by mass analyzers. All mass analyzers employ electric fields, sometimes in conjunction with magnetic fields, to enable discrimination between ions of different mass-to-charge ratio. The discrimination between different ions can be expressed through the concept of resolution. The resolution of a mass spectrometer represents its ability to separate ions of different m/z . An instrument with high resolving power and accuracy in mass measurement is able to distinguish many peaks placed under a single nominal mass and to assign correct composition of each exact mass, respectively. Therefore, instruments with high resolving power are highly essential to identify the thousands of components, in a mass range of 100-1000 Da, found in crude oil.

4.2.1 Definitions

4.2.1.1 Mass Resolution

Resolution (R) is generally calculated in three different ways: (1) 10 % valley definition, (2) 5 % valley definition and (3) full width of the peak at half maximum intensity (FWHM).

10 % valley definition - Generally peaks obtained from mass spectrometers are Gaussian in shape and the definition is $R = m/\Delta m$, where m is the mass of an ion peak and Δm is the distance to another peak overlapping such that there is a 10 % valley between the two peaks.

5 % valley definition – Here, it is calculated on a single ion. Δm is the full width of the peak at 5 % of its maximum intensity.

FWHM - This definition is commonly used for most of the instruments. Here, Δm is expressed in definition itself.

4.2.1.2 Mass Resolving Power

Resolving power ($m/\Delta m_{50\%}$), mostly used in FT-MS, is defined as the ratio of mass to the width of the corresponding mass peak at half-height.

4.2.1.3 Mass Accuracy

The mass accuracy of a spectrometer is the difference observed between the calculated mass of an ion and its observed mass, $\Delta m = m_{\text{calculated}} - m_{\text{observed}}$, expressed relative to the observed mass. It is usually reported in parts per million (ppm):

$$\text{Mass accuracy (ppm)} = \Delta m / m_{\text{observed}} \times 10^6 \quad \text{Eq. 4.1}$$

Generally, instruments capable of providing a mass accuracy of 5 ppm or better are chosen for accurate mass measurements. Moreover, the trend is shifting towards parts per billion (ppb) levels with the advent of modern mass spectrometers.

Here, the mostly used five main types of mass analyzers will be presented with their pros and cons' emphasizing the FT-ICR as this analyzer was used for all the measurements during this dissertation work.

4.2.2 Types of Mass Spectrometers

4.2.2.1 Sector Field

The sector-type system involves a magnetic field that causes ions to be deflected along curved paths. The individual ions are separated spatially according to their unique radius of curvature (ion trajectory) r , which is unique for individual mass/charge (m/z) ratio. The principle involved in the separation of ions in this analyzer can be explained in the following way.

The velocity v , experienced by ion before entering into the magnetic field is given by

$$\frac{1}{2}mv^2 = zV \quad \text{Eq. 4.2}$$

or, solving the velocity term,

$$v = \sqrt{\frac{2zV}{m}} \quad \text{Eq. 4.3}$$

As the ions enter the magnetic field, they experience a force at right angle both the magnetic lines of force and their line of flight. Equating the centripetal and the centrifugal forces,

$$\frac{mv^2}{r} = Bzv \quad \text{Eq. 4.4}$$

Or, rearranging the equation, the radius of curvature of the flight path is proportional to its momentum and inversely proportional to the strength of the magnetic field:

$$r = \frac{mv}{zB} \quad \text{Eq. 4.5}$$

Eliminating the velocity term,

$$r = \frac{1}{B} \sqrt{2V \left(\frac{m}{z} \right)} \quad \text{Eq. 4.6}$$

or, rearranging the above equation,

$$\frac{m}{z} = \frac{B^2 r^2}{2V}, \quad \text{Eq. 4.7}$$

where, B = magnetic field strength

r = radius of curvature of the ion

V = applied potential

In order to obtain the mass spectrum, either the accelerating potential or the magnetic field strength is varied. This is one of the high resolution, sensitivity and high dynamic range instruments. Mass range goes up to 4000 m/z . The typical resolution is 25,000 with maximum of 100,000 for double-focusing instruments. This is applied in all organic MS analysis method, accurate mass measurements, quantitation and isotope ratio measurements. However, it lacks coupling capability with atmospheric ionization source and is not well-suited for pulsed ionization methods (e.g. MALDI).

4.2.2.2 Quadrupoles

Here, a quadrupole field is formed by four electrically conducting, parallel rods. Opposite pairs of electrodes are electrically connected. One diagonally opposite pair of rods is held at $+U_{dc}$ volts and the other pair at $-U_{dc}$ volts. A rf oscillator supplies a signal to the first pair of rods that is $+V \cos \omega t$ and a rf signal retarded by 180° ($-V \cos \omega t$) to the second pair. The equipotential surfaces in the region between the four rods appear as oscillating hyperbolic potentials. The ions, coming from the ionization source, proceed down the longitudinal z -axis, they undergo transverse motion in the x - and y -planes perpendicular to the longitudinal axis. The dc electric fields tend to focus positive ions in the positive plane and defocus them in the negative plane. As the superimposed rf field becomes negative during part of the negative half-cycle of the alternating field, positive ions are accelerated toward the electrodes and achieve a substantial velocity. The following positive half-cycle has an even greater influence on the motion of the ion, causing it to reverse its direction

(away from the electrode) and accelerate even more. The ions exhibit oscillations with increasing amplitudes until they finally collide with the electrodes and become neutral particles. By controlling the ratio V_{dc}/V_{rf} , the field can be established to pass ions of only one m/z ratio down the entire length of quadrupole array. By simultaneously ramping the dc and rf amplitudes, ions of various m/z ratios are allowed to pass through the mass filter to the detector and an entire spectrum can be produced.

This instrument is compact, simple, well-suited to chromatographic coupling, well-suited for coupling to atmospheric ionization source and best-suited for MS/MS study. The mass range goes up to 4000 m/z ; typically 2000 m/z . This type of analyzer is more frequently used in benchtop GC/MS and LC/MS system. This can be used for MS/MS studies as triple quadrupole or in hybrid with sector or TOF. However, limited resolution (maximum 3000) and the lack of interfacing abilities with pulsed ionization techniques limit its versatility.

4.2.2.3 Ion Trap

The ion trap, called as quadrupole ion trap, consists of a ring shaped electrode with curved caps on the top and bottom. Ions are injected from the source through one of the caps, and by applying a combination of voltages to the ring and capping electrodes, the ions can be trapped in a complicated three-dimensional orbit. The electric field is constructed in such a way that the force on an ion is proportional to its distance from the center of the trap. A constant low pressure is maintained in the cell to remove excess energy from the ions, which would otherwise repel each other to the extent that their trajectories became unstable, causing loss of ions from the trap. Only of the order of 300-1000 ions are trapped at a given time, as more ions than this decrease attainable resolution and fewer reduces sensitivity. Once the ions are trapped, the electrode potentials can be manipulated so that the ions' motion become unstable in order of their mass-to-charge ratios and they are ejected from the trap into an external detector, a process called mass-selective ejection. Mass analysis in this way takes less than one tenth of a second, and the resolution obtained is comparable to that of a quadrupole.

This provides high sensitivity, multi-stage mass spectrometry and it can be configured with any other mass analyzers in hybrid instruments. The mass range and resolution are in

the similar range as those of quadrupole instruments. The ion trap finds application in benchtop GC/MS and LC/MS. Unlike the quadrupole, it can also be interfaced with MALDI sources. It is quite useful for MSⁿ and hybrid systems. However, it is not efficient for quantitation and is subject to space charge effects and ion molecule reactions.

4.2.2.4 Time of Flight

The principle involved in the time of flight (TOF) mass analyzer can be described in the following way. A pulse of ions is generated in the source, and accelerated through an electric field into the TOF analyzer. The kinetic energy (*KE*) given to each ion by the electric field is the product of the charge of the ion and the electric field strength:

$$KE = zeV \quad \text{Eq. 4.8}$$

All ions (of the same charge), regardless of mass, enter the field free region with the same kinetic energy. Since kinetic energy can also be represented by the Newtonian equation:

$$KE = \frac{1}{2}mv^2 \quad \text{Eq. 4.9}$$

Equating Eq. 4.8 and 4.9,

$$zeV = \frac{1}{2}mv^2 \quad \text{Eq. 4.10}$$

By rearranging the Eq. 4.10, m/z for a given ion can be determined:

$$m/z = 2eV \left(\frac{t}{L} \right)^2 \quad \text{Eq. 4.11}$$

where z is the charge on the ion, e is the charge of an electron in Coulomb, V is the voltage in volts, t is the flight time of the ion and L is the flight path length of the ion. An entire mass spectrum is generated in a single pulse, and up to 30,000 individual spectra are collected per second. These spectra are summed to obtain a much improved signal to noise ratio.

This instrument has uniqueness of having unlimited mass range. In addition, high speed analysis, detection of all species simultaneously and compatibility with pulsed ionization sources make it popular among the analyzers. There is no theoretical upper limit to the mass range. For instance, instruments typically extend well beyond 200,000 m/z . The best resolution that can be achieved is about 30,000, but in general 10,000 is observed. It is best suited to MALDI. It has found application in hybrid spectrometers and in GC/MS systems.

4.2.2.5 Fourier Transform Ion Cyclotron Resonance

FT-ICR mass spectrometers, first demonstrated by *Comisarow and Marshall*, offered ~100 times higher resolution and mass accuracy than any other analyzers at the time of introduction to market [97]. In addition, till date, the FT-ICR instrument has maintained the uniqueness in providing highest resolution (350,000) and highest accuracy (50 ppb), putting other analyzers far behind. Therefore, it finds more application in the field of proteomics and petroleomics, which involve characterization of ultra-complex mixtures. Moreover, interfacing of both internal and external ionization sources to the analyzer makes it more versatile in the analysis of a wide variety of compounds. Above all, this is quite powerful for tandem mass spectrometry (MS/MS or MSⁿ). Therefore, a short description will be provided in order to demonstrate the operation principles involved in the separation of ions.

Principle of operation. Ions are deflected into a circular path when moving perpendicular to a magnetic field, and if the field is very strong and the velocity of the ion is slow, the ions are forced to move in a circular orbit. This orbit represents cyclotron motion and the frequency of the orbiting ion is characteristic of its mass. The force experienced by the ion is called the Lorentz force (F_L). This force acts as centripetal force (F_{cp}) in order to hold the ions in a fixed circular orbit.

$$F_L = zvB \quad \text{Eq. 4.12}$$

$$F_{cp} = mv^2/r \quad \text{Eq. 4.13}$$

$$zvB = mv^2/r \quad \text{Eq. 4.14}$$

$$\omega = zB/m, \quad \text{Eq. 4.15}$$

where ω : angular frequency, m : mass of ion, z : charge of ion, B : external magnetic field
 r : radius of circular ion path, and v : ion velocity.

A significant feature in this instrument is that all ions of a given mass-to-charge ratio, m/z , have the same frequency, independent of their velocity. This property makes ion cyclotron resonance (ICR) more useful for mass spectrometry, because translational energy “focusing” is not essential for the precise determination of m/z .

The frequency of the trapped ions must be determined in order to obtain a mass spectrum. In FT-ICR cell, all ions are excited using a radiofrequency ‘chirp’ of short duration that rapidly sweeps across a large frequency range. This has the effect of increasing

the orbital radius so the ion trajectory passes close to the walls of the cell. Two of the walls of the cubic cell (shown in Figure 4.1) are designated detection plates and as the ions approach one of the walls electrons are induced to collect on that electrode. The path of the ions takes them back towards the other electrode and the electrons flow back. This migration of electrons is amplified and detected as a sinusoidal image current. The image currents induced in the detection plates contain frequency components originating from all different mass-to-charge ratios. The various frequencies and their relative abundances can be calculated by using Fourier transformation, which converts the time-domain data (image currents) to frequency-domain spectrum that then results in the mass spectrum.

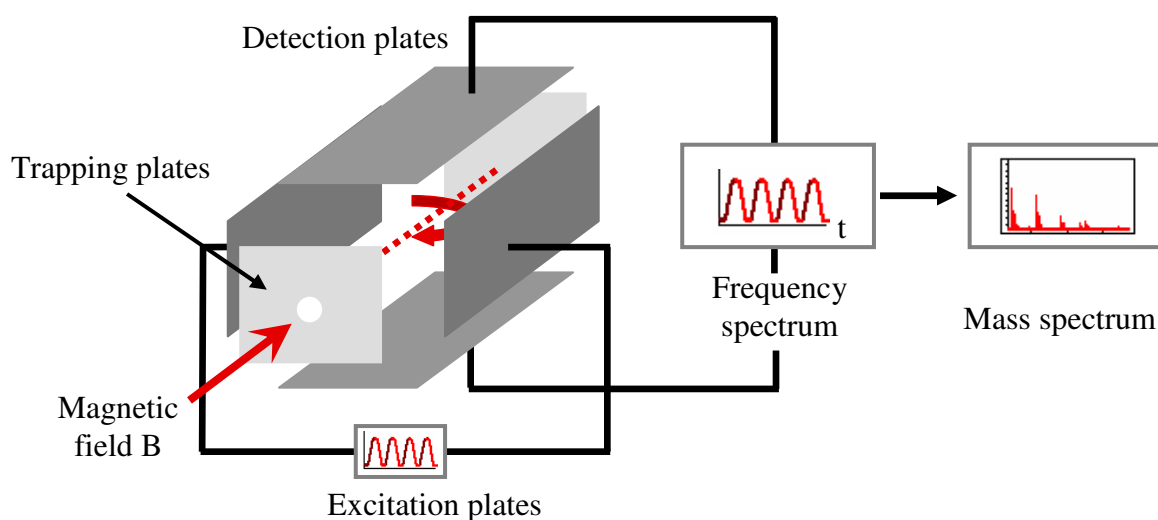


Figure 4.1. Schematic diagram of a cubic FT-ICR cell.

The magnetic field does not constrain ion motion along the direction of the applied magnetic field, a small potential is applied to the trapping plates in order to keep the ions confined within the ICR cell. As the ions are measured non-destructively, repeated measurements can be summed to improve the limit of detection. The pressure in an ICR cell should be extremely low to minimize ion-molecule reactions, space charge effects and collisions that damp the coherent ion motion.

4.3 ESI FT-ICR Mass Spectrometer

In Figure 4.2, a scheme of an FT-ICR instrument, used for our purpose, is shown with the electrospray ion source on the left side. Here the ions are produced and accumulated to ion packages in an octapole. These packages are subsequently transferred through an array of

tube and half-tube lenses into the cyclotron cell of the spectrometer. The cell is placed within a homogenous magnetic field of a super-conducting magnet. Field strengths currently employed range from 4.7 up to 12 T. The magnet used for our studies has a field strength of 7 T, which correlates to a ^1H -Lamor frequency of 300 MHz.

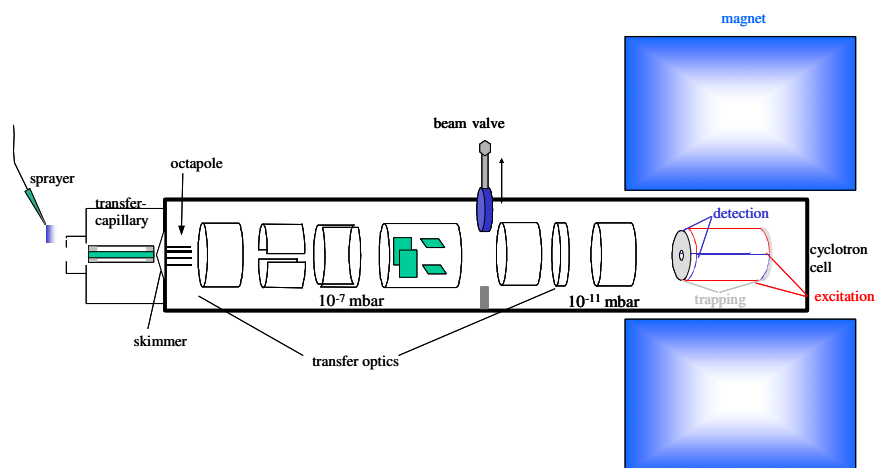


Figure 4.2. FT-ICR MS instrument with an electrospray (ESI) ion source (courtesy of Bruker Daltonic, Bremen, Germany).

4.4 Data Interpretation

The ultra-high resolution and ppm-level mass accuracy of FT-ICR MS allows precise identification of all elemental compositions present in vast complex petroleum samples. The FT-ICR mass spectrum of a gas oil aromatic neutral fraction contained peaks resulting from the resolution of ions having 358 distinct formulas over a mass range of ~ 42 Da unit [98]. C_3/SH_4 , $^{13}\text{C}/\text{CH}$, $^{13}\text{CH}/\text{N}$, CH_2/N , and other mass doublets were baseline-resolved, yielding typical mass measurement inaccuracies of ~ 1 ppm. However, for higher mass range (above 300 Da), as the number of possible elemental compositions increases tremendously and the resolution of the mass spectrometer decreases towards higher mass, special care has to be taken. Although FT-ICR MS provides the best in the sense of accuracy and resolution in mass measurement, it is practically impossible to assign the exact compositions of constituents found in fossil fuels without preliminary knowledge of constituent elements. Therefore, knowledge from previous investigations restricts the elements to C, H, N, S, and O in major constituents with V, Ni or Fe in minor quantity. But, in aromatic fractions, presence of metal elements is highly unusual leaving only the first group elements.

Henceforth, the data interpretation is developed considering the mentioned first group elements with their isotopes.

In addition, we have adopted a data reduction technique, which uses only a few indices, to group and identify compound series in a complicated high resolution mass spectrum [99]. The indices we choose are the nominal mass series (z^*), the Kendrick mass defect (KMD) and the accurate mass of the ionic species.

4.4.1 Nominal Mass Series (z^*)

It is practically impossible to analyze each individual molecular species in heavy petroleum fractions due to the presence of an enormous number of isomers. Therefore, analysis of a petroleum fraction is based on the groupings of the compound series according to their number of hydrogens relative to number of carbons, i.e. $C_nH_{2n+z}X$, where n is the number of carbon atoms, z is the “hydrogen deficiency” relative to mono-olefins or 1-ring naphthenes, X represents heteroatoms such as S, N and O. For instance, C_6H_6 , C_7H_8 , and C_8H_{10} are benzene, toluene, xylenes/ethylbenzene, respectively. This type of compounds are designated as $z = -6$ series. Another example is the $z = -10S$ series that includes benzothiophenes, methylbenzothiophenes and C_n -substituted benzothiophenes, etc. The concept of compound distribution in petroleum fractions as a function of z -series has been introduced over 40 years ago. The constituents of a fuel mixture can be grouped into 14 families according to their nominal molecular masses [100]. The nominal mass series, z^* , is defined for an ion as the remainder of its nominal mass divided by 14, minus 14, i.e. the modulus of $(\text{nominal mass}/14) - 14$. Each nominal mass yields a z^* value between -1 and -14. However, each nominal mass series, z^* , contains several compound types, e.g. the $z^* = -6$ contains compound types of $z = -6$ (benzenes), $-10S$ (benzothiophenes), -20 (phenylnaphthalenes), etc.

4.4.2 Kendrick Mass Defect (KMD)

In the early 1960's, *E. Kendrick* introduced a mass scale based on the mass of a methylene (CH_2) group as exactly 14 mass units, instead of 14.01565 on the $^{12}C = 12.00000$ scale to express organic mass spectral data [101]. The mass of an ion is converted from the ^{12}C mass scale to the Kendrick mass scale by the multiplication of a factor

14.00000/14.01565. For complex mass spectra, in order to extract information, the Kendrick nominal mass and the Kendrick mass defect (KMD) of individual ions are calculated. The Kendrick nominal mass (KNM) is obtained by rounding the Kendrick mass to the nearest integer. The Kendrick mass defect can be obtained as:

$$\text{KMD} = \text{KNM} - \text{Kendrick exact mass.} \quad \text{Eq. 4.16}$$

The advantage of the Kendrick mass scale over the IUPAC mass scale is that the members of a homologous series (namely, compounds with same heteroatom composition and number of rings plus double bonds, but different numbers of CH_2 groups) have identical Kendrick mass defect. The merit of the Kendrick scale over the ^{12}C scale is that the mass defect of each member in each series (same class and same type) will be same whereas all of the compounds in each series have a different mass defect in the ^{12}C scale. Moreover, the Kendrick mass scale provides another advantage over the ^{12}C scale for the determination of nominal masses. The limitation of correct-assignment in nominal masses by the ^{12}C scale is overcome by the Kendrick scale in the characterization of heavy hydrocarbons, which is the subject of discussion in the present work.

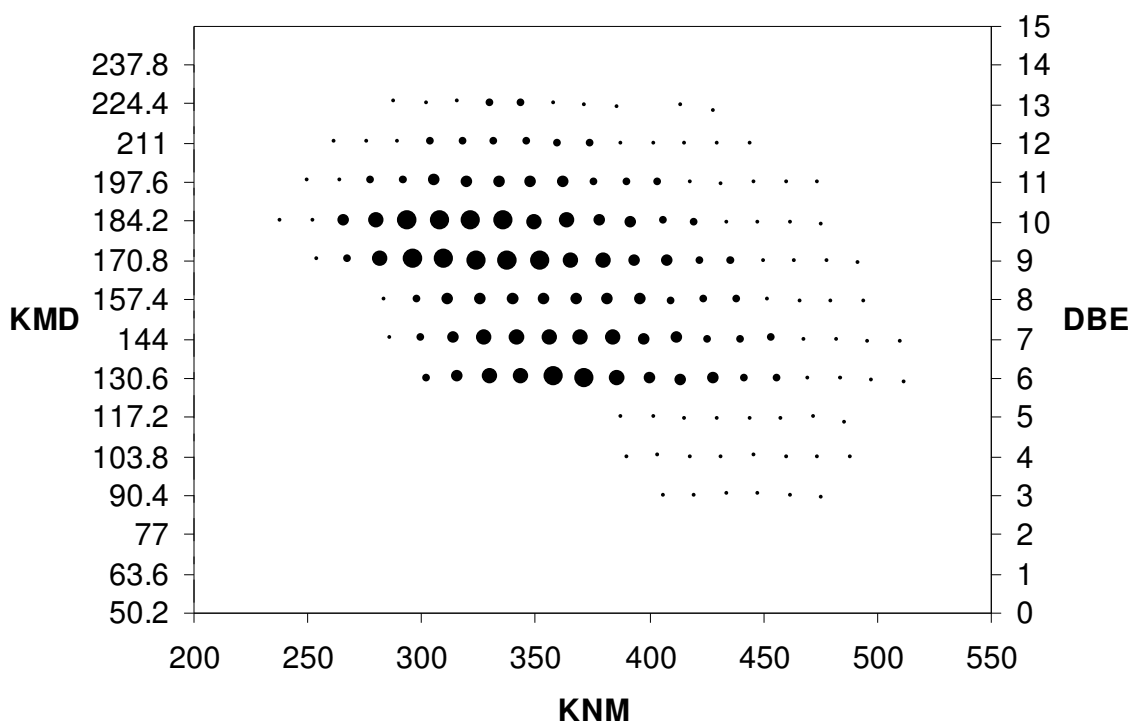


Figure 4.3. Kendrick plot of S1 compounds found in a vacuum gas oil.

As shown in Figure 4.3, the importance of such a display is not simply visual. At low mass (< 300 Da), it is possible to assign a unique elemental composition to each ion, based

on mass resolving power of 300,000. At higher mass, assignment based on mass measurement accuracy alone is no longer unique; however, starting from one unique mass assignment at low mass, the Kendrick plot quickly identifies the other members of a homologous alkylation series, so that mass assignments can extend with confidence to ~900 Da [102]. The second advantage of the Kendrick plot is that it quickly identifies other classes of compounds, as they will not fall on the horizontal lines specified for S1 class compounds in Figure 4.3.

In Figure 4.3, we have represented the right side of vertical scale with double bond equivalent (DBE) in addition to KMD on the left side. The relation between KMD and DBE can be illustrated in the following ways. For thiophene (C_4H_4S), KMD is found to be 90.4, which shows that six hydrogen atoms must be added to the compound to completely saturate it. Thus, two double bonds and one ring fulfill this requirement. For each addition of 13.4 to the KMD of thiophene, one more ring or one more double bond than in thiophene is indicated, and, conversely, each lowering of the KMD of thiophene by 13.4 indicates the deletion of one ring or one double bond. Thus, we can get information of different types of compounds in the thiophene series from the DBEs, which, of course, in their turn are derived from the KMDs.

4.4.3 Multiple Sorting

Here, a multiple sorting technique based on nominal mass series and KMD, to process high-resolution mass spectral data was used as reported in the literature [99]. Mass peaks with their accurate masses are first sorted by z^* and separated into 14 groups with z^* ranging from -1 to -14. Within the same z^* group, the mass peaks are further sorted by their KMD. The pre-sorting of masses with z^* before sorting according to KMD, although KMD has lot of potential in identifying series of compounds, can be explained in the following way. The difference in KMD between $C_{11}H_8O$ and C_7H_6S is only 0.5 millimass units. Therefore, it is quite difficult to distinguish between O- and S- containing compounds without introduction of any mistakes. But, the z^* for $C_{11}H_8O$ and C_7H_6S is -12 and -4 respectively. The z^* values are well separated to distinguish between O- and S-containing heterocycles. Therefore, masses are pre-sorted according to their z^* values prior to KMD sorting. A multiple sorting algorithm for data analysis is shown in Figure 4.4.

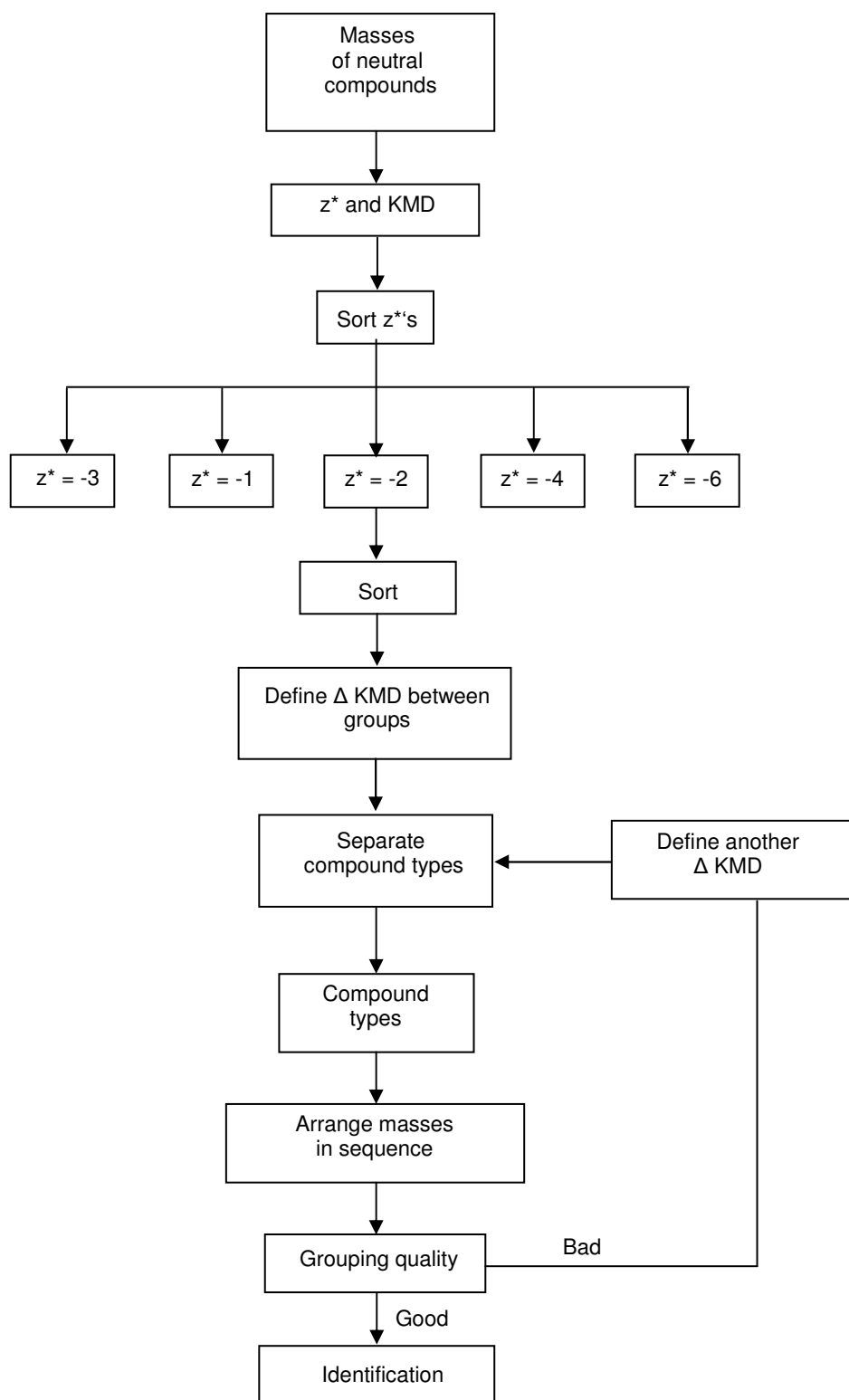


Figure 4.4. Flow diagram of multiple sorting algorithm [99].

4.5 Limitations of MALDI and ESI

The FT-ICR MS measurements with a MALDI ionization interface were done with the sulfur-enriched fraction from a VGO. Although there were some signals, they are of low intensity and do not correlate accurately with sulfur compounds. The low intensity can be due to a lower ionization efficiency of sulfur compounds by MALDI and variation in accuracy can arise from inadequate calibration of FT-ICR mass spectrometer.

Also, the same sample was analyzed with FT-ICR mass spectrometer interfaced with an ESI source. Here, it was not possible to observe any appreciable intense signals. This can be expected due to the lower efficiency of ESI for non-polar compounds, which are present in this fraction of VGO.

Therefore, in order to overcome the limitations by an ionization source like MALDI and ESI, derivatization techniques were followed. We have adopted two derivatization techniques, e.g. methylation and phenylation. The purpose of these derivatizations is to form ions from compounds that are not efficiently ionized by MALDI and ESI, before introduction of them to the ionization source. The formation of charged ions of sulfur compounds in the presence of a large number of PAHs that are not affected by the reaction increases the selectivity for PASHs and very much lowers the problems of space charge effects in the ICR cell.

4.6 Methylation of Sulfur Compounds

The selectivity of the methylation reaction towards sulfur aromatic compounds in the presence of PAHs, which are generally encountered during analysis of sulfur compounds in petroleum fractions, was verified with the reaction of model compounds [103]. The procedure adopted for methylation was described by *Acheson and Harrison* [104]. A mixture of standard compound (1 mmol) and methyl iodide (1.3 mmol) was dissolved in 3 mL of 1,2-dichloroethane (DCE). To it, a solution of 1 mmol silver tetrafluoroborate in 2 mL DCE was added. The reaction was allowed to run for 12 h at room temperature. Then, the silver iodide precipitate was removed by filtration and the DCE was evaporated under a stream of nitrogen. The obtained sulfonium salts were dried under vacuum before mass spectrometric analysis. Three standards, namely benzothiophene, dibenzothiophene and

4,6-dimethyldibenzothiophene, were reacted under the above conditions in order to check the efficiency of methylation reaction.

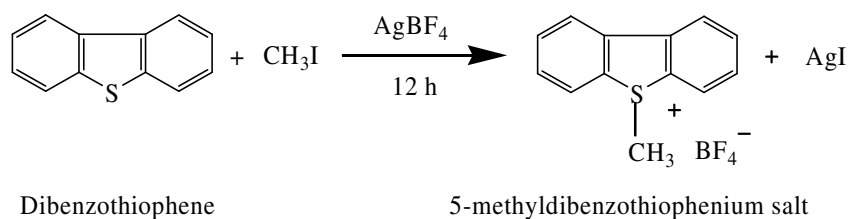


Figure 4.5. Methylation of dibenzothiophene.

4.7 Phenylation of Sulfur Compounds

The procedure for the phenylation was reported in the literature [105]. A mixture of standard compound (1 mmol) and diphenyliodonium triflate (1.3 mmol) was dissolved in 3 mL of DCE. To it, 0.01 mmol of cupric acetate was added. The reaction was allowed to continue for 48 h at room temperature. After that, the filtrate was collected and the solvent was evaporated under nitrogen. Three standards, namely benzothiophene, dibenzothiophene and 4,6-dimethyldibenzothiophene, were reacted under the above conditions in order to check the efficiency of phenylation reaction.

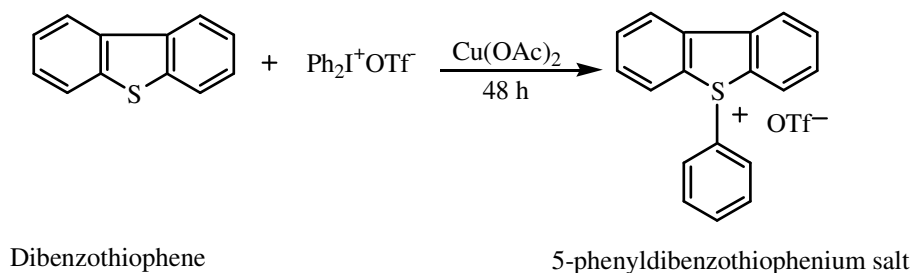


Figure 4.6. Phenylation of dibenzothiophene.

4.8 MALDI FT-ICR MS of Derivatized Sulfur Compounds

The PASH fraction of a VGO was isolated by ligand exchange chromatography on a Pd(II)-bonded phase as described in the Chapter 8. The fraction was divided into two parts, one part was methylated, and other part was phenylated as described in the earlier sections. For the methylated sample, 15.02293 is subtracted from the masses obtained from FT-ICR mass spectrometry in order to convert them into neutral masses. This number corresponds to the mass of the CH_3^+ ion. Then the neutral masses are sorted according to the data interpretation procedure (Section 4.4). In this sample, a large number of S1 compounds were identified. The masses observed ranged from 250 Da to ~600 Da. The double bond equivalents range from 3 to 14.

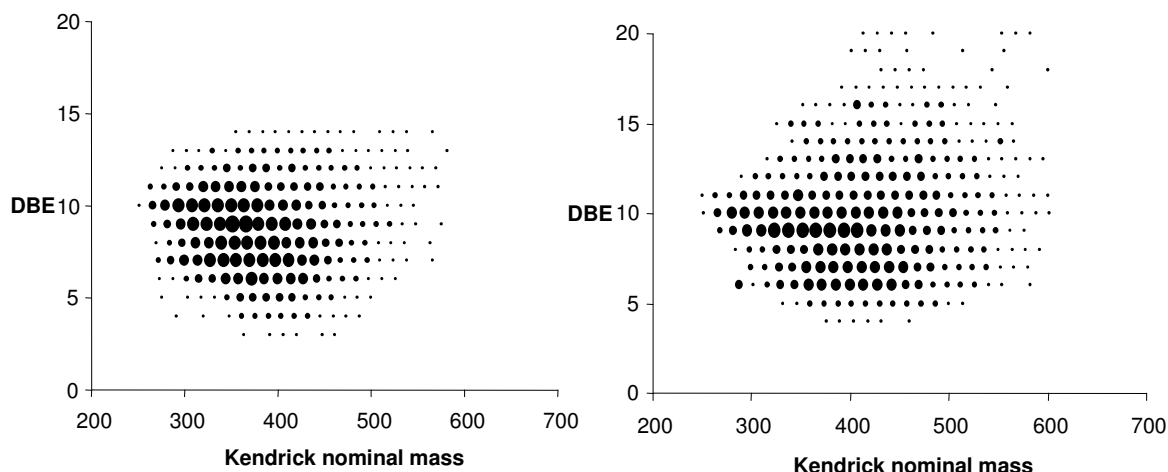


Figure 4.7. Kendrick plots of S1 compounds of a VGO from two derivatizations; (left) methylation and (right) phenylation

For the phenylated sample, similarly the masses obtained are converted into their neutral masses by subtracting a factor of 77.03868. The neutral masses obtained are further sorted according to the Kendrick scale, which facilitates the assignment of a molecular composition to the constituents. The similarity observed between the two derivatization is that abundant masses fall in the range of 250-450 Da and the more intense DBEs are in the range of 6 to 12. However, in case of phenylation, the highest detectable DBE was 20 whereas for methylation it was only 14 without significant change in the mass range. As the intensity of DBE 15 to 20 is low compared to other DBEs, this effect may be originating from extraneous factors like different concentration of the samples. In both the cases, the intense mass range falls between 250 to 500 Da. In addition, the distribution pattern remains

almost same among different DBEs and the intense series are represented by DBE 9 and 10. The data can be further analyzed in detail through the generation of pseudograms with the relative intensity of masses obtained from mass spectrometer. The pseudograms, generated for each DBE separately, give the distribution pattern of alkylated compounds in a particular group of compounds.

4.9 Generation of Pseudograms

The pseudograms were generated by the data obtained using the following Gaussian function:

$$y(x) = a \cdot \exp(-(((x-b)/c)^2)), \quad \text{Eq. 4.17}$$

where a , b and c represent the relative intensity of the mass of interest, this particular mass and the selected standard deviation, respectively. Y values were generated using the above equation in an Excel spreadsheet. In petroleum research, gas chromatography has been thoroughly used in the characterization of high molecular weight aromatic compounds although this technique is not the most appropriate one for large molecules. Therefore, pseudograms, as we have named, generated from MS data can aid to compare the previous data obtained from gas chromatography during last decades. With this mode of presentation, the alkyl distribution patterns of one particular type of compounds, if there is any difference, in different variety of samples can be clearly observed. This visualization technique has been further applied in the following chapters.

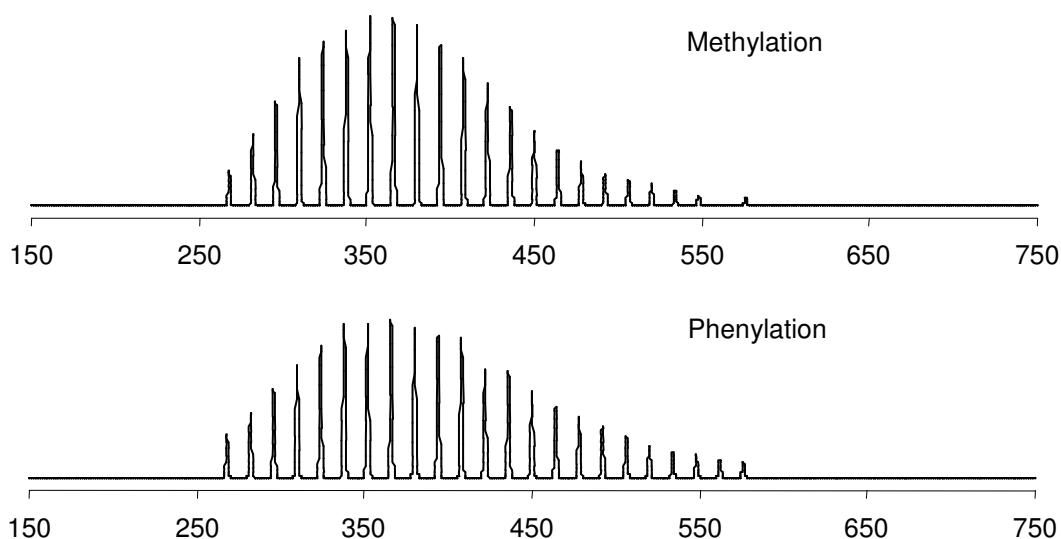


Figure 4.8. Distribution patterns of alkylated dibenzothiophenes (DBE 9) as determined by MALDI FT-ICR MS for a VGO.

Here, the distribution pattern of alkylated dibenzothiophenes determined from both the derivatizations is found to be very similar.

4.10 ESI FT-ICR MS of Derivatized Sulfur Compounds

The PASH fraction of a VGO obtained from Pd(II)-bonded phase was divided into two parts (same VGO to that of Chapter 8). One part was selectively methylated with methyl iodide whereas other part was phenylated with diphenyliodonium triflate as described in the earlier sections. The masses obtained as methylated or phenylated were converted to neutral masses. The neutral masses obtained were converted to Kendrick masses and the resulting Kendrick masses were further processed using several multiple sorting procedures as described in the Section 4.4 in order to assign elemental compositions of sulfur compounds.

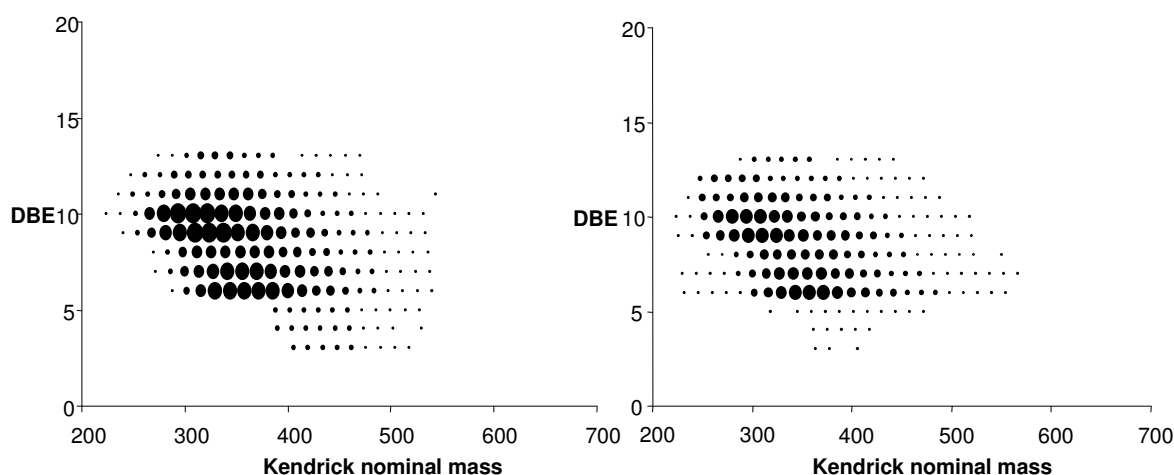


Figure 4.9. Kendrick plots of S1 compounds of a VGO from two derivatizations; Methylation (left) and phenylation (right).

In both cases (methylation and phenylation), the highest DBE observed was 13. The DBE series covers from 3 to 13. The highest mass goes up to ~550 Da. The range of DBE and mass is comparable to that obtained from MALDI FT-ICR MS. The distribution pattern of alkylated compounds at different DBEs is also comparable to that of MALDI FT-ICR MS.

The phenylation works similarly to that of methylation. Here, the highest detectable DBE was 13 for both the cases. The most intense masses cover between 250 to 450 Da. The derivatization techniques complement each other with respect to mass range, DBE range and

the distribution pattern of alkylated S1 compounds at different DBEs. Also, for crucial investigation, pseudograms were produced for alkylated dibenzothiophenes for both derivatization techniques.

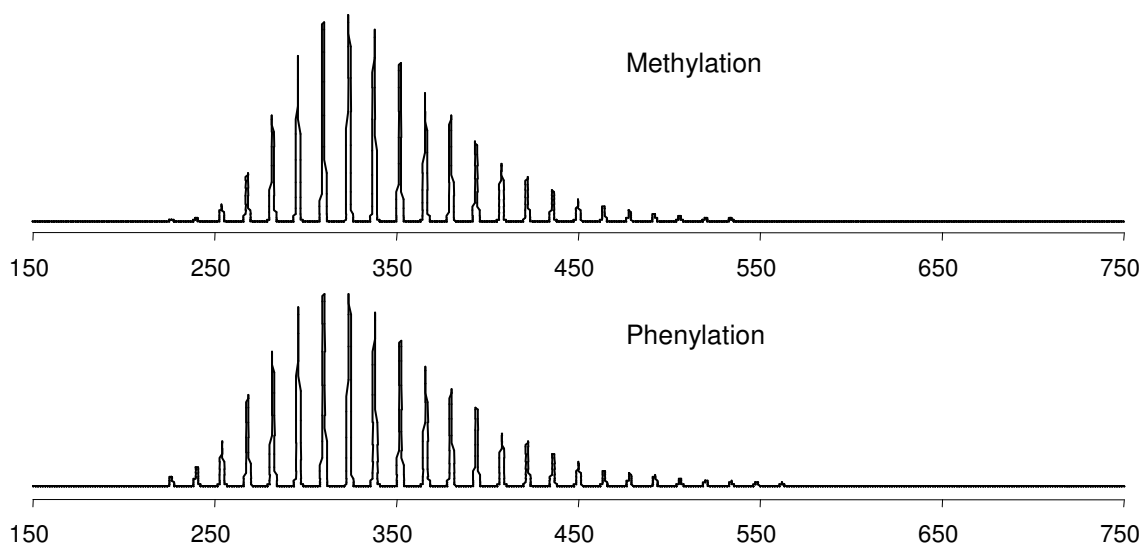


Figure 4.10. Distribution patterns of alkylated dibenzothiophenes as determined by ESI FT-ICR MS.

The distribution pattern of alkylated dibenzothiophenes is almost identical for both derivatization techniques. This is a result of the similar reactivity of dibenzothiophenes to both phenylation and alkylation reactions. Therefore, in principle, both the derivatization techniques are quite efficient for production of charged ions in sulfur compounds.

4.11 Summary

In principle, both the ionization techniques (ESI and MALDI) work well with the derivatized compounds. However, the similarity in distribution pattern of alkylated dibenzothiophenes among two derivatization techniques was more comparable for ESI to that of MALDI. From our experience, it is found that the phenylation reaction proceeds slowly with sterically hindered dibenzothiophenes compared to that of methylation. This limitation makes the methylation reaction the preferred derivatization and was used with all the petroleum fractions, investigated during this dissertation work, before being characterized by ESI FT-ICRMS.

5. Pattern of Sulfur Heterocycles in Vacuum Gas Oils

Fluid catalytic cracking, hydrocracking, and catalytic reforming, secondary petroleum refinery processes, are mostly used in order to sustain the supply of lighter and middle distillates, used as a direct source of energy, from heavy distillates such as vacuum gas oils (VGOs). However, the presence of heteroatoms (N and S) in vacuum gas oil plays a major role, acting as poisons for catalysts. Sulfur has the major contribution towards reduction of catalytic activity, being the most abundant atom out of all heteroatoms. Therefore, removal of sulfur is highly desirable in order to make the above-mentioned processes more efficient and effective. This development has also been driven by the need to comply with strict legislation in many countries with respect to the sulfur content of fuels that has as a goal to limit the sulfur concentration to 10 $\mu\text{g/g}$.

The most common and widely used method for removal of sulfur is hydrodesulfurization (HDS) which operates at high hydrogen pressure and at elevated temperature. The reactivity of compound classes towards HDS process in gas oil follows: Non-thiophenic sulfur compounds > thiophenic sulfur compounds [106]. HDS of VGO is more difficult compared to lighter distillates [107] which can be expected due to the presence of more thiophenic compounds with variety of aromatic network and alkyl groups substituted at different possible and probable positions. In lighter distillates e.g. diesel, the rate of desulfurization for alkylated benzothiophenes is higher than that of alkylated dibenzothiophenes and simultaneously certain positions (4-, 6- and 1-) with alkyl groups of dibenzothiophenes are more refractory to the HDS process [27,28,30,108]. Due to limitation in volatility for high molecular weight compounds, it is impossible to analyze high molecular weight polycyclic aromatic sulfur heterocycles (PASHs) present in vacuum gas oils by gas chromatography. Thus, many investigations were carried out using liquid chromatography as a separation technique and mass spectrometry as an identification tool to reveal patterns of sulfur aromatics in higher boiling fractions. Although research in this field has crossed half a century, it remains a challenging task to find one satisfactory method for the characterization of a large number of PASHs of high molecular weight. The detailed structural information of PASHs will help in the development of better catalysts required for the HDS process.

In the present work, three vacuum gas oils of different boiling ranges and different sulfur content were included for the investigation. The aim was to establish the correlation of the distribution of sulfur compounds (in both alkyl carbons and size of aromatic rings) originating from the vacuum gas oils of different boiling ranges. The analytical protocol involves isolation of the aromatic fraction, separation on a Pd(II)-bonded phase, and characterization of the sulfur compounds with FT-ICR MS.

5.1 Experimental Section

5.1.1 Sample

Three vacuum gas oils from Iranian Light crude oil of three boiling ranges were supplied from Institut Français du Pétrole, Vernaison, France. The boiling ranges were 390-460 °C, 460-520 °C and 520-550 °C and the sulfur content was 1.12 wt %, 1.33 wt % and 1.77 wt %, respectively. Chemicals for synthesis and HPLC grade solvents were from Sigma-Aldrich (Taufkirchen, Germany). The aromatic fractions from all the three vacuum gas oils were isolated as follows. About 1-1.5 g of each sample was taken for the analysis. The sample was loaded on a glass preparative column (200 mm x 28 mm) filled first with 20 g of silica gel and then with 35 g of alumina. Before using silica and alumina as adsorbents, both were activated at 180 °C for 16 h separately. The adsorbents were only once used. The aliphatics were collected using 120 mL n-heptane as eluent and the aromatics were eluted by 360 mL of a 2:1 (v:v) mixture of n-heptane and toluene. The detailed analysis scheme is presented in Figure 5.1.

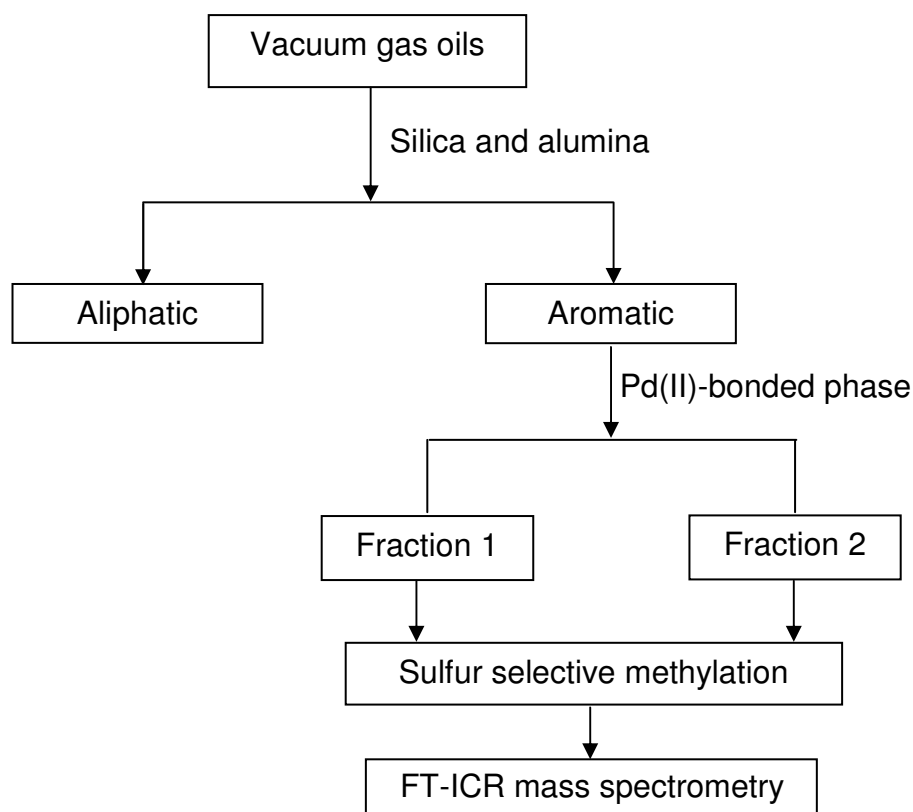


Figure 5.1. Analysis scheme for sulfur aromatics present in vacuum gas oils.

5.1.2 Ligand Exchange Chromatography

The stationary phase, a Pd(II)-containing complex based on 2-amino-1-cyclopentene-1-dithiocarboxylate covalently bonded to silica gel, used for ligand exchange chromatography, was synthesized with 10 μm LiChrosorb Si 100 (Merck, Darmstadt, Germany) as described in the literature [109-111]. About 10 g of Pd(II)-bonded silica gel was packed into a stainless steel column (250 mm x 8 mm) with the slurry method at a pressure of 350 bar using a Knauer pneumatic pump. Methanol was used for making the slurry and the same solvent was used for the column filling. Then, the packed column was washed with methanol, dichloromethane and cyclohexane successively. After washing with the three solvents, the selectivity of the column was tested with a standard mixture containing benzothiophene, dibenzothiophene, and benzonaphthothiophene. After that, the Pd(II)-bonded column was used for the fractionation of real-world samples. The first fraction (Fraction 1) was eluted with cyclohexane:dichloromethane (7:3 v/v) for 15 minutes and the second fraction (Fraction 2) was eluted after addition of 0.5 % isopropanol to the previous mobile phase. The flow rate maintained throughout the whole separation was 3 mL/min.

5.1.3 Sulfur Selective Methylation

About 50 mg of the aromatic fraction from each vacuum gas oil was separated on a Pd(II)-bonded column (250 mm x 8 mm) into two fractions (called Fraction 1 and Fraction 2). To each fraction, an excess of methyl iodide (50 μ L) and silver tetrafluoroborate (40 mg) was added in 3 mL of 1,2-dichloroethane (DCE). The mixture was allowed to run for 48 h at room temperature to ensure the complete methylation of all sulfur compounds in the sample. Then, the filtrate was collected and the solvent was evaporated by a stream of nitrogen to obtain methyl thiophenium salts [103].

5.1.4 High-Resolution Mass Spectrometry

Mass spectra were acquired using an APEX III Fourier transform ion cyclotron resonance mass spectrometer (Bruker Daltonics, Bremen, Germany) equipped with a 7 T actively shielded super conducting magnet and an Agilent ESI source. The samples were introduced in a 1:1 (v/v) solution of dichloromethane/acetonitrile and injected in the infusion mode with a flow rate of 2 μ L/min detecting positive ions. The spray voltage was maintained at 4.5 kV. After ionization, the ions were accumulated for 0.5 s in the octapole before transfer to the cyclotron cell. For a better signal-to-noise ratio, at least 64 scans were accumulated. Internal and external calibrations were done using a mixture of the Agilent electrospray calibration solution of masses 622.02896 and 922.00980 with the addition of indolacrylic acid of masses 397.11589 $[2M+Na]^+$ and 584.17923 $[3M+Na]^+$ covering the whole range of masses in the samples. All the measurements by FT-ICR mass spectrometer were performed in collaboration with Max-Planck-Institute of coal research, Mülheim, Germany.

5.1.5 Data Analysis

All the data obtained from the mass spectrometer were imported into an Excel spreadsheet. Each signal in the mass spectrum corresponds to the methylated form of parent masses. In order to assign elemental composition of components present in vacuum gas oils, all the masses, measured as $[M+CH_3]^+$ were converted to neutral masses by subtracting 15.02293 from the measured masses. Then IUPAC masses were converted to the Kendrick mass scale [101] and Kendrick masses were further sorted according to the procedure explained in the Chapter 4.

5.2 Results and Discussion

Following the separation on the Pd(II) column, the PASHs collected in the two fractions were methylated and investigated by FT-ICR MS. The number of PASHs in Fraction 1 was less compared to Fraction 2 for each boiling range, as is illustrated in Figures 5.2 and 5.3, but it increased with increasing boiling temperature. The complexity of the sulfur-enriched Fraction 2 remains very high even after some PASHs have been separated into Fraction 1 (Figure 5.3). The number of assigned S1 compounds (compounds containing one sulfur atom) from Fraction 1 was 11, 94 and 106 in the three boiling ranges in increasing order of distillation temperature, and the number of S1 compounds in Fraction 2 was 188, 225 and 281, respectively. This corroborates the trend of an increasing number of S1 members with increasing boiling temperature as was observed by low-voltage electron ionization FT-ICR MS [77], but in this study the number of compounds identified is significantly higher than in the literature one.

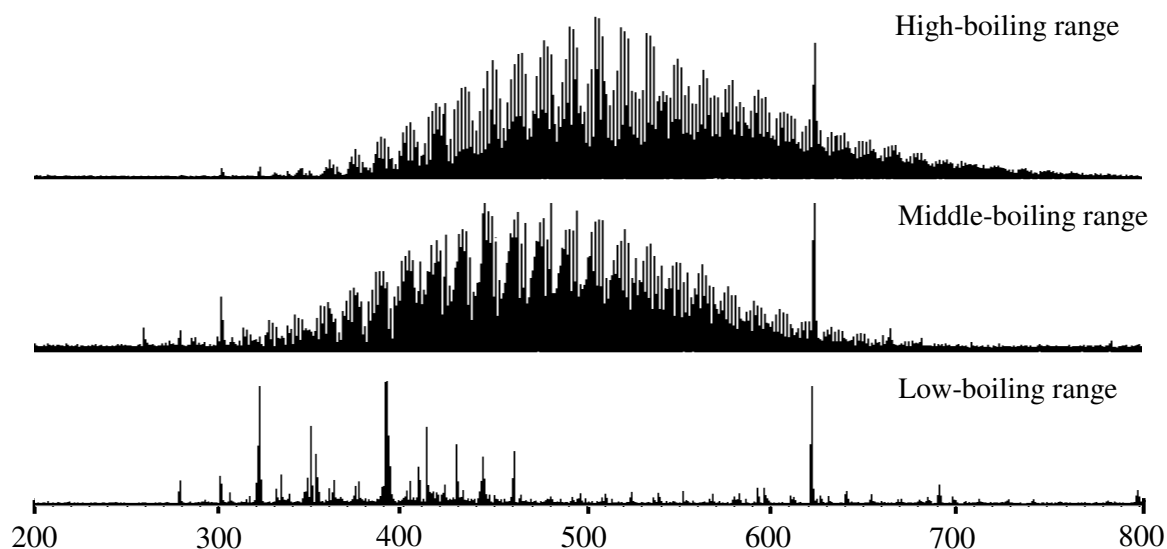


Figure 5.2. ESI FT-ICR mass spectra of Fraction 1 from Pd(II)-bonded stationary phase of three VGOs of different boiling ranges.

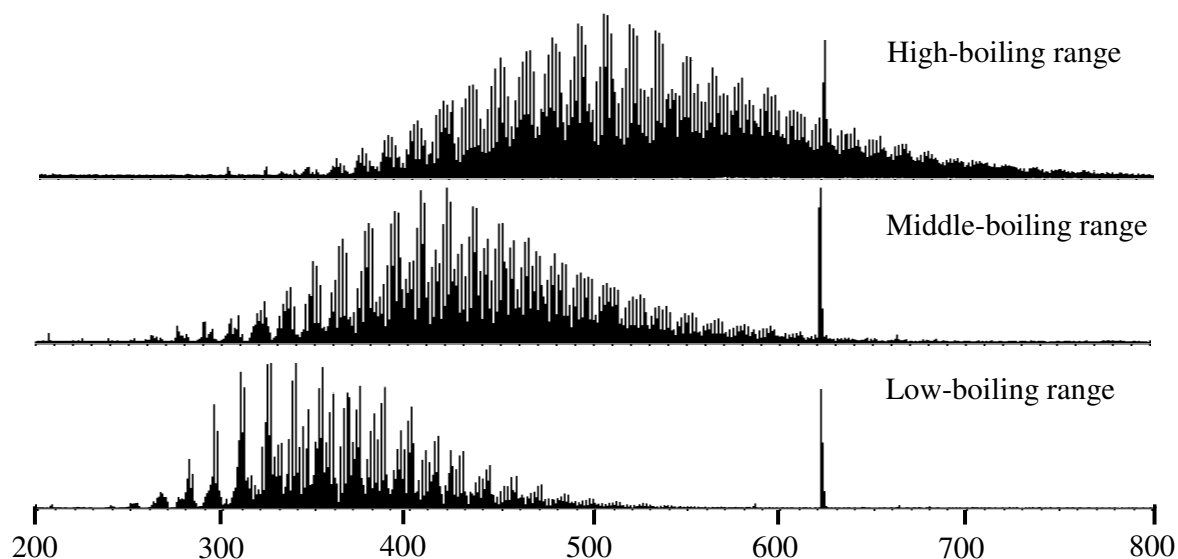


Figure 5.3. ESI FT-ICR mass spectra of Fraction 2 from Pd(II)-bonded stationary phase of three VGOs of different boiling ranges.

In order to get more information of molecular weight distribution patterns at a glance, both number-average molecular weight, M_n , and weight-average molecular weight, M_w for S1 compounds in the second fractions of all three VGOs were calculated as described in the literature [112].

$$M_n = \frac{\sum N_i M_i}{\sum N_i} \quad \text{Eq. 5.1}$$

$$M_w = \frac{\sum N_i M_i^2}{\sum N_i M_i}, \quad \text{Eq. 5.2}$$

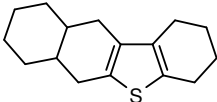
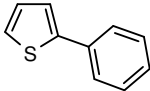
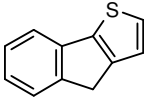
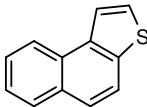
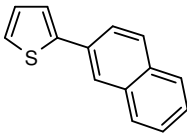
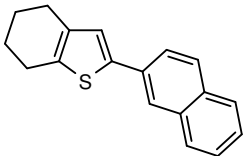
where N_i is the relative abundance of ions of mass M_i

The mass distribution pattern for the low-boiling range ($M_n/M_w = 358/366$) was centered at about ~360 Da, for the middle one (423/434) at about ~430 Da, and for the higher one (508/519) at about ~510 Da. The information obtained from the above results show the expected trend in shifting centered-mass toward the higher side with increase in boiling range. This is a result of two factors, namely of a larger number of carbon atoms in the substituents and of larger ring systems being present in the higher-boiling fractions. This structural information can be deduced from the DBE and from the retention on the Pd(II) phase and will be discussed.

5.2.1 Low-Boiling Range VGO

The number of S1 compounds in Fraction 1 was negligible and their relative abundance was equally low (Figure 5.2). DBE 3, 4 and 5, found in Fraction 1, can correspond to thiophenes, naphthenothiophenes and cyclopentenothiophenes with knowledge from retention properties of some model thiophenic compounds on Pd(II)-bonded phase [113]. The compounds in Fraction 1 showing DBE 6 and 7 with a mass range from about 350 Da to 450 Da probably are not benzothiophenes as all our previous experience points to the conclusion that this group of PASHs elutes in Fraction 2 on Pd(II)-bonded phases [113]. Therefore, the sulfur aromatics in this fraction may be suggested to belong to another class of compounds such as dodecahydrobenzonaphthothiophenes with DBE 6 and phenylthiophenes of DBE 7 (Table 5.1).

Table 5.1 Examples of typical sulfur-containing compounds eluting in Fraction 1 on Pd(II) phase.

Possible structure	DBE	Compound type	Nominal mass
	6	Dodecahydrobenzonaphthothiophene	246
	7	Phenylthiophene	160
	8	4H-Indeno[1,2- <i>b</i>]thiophene	172
	9	Naphtho[2,1- <i>b</i>]thiophene	184
	10	2-(2-Naphthyl)thiophene	210
	11	2-(2-Naphthyl)tetrahydrobenzothiophene	264

The number of S1 compounds in Fraction 2 (Figure 5.3) was considerably higher than in Fraction 1 (Figure 5.2). Here the masses range from 225 Da to 550 Da with DBE 13 being the highest. We were able to detect some compounds of DBE 3, 4 and 5 in minute amounts, as shown in the Figure 5.4, although these parent groups mainly eluted in Fraction 1. The mass range was between 390 Da and 530 Da for all three DBEs indicating the presence of alkylated thiophenes, alkylated naphthenothiophenes and alkylated cycloalkenothiophenes. It is not yet known what kind of substitution can be expected for such compounds that would lead them to be found in this fraction so that synthetic standards cannot be prepared rationally.

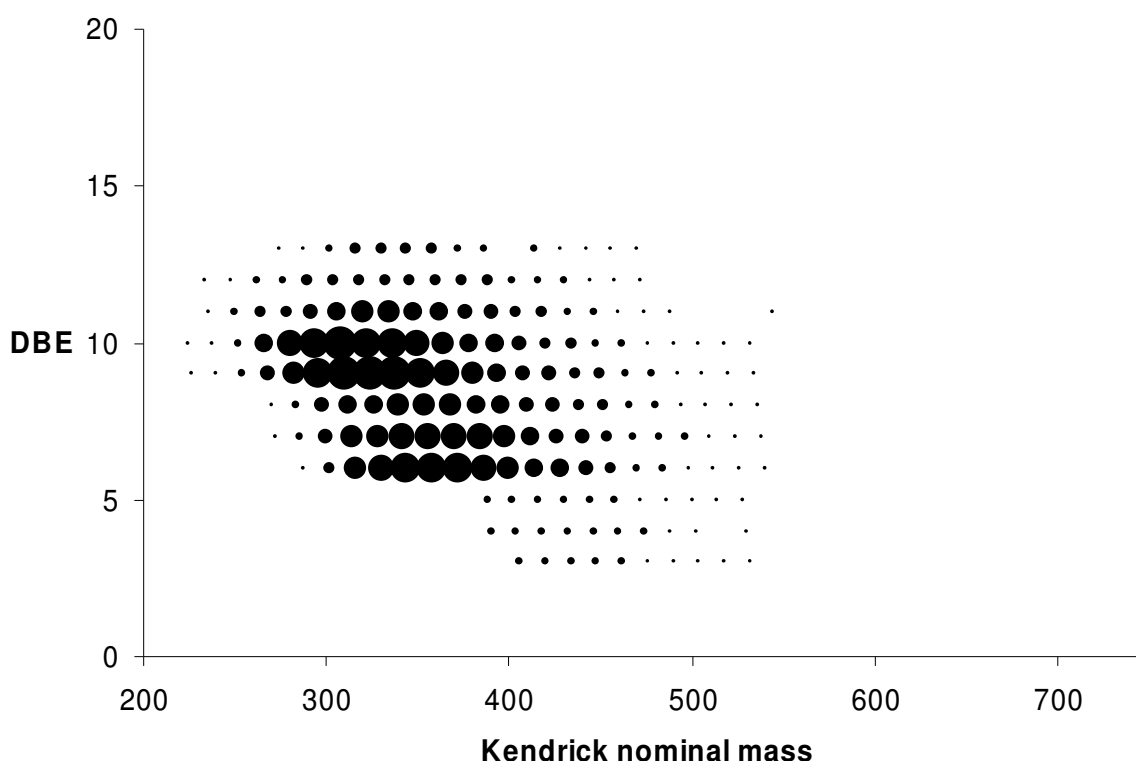


Figure 5.4. Kendrick plot of Fraction 2 of low-boiling fraction.

DBE 6 with masses from 288 Da to 540 Da represents major constituents and it is reasonable to postulate that they correspond to benzothiophenes with alkyl substituents from 11 to 29 CH_2 units. The intense peaks in the mass range 300 Da to 400 Da may indicate a high abundance of those alkylated compounds in the sample although the relative abundance of ions in mass spectra does not necessarily correlate exactly with the relative abundance of the compounds in the original mixture. This is a consequence of the methylation used for producing the ions that may run with somewhat different yields depending on the substitution pattern. DBE 7 can correspond to tetrahydrodibenzothiophenes with 6 to 25

alkyl carbons. The abundant masses fall in the same mass range as that of the benzothiophene series.

The next higher row of homologues shows a DBE of 8 and can correspond to indenothiophenes (Table 5.1) and indanylthiophenes or compounds from the DBE 6 and DBE 7 rows that possess two and one more naphthenic rings, respectively. The masses range from 270 Da to 536 Da and the intensity of the representatives of this class is less, as indicated in Figure 5.4. DBE 9 most probably represents alkylated dibenzothiophenes (or naphthothiophenes) with 3 to 25 alkyl carbon atoms. The relative abundance is higher than that of the previous DBEs. DBE 10 can represent acenaphthenothiophenes or dibenzothiophene with one naphthenic ring and contains compounds with masses between 224 Da and 532 Da. Phenylbenzothiophenes also display this DBE. The relative intensity of the ions in dependence of the mass is very similar to that of the DBE 9 series.

Acenaphthylenothiophenes, phenylbenzothiophenes with one naphthenic ring or two naphthenic rings attached to dibenzothiophene can represent the DBE 11 series with masses of 236 Da to 544 Da. The row at DBE 11 can be assigned to acenaphthylenothiophenes with 2 alkyl carbons to 24 alkyl carbons. Benzonaphthothiophenes are one of the most probable series for DBE 12 and they cover masses from 234 to 472 Da. That means that compounds possessing from 0 to 17 alkyl carbon atoms are detected. The next, and highest, DBE for this fraction is 13 and can represent naphthenophenanthrothiophenes or benzonaphthothiophenes with one naphthenic ring with a mass range from 274 Da to 470 Da.

As the DBE increases, the number of possible parent structures increases sharply, making it more difficult to identify the basic ring structure. In previous investigations [114] on VGOs, GC/MS showed that benzothiophenes, dibenzothiophenes and benzonaphthothiophenes are major classes of compounds so that we are confident suggesting that DBE 6, 9 and 12 are formed, at least predominantly, by these compounds.

5.2.2 Middle-Boiling Range VGO

There are many more S1 compounds in Fraction 1 of the VGO of the middle-boiling range compared to the low-boiling VGO discussed above. The range of DBEs goes from 3 up to 9 with masses from about 250 to 550 Da. The DBE 5 and 6 series show the maximum

numbers of compounds with masses from about 300 to 550 Da. The probable structures in this fraction can be assigned on the basis of the liquid chromatographic retention on the Pd(II)-bonded stationary phase as shown in Table 5.1. DBE 6, 7, 8 and 9 are shown by dodecahydrobenzonaphthothiophenes, phenylthiophenes, 4*H*-indeno[1,2-*b*]thiophenes, possibly naphtho[2,1-*b*]thiophenes, 2-(2-naphthyl)thiophenes and 2-(2-naphthyl)tetrahydrobenzo- thiophenes as representatives of the more probable structures. In Fraction 2, it was possible to observe a larger number of members in addition to a significant change in the distribution pattern along different DBEs compared to that of the low-boiling VGO (Figure 5.5). Not only is the highest observed DBE now 15, compared to 13 of the low-boiling VGO, but the relative abundance pattern across the DBE rows has been shifted towards higher numbers. The dominating series are formed by DBE 9, 10, and 11 followed by 6 and 7.

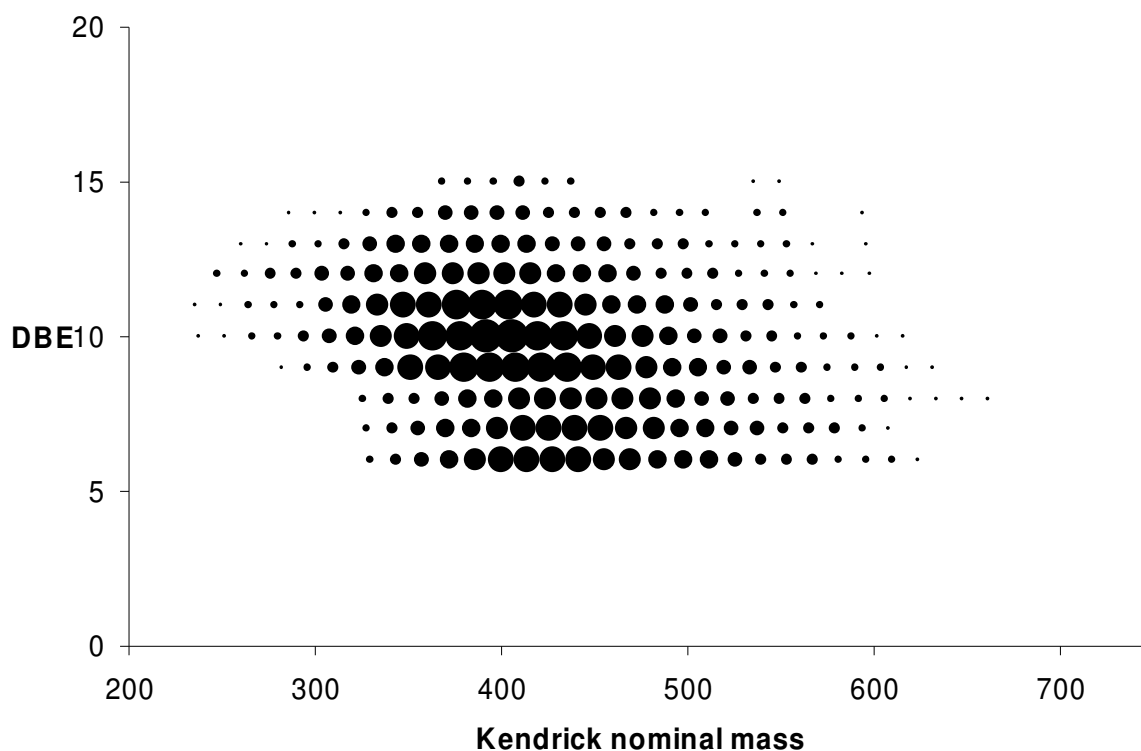


Figure 5.5. Kendrick plot of Fraction 2 of middle-boiling fraction.

With an increase in boiling range, the complexity of the aromatic systems increases both with respect to higher mass (about 650 Da) and the variety of aromatic parent structures (DBE attains values from 6 to 15). As explained in the earlier section, DBE 6 can be formed by alkylated benzothiophenes, now with 14 to 35 alkyl carbons with the highest abundance

in the mass range from 350 Da to 450 Da. In the dibenzothiophene series the lowest mass compound contains 13 CH₂ units, four more than that in the low-boiling fraction, and the highest mass compound shows 32 CH₂ units, seven more than that in the low-boiling VGO. The benzonaphthothiophenes of DBE 12 are represented by compounds with from one to 26 alkyl carbons.

In this fraction, DBE 13 is more abundant compared to previous VGO with masses going up to 596 Da. The next two higher DBEs, i.e. 14 and 15, were not detected in the low-boiling fraction. Pyrenothiophenes with 2 to 24 alkyl carbons are examples for compounds that can be assigned to the DBE 14 series. The highest DBE 15 for this fraction is only weakly represented with masses up to 550 Da.

5.2.3 High-Boiling Range VGO

In Fraction 1, the number of assigned S1 compounds was not significantly larger than that of the middle-boiling fraction but the distribution pattern along the DBE rows was remarkably different. The compounds extend from DBE 6 to DBE 13 with masses from 280 Da to about 530 Da. The most abundance series comprises compounds of DBE 9, 10 and 11. The most abundant masses in these DBEs fall in the range of about 340 Da to 500 Da. Here also the trend of shifting masses toward higher DBEs with an increase in boiling temperature is observed. DBE 12 and 13 can correspond to series of compounds of thiophenes attached to aromatic or naphthenic compounds of DBE 9 and DBE 10 respectively in a non-condensed way. At such higher DBEs, it is practically impossible to assign aromatic ring size without a further fractionation on the basis of aromatic ring size as no mass spectrometer providing only molecular mass information is able to distinguish between isomers of naphthenic and aromatic rings.

In Fraction 2, the initial member detected represents mass of 316 Da having DBE 13, where as mass of 236 Da with DBE 11 and 224 Da with DBE 10 represent initial mass of middle- and low-boiling fractions. The relative abundance of compounds shifts to a great extent toward higher DBEs. Figure 5.6 shows that the most intense series are formed by the PASHs of DBE 9 through 13 followed by DBE 6, 7 and 8. The highest DBE in this boiling range is 17 with a mass range of about 300 Da to 750 Da. At higher boiling ranges, the small

increase in boiling temperature is reflected in a significant change in higher masses with DBE.

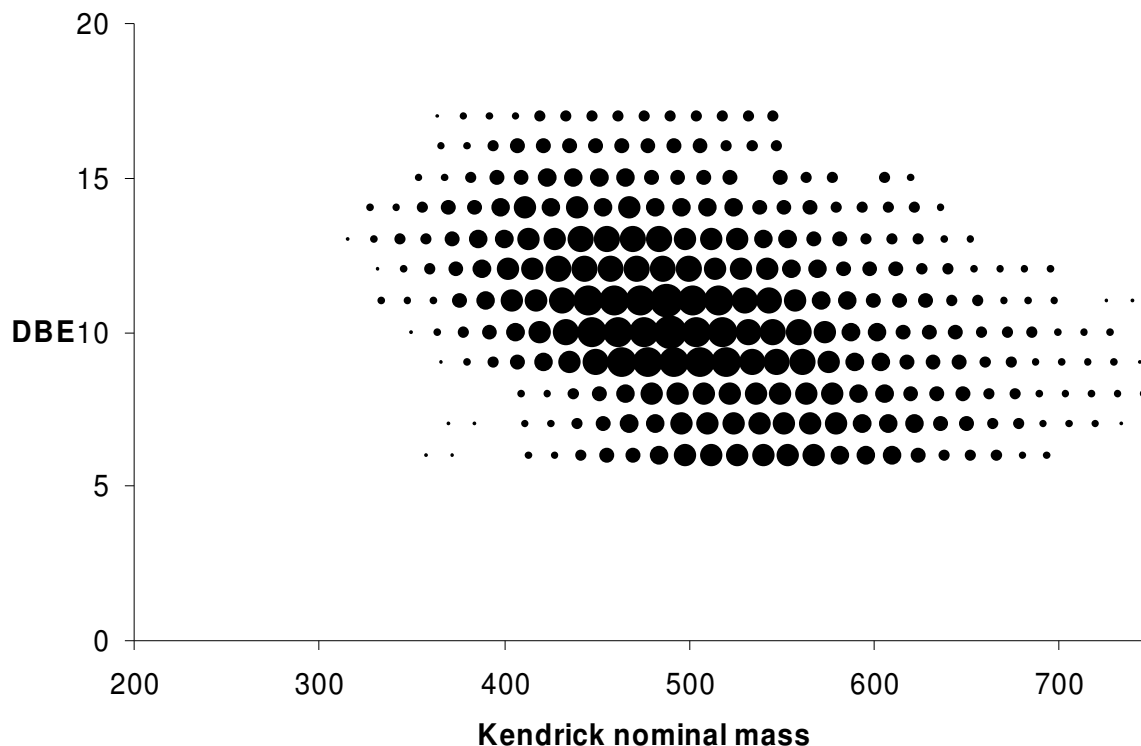


Figure 5.6. Kendrick plot of Fraction 2 of high-boiling fraction.

Benzothiophenes with 16 to 40 alkyl-chain carbon atoms are observed compared to 14 to 35 in the middle-boiling range. In this fraction dibenzothiophenes contain from 13 to 40 alkyl carbons. The DBE 10, 11 and 12 series comprise masses from about 350 Da to 720 Da. DBE 16 can be represented by cholanthrenothiophenes or compounds containing one dibenzothiophene and one naphthalene ring system with between 5 and 18 alkyl carbons. Benzopyrenothiophenes with 5 to 17 alkyl carbons are but one example for compounds of DBE 17. For more information on structure of sulfur-containing aromatic compounds that are generally encountered in fossil fuels are presented in Table 6.1.

The distribution pattern of alkylated benzothiophenes, at DBE 6, present in different boiling ranges can be clearly observed in Figure 5.7. In order to realize the significant change in distribution pattern at a glance, we have presented pseudograms of all the three vacuum gas oils for DBE 6. For the said reason, the pseudograms were generated using nominal masses and relative intensity, obtained from mass spectrometer, with a Gaussian function as described in the Chapter 4.

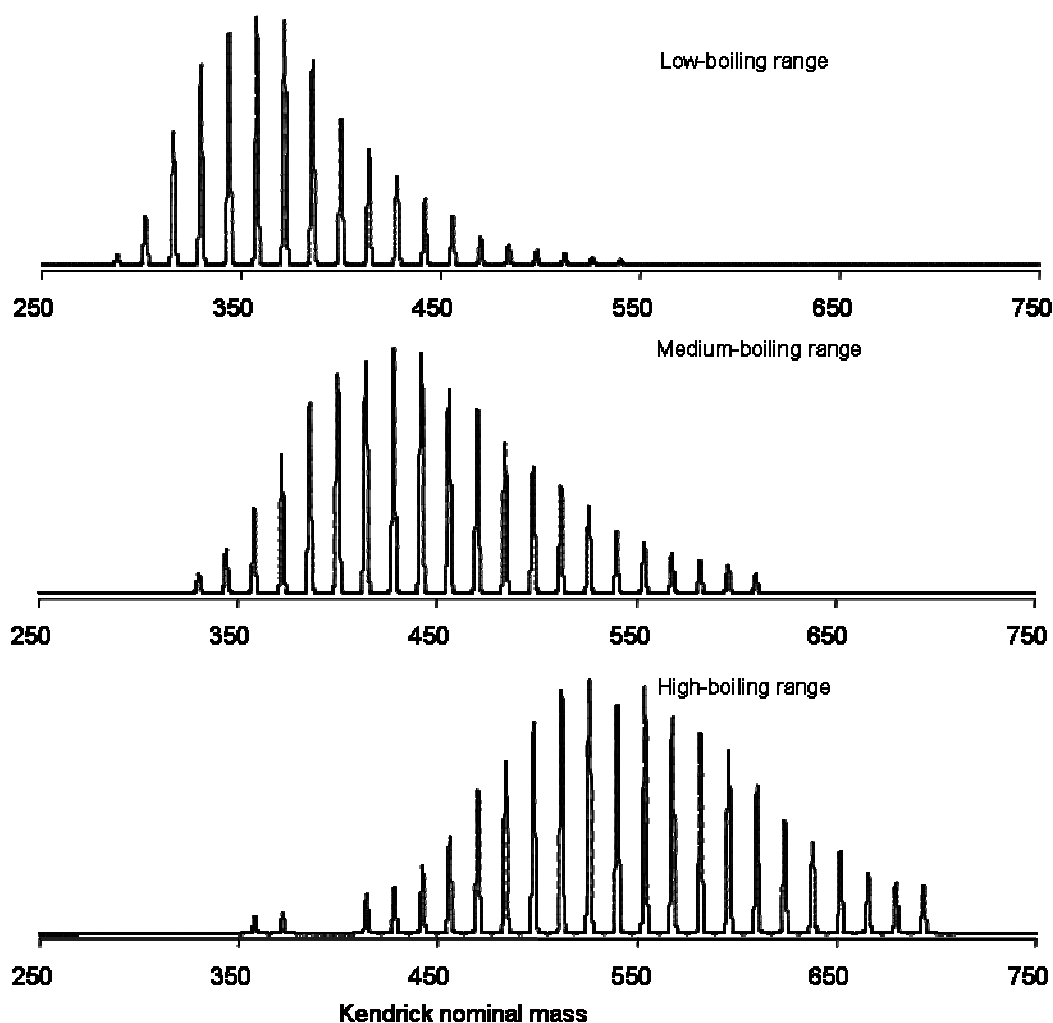


Figure 5.7. Distribution of alkylated benzothiophenes (DBE 6) in VGOs.

With the present mode of presentation, it is quite evident that the increase in boiling range plays a significant role in increasing the probability of finding high molecular weight compounds in one group of compounds. For instance, the case of alkylated benzothiophenes can be taken into account for the illustration of the said purpose. Here, the increase in mass of benzothiophenes can be due to presence of long alkyl chains or due to presence of short alkyl chains at different positions of benzothiophenes. It is clearly observed that most abundant masses for low-, medium- and high-boiling range vacuum gas oils fall around ~350 Da, ~450 Da and ~550 Da, respectively.

In the earlier study, sulfur compounds in non-polar fraction of vacuum gas oil (boiling range 340-530 °C) were analyzed by ligand exchange chromatography combined with high-performance liquid chromatographic separation on the basis of aromatic ring number, with subsequent capillary GC/MS for identification [114]. Although it was a systematic approach towards speciation of sulfur heterocycles in a VGO, the use of GC precluded identification of high molecular weight compounds present enormously in high boiling fractions. Recently, low-voltage electron ionization FT-ICR MS was used to identify a large number of hydrocarbons with a substantial amount of sulfur-, nitrogen- and oxygen-containing heterocycles in the three vacuum gas oils of different boiling ranges [77]. However, the number of sulfur compounds detected was considerably lower than in our observation. In the present study, the inclusion of ligand exchange chromatography (LEC) and FT-ICR MS provide a better technique for characterization of large number of sulfur heterocycles compared to earlier studies. Here, the use of LEC helps to identify a large number of isomers, which were not revealed by earlier two investigations.

5.3 Summary

The detailed analysis using liquid chromatography and FT-ICR MS gives an idea about the pattern of sulfur aromatics present in vacuum gas oils of different boiling ranges. Although the sulfur content in three vacuum gas oils was within about 0.5 wt % of each other, the change in relative abundance of masses along different double bond equivalents was remarkably high. The isomers of S1 compounds found in Fraction 1 were less compared to Fraction 2 but revelation of these types of isomers was possible only with the coupling of ligand exchange chromatography to FT-ICR MS. Catalytically cracked VGOs may give rise to a number of isomers (non-condensed thiophenes) found in Fraction 1 depending on the type of catalysts used for the cracking process. Therefore, this technique has tremendous potential for speciation of sulfur aromatics in low-sulfur petroleum products derived from high-boiling fractions.

6. Distribution of Sulfur Heterocycles in Crude Oils

The presence of sulfur in crude oils hampers the oil economy and poses a potential threat to the environment. Therefore, in order to improve the oil quality by removing sulfur, making profit of billion-euros, some companies are envisaging to carry out desulfurization of total crude oil before putting on the market. At present, both the causes (environment and oil economy) push towards a common goal, i.e. to develop an efficient desulfurization technique, which in turn needs the detailed structural information of sulfur aromatics present in crude oils.

In the present work, it was aimed for the speciation of sulfur heterocycles present in three Arabian crude oils namely Arabian Heavy, Arabian Medium and Arabian Light. Here, the important aspect is to establish the distribution pattern of sulfur heterocycles present in different oils obtained from different sources and to look for any systematic variation of the PASHs with the sulfur content of the crude. The analytical procedure follows the isolation of aromatic fraction, separation of thiophenes attached to aromatic rings in a condensed fashion and thiophenes attached to aromatic rings in a non-condensed fashion by a Pd(II)-bonded stationary phase, and identification of the PASHs in both fractions with FT-ICR MS.

6.1 Experimental Section

6.1.1 Sample

Three Arabian crude oils, namely Arabian Heavy (AH), Arabian Medium (AM) and Arabian Light (AL), were provided by Saudi Aramco, Dhahran, Saudi Arabia. The sulfur content and API gravity of AH, AM and AL were 2.9, 2.5, and 1.8 wt %, and 27, 29 and 32, respectively. The aromatic fractions from all the three oils were isolated by a dual-packed (silica and alumina) open tubular column as depicted in the Section 5.1.1.

6.1.2 Ligand Exchange Chromatography

Pd(II)-bonded silica phase was synthesized using 10 μm LiChrosorb Si 100 (Merck, Darmstadt, Germany) as described in the literature [109-111] and the ligand exchange chromatography was performed as described in the Section 5.1.2.

6.1.3 Sulfur Selective Methylation

About 50 mg of the aromatic fraction from each crude oil was separated on Pd(II)-bonded stationary phase into two fractions and both the fractions were methylated as reported in the Section 5.1.3.

6.1.4 High-Resolution Mass Spectrometry

Mass spectra were acquired using an APEX III Fourier transform ion cyclotron resonance mass spectrometer (Bruker Daltonics, Bremen, Germany) equipped with a 7 T actively shielded super conducting magnet and an Agilent ESI source and the conditions maintained for the measurements are described in the Section 5.1.4.

6.1.5 Data Analysis

All the masses obtained from FT-ICR mass spectrometer were imported to an Excel spreadsheet. Each mass corresponds to the methylated form of parent molecule, as there were no observable signals without methylation at same condition of mass measurements. In order to assign elemental composition of original components, all the masses obtained as $[M+CH_3]^+$ were converted to neutral masses by subtracting 15.02293 from the measured masses. Then IUPAC masses were converted to the Kendrick mass scale [101] and the Kendrick masses were further sorted according to the procedure explained in the Chapter 4.

6.2 Results and Discussion

The first step towards characterization of sulfur aromatics was isolation of aromatic fraction from three crude oils and subsequent separation of aromatic fractions into well-defined two fractions namely Fraction 1 and Fraction 2 by ligand exchange chromatography (shown in Figure 6.1).

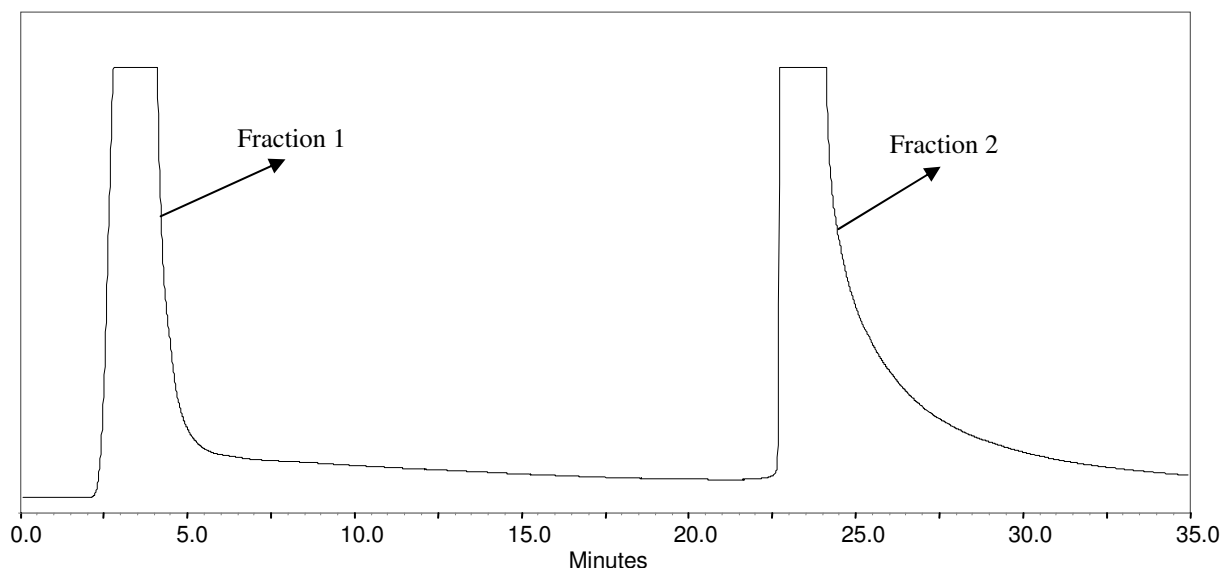


Figure 6.1. Fractionation on Pd(II)-bonded phase of the aromatic fraction from crude oils.

Here, Fraction 1 contains thiophenes attached to aromatic rings in a non-condensed fashion, e.g. phenylthiophene together with all the polycyclic aromatic hydrocarbons, whereas Fraction 2 contains thiophenes attached to aromatic rings in a condensed fashion, e.g. benzothiophene and higher homologous. The above-mentioned selectivity of Pd(II)-bonded phase was verified by investigating a series of model compounds [113]. Both the fractions obtained from the liquid chromatographic separation were methylated at the sulfur atom selectively in order to produce charged sulfur-compounds before introduction to the ESI source, as the ESI technique is not efficient for non-polar compounds [115]. The formation of charged-sulfur-compounds with methyl iodide was found to be quite efficient for high-boiling fractions, namely vacuum gas oil and vacuum residue [103,116], and the same technique was extended here for crude oils.

6.2.1 Identification of Sulfur Heterocycles with FT-ICR MS

In this study, we have assigned elemental compositions to all compounds containing one sulfur atom. It is practically impossible to extract any information from the mass spectra without further sorting using the Kendrick mass scale due to the complexity of the sample. This can be realized from mass spectra of condensed thiophenes from all three samples (shown in Figure 6.2). For simplicity, we have introduced the DBE (double bond equivalent) concept in place of KMDs in all following figures (Figure 6.3 - 6.6) to convey essential information about the number of rings and double bonds without going into detail about

KMDs. The DBE always represents the sum of the total number of rings and double bonds present in a compound.

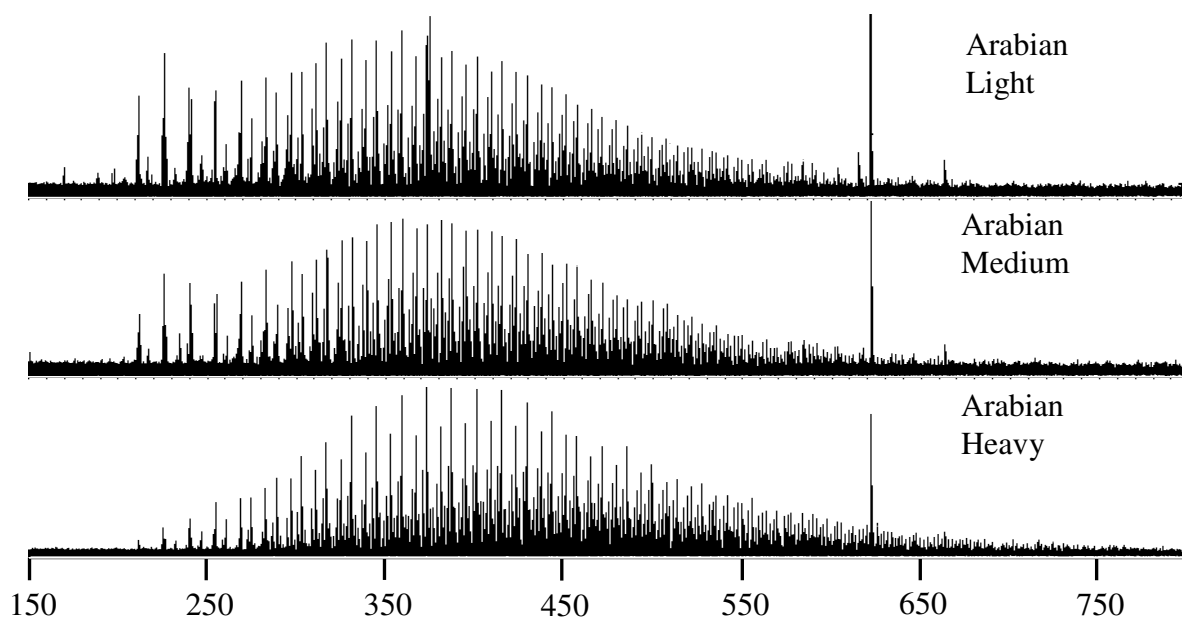
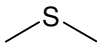
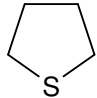
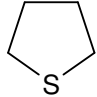
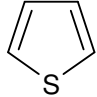
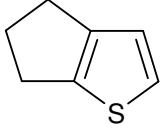
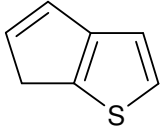
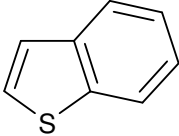
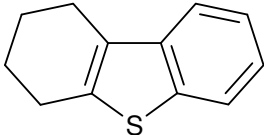
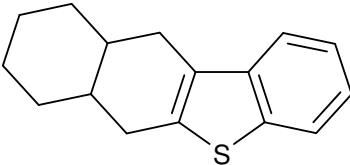
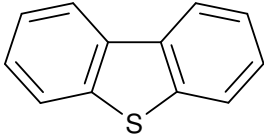
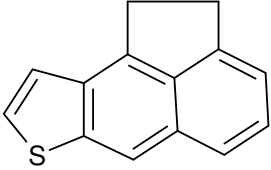
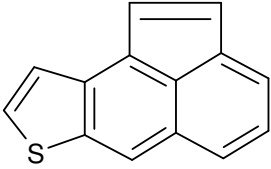
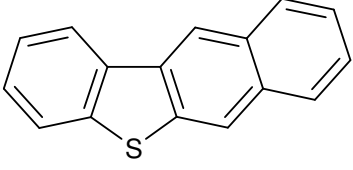
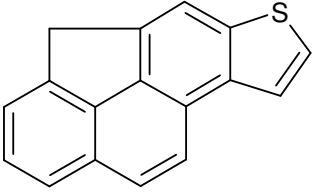
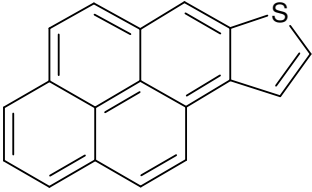
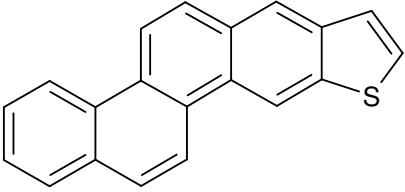
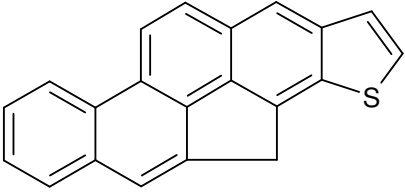
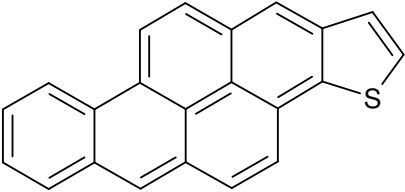


Figure 6.2. ESI FT-ICR mass spectra of Fraction 2 from Pd(II)-phase of three Arabian crude oils.

In the present samples, AH contained detectable amounts of PASHs in the first fraction from the Pd column. In the second fraction of the three samples, we find compounds containing one sulfur atom and showing up to 12 DBE numbers. It is important to note that for the lowest DBEs, practically only one ring system is likely (crude oils rarely contain appreciable amounts of alkenes), but for higher DBEs, several parent ring systems are a possibility. At the moment, there is no conclusive way to tell which systems are predominantly present at a certain DBE. The ring systems suggested for larger DBEs therefore should only be taken as examples. The nominal mass given in Table 6.1 is that for the unsubstituted parent compound. Most compounds present will be heavily alkylated.

Table 6.1 Examples of typical sulfur-containing compound types in crude oils.

Possible structure	DBE	Compound type	Nominal mass
	0	Mercaptan\Sulfide	62
	1	Tetrahydrothiophene	88
	2	Dihydrothiophene	86
	3	Thiophene	84
	4	Naphthenothiophene	124
	5	Cyclopentenothiophene	122
	6	Benzothiophene	134
	7	Tetrahydrodibenzothiophene	188
	8	Octahydrobenzonaphthothiophene	242
	9	Dibenzothiophene	184

	10	Acenaphthenothiophene	210
	11	Acenaphthylenothiophene	208
	12	Benzonaphthothiophene	234
	13	Naphthenophenanthrenothiophene	246
	14	Pyrenothiophene	258
	15	Chrysenothiophene	284
	16	Cholanthrenothiophene	296
	17	Benzopyrenothiophene	308

6.2.2 Arabian Heavy

In the second fraction, the sulfur aromatics present range from DBE 6 to DBE 17. In Figure 6.2 (bottom) the ICR mass spectrum for the Arabian Heavy, Fraction 2, is depicted. The corresponding Kendrick plot of the AH sample, Fraction 2, is reproduced in Figure 6.3. It shows the absence of open-chain sulfides, tetrahydrothiophenes, dihydrothiophenes, thiophenes, naphthenothiophenes and cyclopentenothiophenes (DBE = 0, 1, 2, 3, 4 and 5 respectively). This is as expected since such compounds should not be found in the polycyclic aromatic fraction from the silica/alumina column and, if present, many of them should be irreversibly adsorbed on the Pd(II) column except for a few isomers, as we already found in a separate study [116].

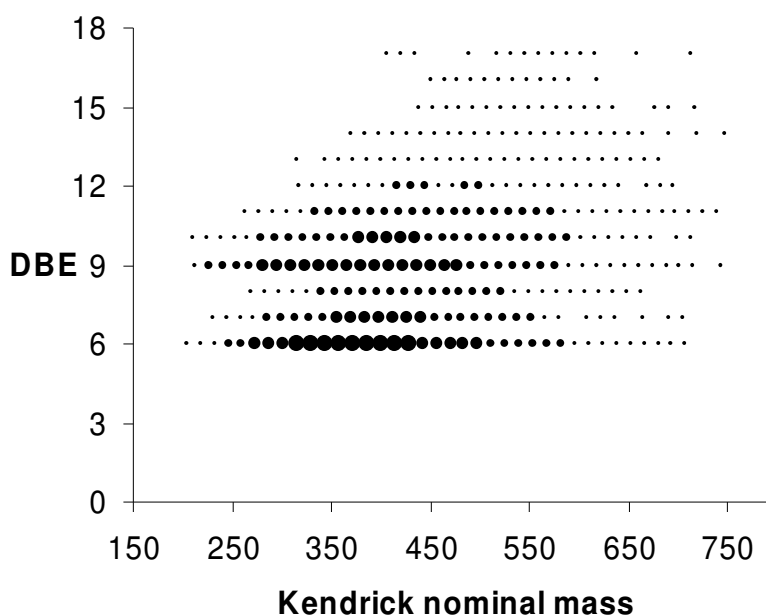


Figure 6.3. Kendrick plot of Arabian Heavy Fraction 2.

The presence of benzothiophenes (DBE 6) and dibenzothiophenes (DBE 9) shows the two most abundant types of compounds, as is expected for a crude oil. The intensity of the mass spectrometric signals decreases gradually from DBE 6 to DBE 8 which is seen in Figure 6.3. (In the Kendrick plots, the area of the circles is a rough measure of the signal intensity.) The next higher compound types of appreciable intensity belong to the dibenzothiophenes (DBE 9) series. From the mass spectrometric data, it is not possible to distinguish between dibenzothiophenes and the isomeric naphthothiophenes. The intensity of compounds with higher DBEs than 9 decreases gradually till DBE 17.

The mass range for all compounds in this sample goes from ca 200 Da to 750 Da. No doubt lighter compounds are also present, such as dibenzothiophene itself and the monomethyldibenzothiophenes, but they probably are lost in the sample preparation which involves some evaporation of high-boiling solvents (toluene). On the other hand, the lighter congeners may well be very minor compounds since the intensity of the sum of all compounds with a common x in the formula $C_x\text{DBTs}$ (and for other series as well) increases to a maximum for a certain x . This is well illustrated in the mass spectra shown.

The benzothiophene series starts at mass 204 and continues till 708 Da which indicates the presence of C_5 -benzothiophenes to C_{41} -benzothiophenes. DBE 7 can represent the 1,2,3,4-tetrahydrodibenzothiophene series but it is not possible to assign the exact size of the naphthenic ring. This series contains from three CH_2 to 37 CH_2 in the side chains. The next higher homologues (DBE 8) can be those of the octahydrobenzonaphthothiophene series (or dihydrodibenzothiophene series) containing from 2 carbon atoms up to 32 carbon atoms in the alkyl side chains. DBE 9 represents the series of dibenzothiophenes which is the most abundant series next to the benzothiophenes. Here alkyl side chains are found with from two carbon atoms to 40 carbon atoms. Also, it is found that both benzothiophenes and dibenzothiophenes are not only strong in intensity but possess the longest alkyl side-chains. Here are mainly discussed ring systems with the most unsaturated system possible. As will be shown in the Chapter 8, it may be more likely that a large number of naphthenic rings are present.

As the DBE increases gradually, the probability of finding isomers of parent compounds also increases to a greater extent. The next higher series (DBE = 10) might consist of the acenaphthenothiophenes ($C_{14}H_{10}S$) or benzothiophenes with a phenyl group as a substituent. The compounds here contain up to 36 alkyl carbons. If DBE 11 is considered as acenaphthyloothiophenes, the series starts with four alkyl carbon atoms and ends with 38 alkyl carbon atoms. DBE 12 can correspond to the benzonaphthothiophenes or anthracenothiophenes. This series contains alkyl groups with from six carbon atoms up to 33 alkyl carbon atoms. DBE 13 can represent benzonaphthothiophenes with one naphtheno ring or dibenzothiophenes with one phenyl group as a substituent as well as several other parent systems. Similarly, DBE 14 and DBE 15 can correspond to pyrenothiophenes and chrysenothiophenes where both start with eight alkyl carbon atoms and continue till 35 and

33 alkyl carbon atoms, respectively. The highest DBE recorded in this sample is 17, which can be benzopyrenothiophenes, displaying from seven up to 32 alkyl carbon atoms.

In the first fraction from the Pd(II)-column, we are able to find compounds with one sulfur atom but there are not many representatives present in this fraction. Figure 5.5 indicates that DBE 6 is the first and also the dominating one, followed by DBE 7. The highest mass is around 650 Da. From DBE 8 to DBE 11, the number of members is smaller with low abundance. It is unclear whether DBE 6 represents benzothiophenes, as would be the first assumption. Extensive studies on the Pd(II)-bonded stationary phase with a variety of standard compounds showed that all benzothiophenes eluted in the second fraction [113]. It is of course still conceivable that these compounds have some particular molecular feature that makes them very poorly retained on Pd(II), such as thiophenes with three saturated rings somewhere in the molecule. The identity of this group of compounds thus is still not clarified with our present research and which is expected to be identified with further research.

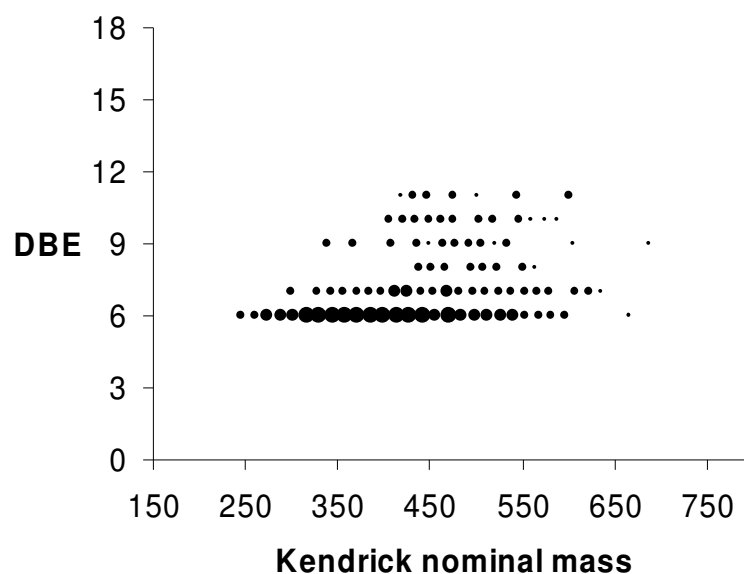


Figure 6.4. Kendrick plot of Arabian Heavy Fraction 1 from Pd(II)-phase.

DBE 7 can correspond to phenylthiophenes. Other structures are also known that have this DBE and contain non-condensed thiophenes. Such thiophenes have been demonstrated to elute in the first fraction in our previous studies with reference compounds [113]. Higher DBEs, up to 11, can be presumed to be different naphthenic rings or aromatic rings in a

non-condensed way connected to a thiophene (Table 5.1). The case of naphtho[2,1-*b*]thiophene is not conclusive since only the parent compound has been studied so far; in most compounds, alkylated derivatives – as are expected in any natural crude – are more strongly retained on Pd(II) than the parent compound and in this case they might well come in the second fraction.

6.2.3 Arabian Medium

In the second fraction of the Arabian medium oil, the sulfur aromatics display DBEs from 6 to 14. Figure 6.5 shows the absence of open-chain sulfides, tetrahydrothiophenes, dihydrothiophenes, thiophenes, naphthenothiophenes and cyclopentenothiophenes (which would have DBE = 0, 1, 2, 3, 4 and 5, respectively) in this fraction. The dominating series are the benzothiophenes and dibenzothiophenes, which is similar to that of AH. It follows the same pattern as that of the AH sample with the exception of the higher mass range. For dibenzothiophenes, the highest mass recorded is 670 in place of 750 Da. The highest DBE is 14 in place of 17. The distribution pattern of compounds of different DBE is demonstrated in tabular form with comparison to the other two oils in Table 6.2. In case of AM, there were no S1 compounds in the first fraction from Pd(II)-phase.

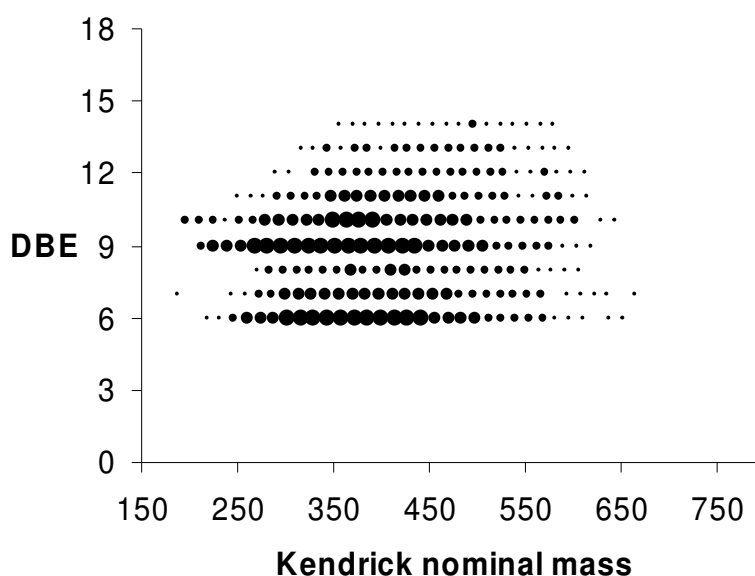


Figure 6.5. Kendrick plot of Arabian Medium Fraction 2.

Table 6.2 Distribution of the number of alkyl carbons at different DBEs of three Arabian crude oils.

Typical Compounds	DBE	Parent mass	Alkyl carbon distribution		
			AH	AM	AL
Benzothiophenes	6	134	5-41	6-37	3-32
Tetrahydrodibenzothiophenes	7	188	3-37	0-34	1-31
Octahydrobenzonaphthothiophenes	8	242	2-32	2-26	1-29
Dibenzothiophenes	9	184	2-40	2-31	2-33
Acenaphthenothiophenes	10	210	0-36	0-32	5-29
Acenaphthylenothiophenes	11	208	4-38	3-29	1-29
Benzonaphthothiophenes	12	234	6-33	4-27	4-29
Naphthenophenanthrenothiophenes	13	246	5-31	5-25	4-24
Pyrenothiophenes	14	258	8-35	7-23	9-21
Chrysenothiophenes	15	284	8-33	n.d.	n.d.
Cholanthrenothiophenes	16	296	11-24	n.d.	n.d.
Benzopyrenothiophenes	17	308	7-32	n.d.	n.d.

n.d. refers to not detected.

6.2.4 Arabian Light

In the second fraction from the Pd(II)-column, the sulfur aromatics range from DBE 6 to DBE 14. Figure 6.6 shows the absence of open-chain sulfides, tetrahydrothiophenes, dihydrothiophenes, thiophenes, naphthenothiophenes and cyclopentenothiophenes (DBE = 0, 1, 2, 3, 4 and 5, respectively) in this fraction. Here, the most intense series are the same as in the case of the AH and AM samples. They follow a similar pattern to those of the AM sample with a similar high mass limit of about 650 Da. The highest DBE is 14. Also, there is no significant difference in pattern of compounds at different DBEs. The distribution pattern of compounds at different DBE is represented in Table 6.2. Here, the case of S1 compounds in Fraction 1 is similar to that of AM oil, i.e. the S1 compounds are either not present in the sample or below the detection limit.

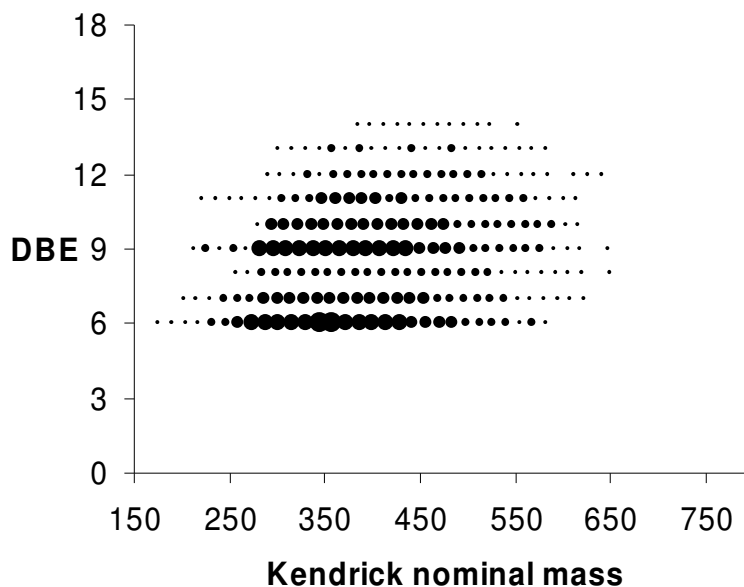


Figure 6.6. Kendrick plot of Arabian Light Fraction 2 from Pd(II)-phase.

6.2.5 Comparison with the GC Techniques

Previous methods for the analysis of PASHs in crude oil rely heavily on GC. However, the inherent thermal limit for GC equipment allows the analysis only of more volatile components. For instance, in the literature benzothiophenes with up to 16 alkyl carbon atoms have been found in a vacuum gas oil [114] but with the MS technique employed here, we have been able to find benzothiophenes with up to 30 alkyl carbon atoms in a somewhat lower boiling vacuum gas oil [116], and in a vacuum residue we identified benzothiophenes with up to 47 side chain carbon atoms [103]. Likewise, GC characterization was capable of identifying up to C₅-benzonaphthothiophenes (of 304 Da) in the crude oils [37,117], with the present MS method, we find benzonaphthothiophene with no less than 33 alkyl carbons in the AH. Furthermore, the discrimination against higher-boiling compounds in GC distorts the pattern of the analytes if they have widely differing boiling points.

Here, the distribution pattern of alkylated S1 compounds are presented in a form that we have named pseudograms. For this purpose, the intensity of masses are converted into Gaussian peaks, the peak intensities are normalized to the one peak of the highest intensity and then peaks are distributed along a mass scale, thus turning the mass spectral data into a visual form that resembles a chromatogram, examples of which are shown in Figures 6.7 and 6.8. In Figure 6.7, the compounds of DBE 6 (corresponding to the alkylated

benzothiophenes) from the three oils are represented in this manner, illustrating the ease with which the series of alkyl derivatives can be compared for different samples. It is immediately clear that the most abundant members of these series carry 12 to 20 alkyl carbon atoms and that the number of alkyl carbons decreases from AH to AL.

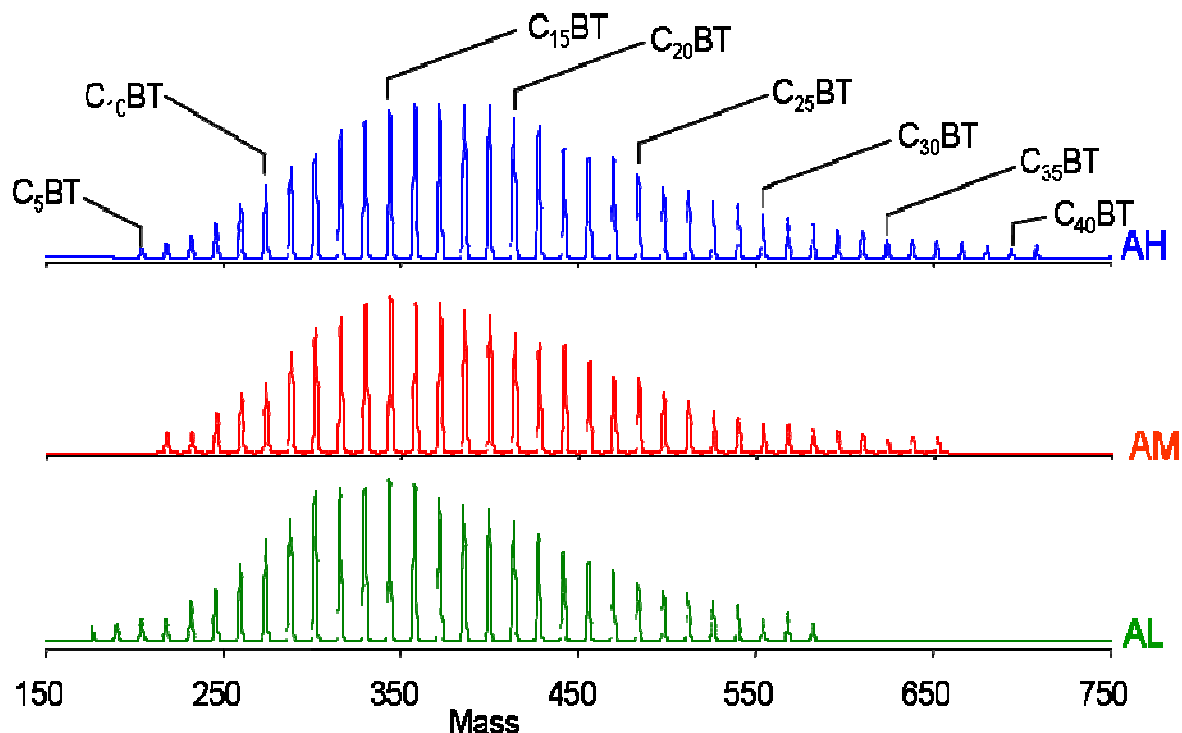


Figure 6.7. Pseudograms showing the distribution of alkylated benzothiophenes (C_xBT) of the three Arabian crude oils.

In Figure 6.8, we depict this for the benzothiophenes (DBE 6), dibenzothiophenes (DBE 9) and benzonaphthothiophenes (DBE 12) in AH. Here the mass scale of the pseudograms are adjusted so that “peaks” representing compounds of the same number of alkyl carbons are aligned along the x-axis. Therefore, it is quite easy, at a glance, to learn that benzothiophenes and dibenzothiophenes are represented with higher alkyl numbers than the benzonaphthothiophenes and that the distribution of alkyl carbons has its maximum at larger numbers for benzothiophenes than for dibenzothiophenes and benzonaphthothiophenes.

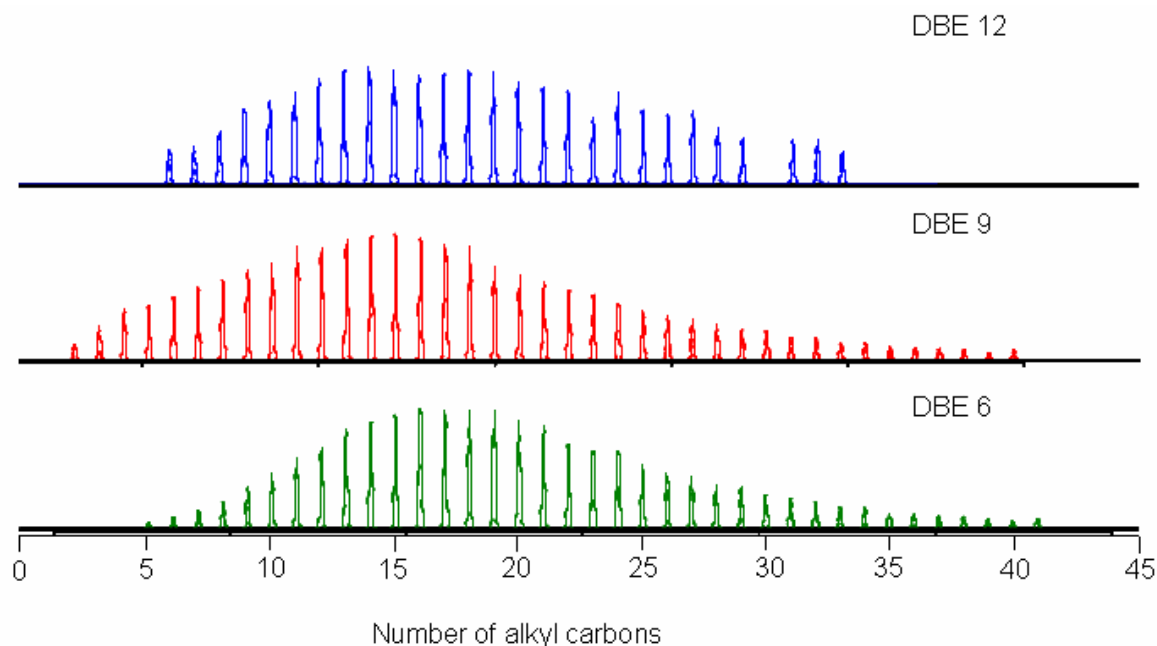


Figure 6.8. Pseudogram showing the distribution of alkylated condensed thiophenes of the Arabian Heavy crude oil, with benzothiophenes at DBE 6, dibenzothiophenes at 9 and benzonaphthothiophenes at 12.

6.2.6 Limitations of FT-ICR MS

It was previously reported that sulfur heterocyclic compounds from a vacuum residue, not from the Arabian crude oils analyzed here, comprise large number of S1 compounds (with DBE going up to 20), some S2 compounds, and a few compounds with three sulfur atoms with masses up to 850 Da [103]. However, here we did not see a higher DBE than 17 and a higher mass than ca 750 for S1 compounds in the Arabian whole crude oils. In addition, we were also not able to see detectable amount of S2- and S3-containing compounds. This may indicate that the compounds not observed here are suppressed by the presence of abundant number of low-molecular weight S1 compounds. Here, the sensitivity of FT-ICR mass spectrometer limits the access to the minor compounds of higher DBEs, higher masses, including multi-sulfur containing compounds although those compounds are indeed present in the sample. Therefore, MS is not useful in this case to preferentially discern the minor compounds unless the major ones are removed. In the future, it is expected that the electronic development of FT-ICR mass spectrometer can reveal the presence of minor components in such complex samples.

6.3 Summary

In this study, we identified a large number of high molecular weight sulfur aromatics in three Arabian crude oils of different origin. The pattern of the sulfur aromatic compounds varies from sample to sample in different ways. The highest DBE is 17 for AH whereas for AM and AL it is found to be 14. This shows that the heavy oil contains somewhat larger aromatic parent systems and the lighter oils have smaller aromatic parent systems. This phenomenon is correlated with the total sulfur content of the oils. The masses of the heaviest compounds are ca 750 Da in AH but only ca 650 Da in the other two oils. Only in AH, there was a detectable amount of sulfur compounds that elute in the first fraction from the Pd(II) column. Such compounds are considered to contain thiophene rings, which are not condensed with other aromatic groups, although they may contain aromatic substituents. They are present here only in one oil but not found in AL and AM, probably due to their low concentration in these oils. Despite having three oils characterized as being from “light” to “heavy”, their sulfur content varies within limit of 1 percentage point (1.8 – 2.9 %). The significant relation is that an increase in sulfur content increases the probability of finding non-condensed thiophenes in the first fraction and also mass ranges higher compared to low-sulfur oils.

7. Recalcitrant Sulfur Aromatics in Desulfurized Vacuum Gas Oil.

Both from an environmental and an industrial point of view, the minimization of sulfur content in petroleum-derived fuel is highly desirable [16,118-120]. Hydrodesulfurization (HDS) remains the technique of choice for the oil industry although the operating conditions are quite harsh. Sulfur removal is relatively easier for low-boiling fractions compared to high-boiling fractions. Therefore, characterization of sulfur compounds present in high-boiling fractions is quite essential in order to develop better catalysts required for the HDS process. To date, there is a fundamental understanding of sulfur removal chemistry for gasoline/diesel, but the molecular-level understanding of the ultra complex high-boiling fraction desulfurization chemistry is limited. The reason can be due to presence of highly branched alkyl groups, often substituted at many possible positions in a variety of aromatic frameworks.

Here, we have included two vacuum gas oils, namely ‘Feed’ and ‘Effluent’, for our investigation. The aim of this task was to determine the order of reactivity, i.e. most reactive and most recalcitrant, among different types (having different number of aromatic rings) of sulfur aromatics in a high-boiling fraction towards the HDS process. To achieve the goal, we have adopted isolation of aromatic fraction, separation of aromatic fraction by ligand exchange chromatography, and identification with FT-ICR MS.

7.1 Experimental Section

7.1.1 Sample

The samples, Iranian Light vacuum gas oils before (‘Feed’) and after (‘Effluent’) hydrotreatment, are obtained from Institut Français du Pétrole, Vernaison, France. The catalyst used for the hydrotreatment was NiMo on alumina from Axenes. The aromatic fractions from two vacuum gas oils were isolated by a dual-packed (silica and alumina) open tubular column as depicted in the Section 5.1.1.

7.1.2 Sulfur Mass Fraction in Vacuum Gas Oils

The sulfur content in both 'Feed' and 'Effluent', and further fractions were determined by combustion/UV fluorescence technique. Cyclohexane was added to all the samples in separate vials. The samples were dissolved in an ultrasonic bath. Then, the samples were measured. Calibration was done with sulfur standards in cyclohexane. Three independent analyses were done for each sample. All the measurements were done at Bundesamt für Materialforschung und -prüfung, Berlin, Germany.

7.1.3 Ligand Exchange Chromatography

The stationary phase, Pd(II)-containing complex based on mercaptopropano silica gel, used here for the ligand exchange chromatography was synthesized with 10 μm LiChrosorb Si 100 (Merck, Darmstadt, Germany) as developed in our group [121]. The packing, washing and testing the selectivity of the column were similar as described in the Section 5.1.2. Also, the conditions for the separation of petroleum samples were similar to that of previous Pd(II)-phase with exception to 1 % isopropanol in place of 0.5 % isopropanol.

7.1.4 Sulfur Selective Methylation

The sulfur atom is methylated selectively in a reaction with methyl iodide and silver tetrafluoroborate, yielding methyl thiophenium salt as described in the Section 5.1.3.

7.1.5 High-Resolution Mass Spectrometry

Mass spectra were acquired using an APEX III Fourier transform ion cyclotron resonance mass spectrometer (Bruker Daltonics, Bremen, Germany) equipped with a 7 T actively shielded super conducting magnet and an Agilent ESI source and the conditions maintained for the measurements are described in the Section 5.1.4.

7.1.6 Data Analysis

The IUPAC masses obtained as methylated form of the parent compounds are converted to neutral masses. The obtained neutral masses are converted to Kendrick mass scale and Kendrick masses were further sorted according to the procedure given in the Chapter 4.

7.2 Results and Discussion

The sulfur content in the samples namely ‘Feed’ and ‘Effluent’ are found to be 1.77 and 0.12 wt % respectively. Both the samples were fractionated into saturate and aromatic fractions. The sulfur amount in the aromatic fraction of ‘Feed’ and ‘Effluent’ was found to be 2.95 and 0.21 wt % respectively, whereas saturate fraction of ‘Feed’ and ‘Effluent’ contains 8.91 ppm and 3.09 ppm respectively. It is evident that sulfur compounds are much more concentrated in the aromatic fraction compared to that of the saturate one. Therefore, our research focuses on characterization of sulfur aromatics present in VGO. The aromatic fractions obtained from both the samples were further separated on the Pd(II)-phase (Section 7.1.3) into condensed thiophenes (Fraction 2) and non-condensed thiophenes (Fraction 1) together with all the polycyclic aromatic hydrocarbons.

The separation of the aromatic fraction from ‘Feed’ gives a rough estimate that both the fractions are of equal intense in UV absorption (shown in Figure 7.1) though it cannot be related to the abundance of molecules in those fractions. As Fraction 1 contains both sulfur and non-sulfur compounds, it is less informative for a comparison between ‘Feed’ and ‘Effluent’ samples. However, the relative UV intensity of Fraction 2 of the ‘Feed’ can be compared with ‘Effluent’ Fraction 2 in order to find out the fate of sulfur aromatics during the course of the HDS process.

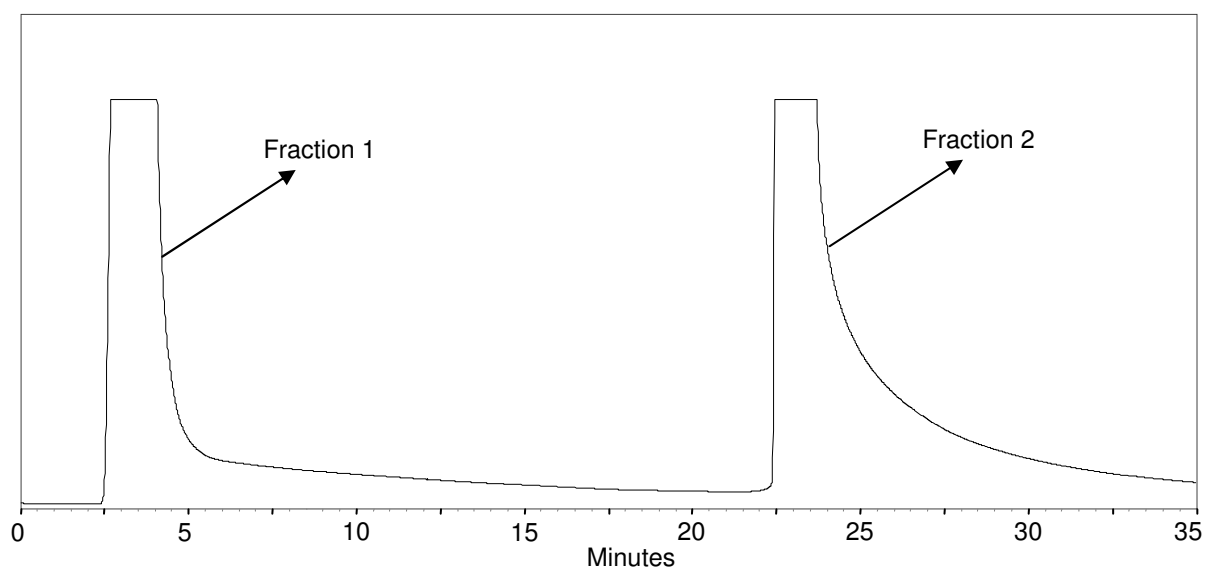


Figure 7.1. Separation of ‘Feed’ aromatic fraction by Pd(II)-bonded phase.

As discussed in the earlier section, the intensity of Fraction 2 from 'Effluent' can be compared with Fraction 2 from 'Feed'. It is found that most of the condensed thiophenes are lost during the HDS process as the concentration of both samples, taken for separation, were of a similar range. In addition, the UV area displayed by Fraction 2 is similar to that of Fraction 1 in the case of 'Feed' whereas the area by Fraction 2 is significantly smaller than that of Fraction 1 for 'Effluent', corroborating the loss of condensed thiophenes (shown in Figure 7.2).

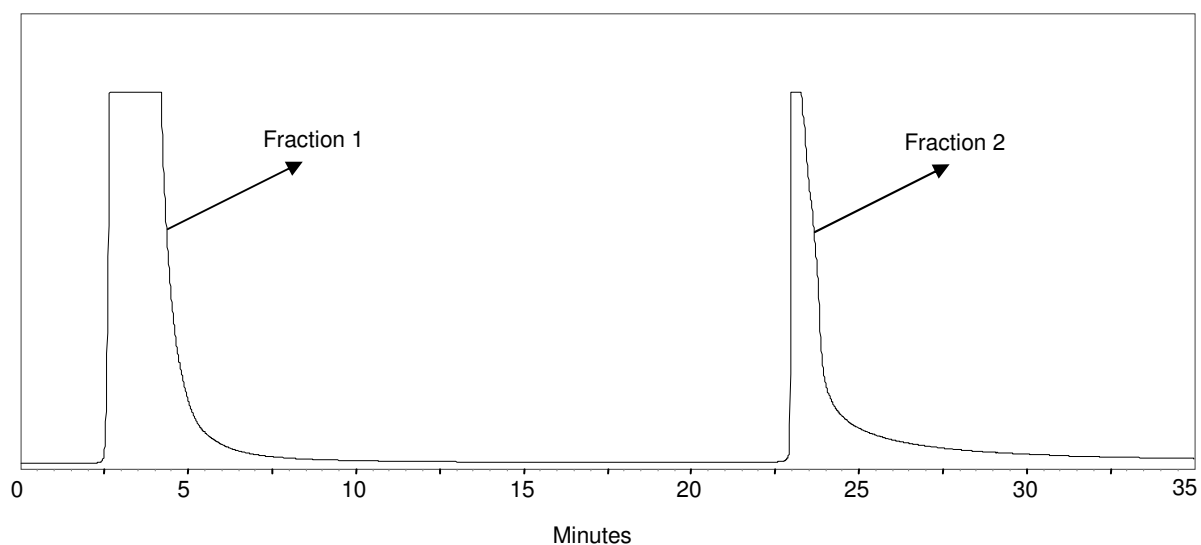


Figure 7.2. Separation of 'Effluent' aromatic fraction on Pd(II)-bonded phase.

The loss of condensed thiophenes is further verified by mass spectrometry. The reduction in complexity of the mass spectrum for the Effluent Fraction 2 (shown in Figure 7.3) gives an indication that an appreciable amount of condensed thiophenes is lost during the HDS process. However, it is quite difficult to find out the type of compounds lost without any further sorting of this complex spectrum.

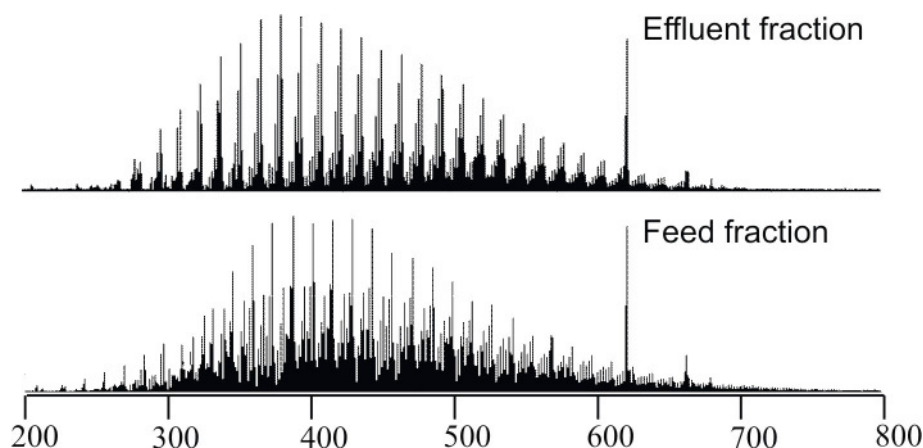


Figure 7.3. ESI mass spectra of the condensed-thiophene fractions in Feed (bottom) and Effluent (top) of an Iranian Light vacuum gas oil.

In case of the first fraction from ‘Feed’, it was possible to observe a number of S1 compounds. S1 compounds that elute in Fraction 1 correspond to thiophenes substituted with aromatic rings in a non-condensed fashion as shown in a previous study. Here, the DBE members go from 4 to 16. Surprisingly, there were no compounds corresponding to thiophenes (DBE = 3) as shown in Figure 7.4. But, the first series of compounds observed were naphthenothiophenes (DBE = 4), which is thiophene attached to a naphthenic ring. The mass, for this fraction, ranges from ~350 Da to ~750 Da. The most abundant series falls in the DBE range of 6-13. The probable structures corresponding to these DBEs in the Fraction 1 from Pd(II)-phase was well described in the Chapter 5.

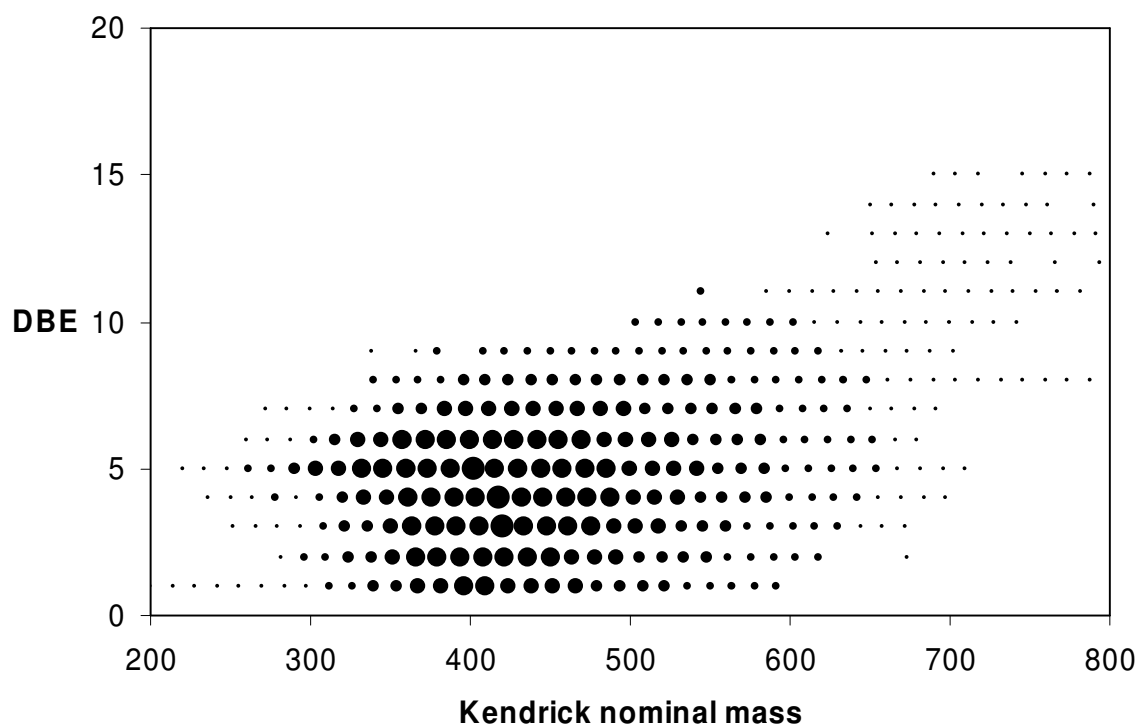
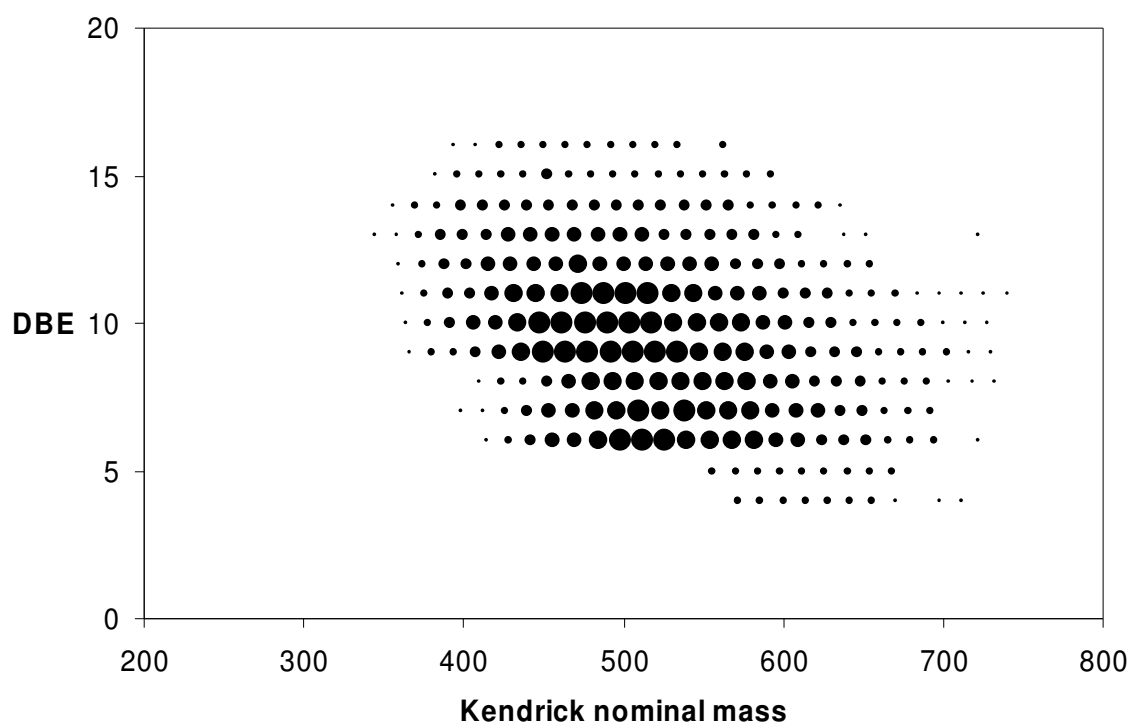


Figure 7.4. Kendrick plots of S1 compounds in Fraction 1 from 'Feed' (top) and 'Effluent' (bottom).

As shown in Figure 7.5, for the Fraction 2, the DBE series goes from three to 16 and the mass ranges from ~200 Da to ~800 Da. The most intense row of dots, corresponding to DBE 6, consists of benzothiophenes possessing from 7 to 43 carbon atoms in side chains. The DBE 7 series can be represented by naphthenobenzothiophenes where one saturated ring is present in the compound. The somewhat less intense series of DBE 8 may be derived from benzothiophenes containing two saturated rings.

The compounds of DBE 9 are again present at higher intensity and they are no doubt dibenzothiophenes with 2 to 42 alkyl carbons. Alternative structures may be the isomeric naphthothiophenes or benzothiophenes with three naphthenic rings. In this way one can climb the series of DBEs and suggest suitable parent ring structures. The DBE 11 series may represent phenanthro[4,5-*bcd*]thiophenes, known to be present in VGOs [114] or dibenzothiophenes with two saturated rings. Benzonaphthothiophenes have a DBE of 12 and in this sample, they display up to 39 alkyl carbon atoms. As the DBE increases, the number of possible parent ring-systems increases so that further data are necessary to discuss meaningfully the likely parent structures.

As described earlier in the Section 1.6.1, sulfur removal from petroleum fractions proceeds via a) direct extraction, which involves sulfur removal in a single hydrogenolysis step, and b) hydrogenation, which involves hydrogenation of the aromatic ring(s) of the sulfur compound prior to the hydrogenolysis step [122]. Hydrogenation of the aromatic ring(s) facilitates the hydrogenolysis step by diminishing the steric hindrance and increasing the electron density on the sulfur atom.

After HDS, the distribution pattern of S1 compounds in the first fraction changes significantly (shown in Figure 7.4). The major changes observed (1) that aromatic rings attached to thiophenes get saturated through the hydrogenation process, (2) Higher members (650-800 Da) at DBEs 12-15 are more resistant to desulfurization compared to members at lower ends, and (3) the most intense series 6-13 (before HDS) shifts to 1-7 (after HDS). In addition, the presence of compounds below 300 Da can be expected due to removal of alkyl chains during HDS process. The most unusual occurrence of compounds exhibiting DBE less than three in the aromatic fraction can only be explained with further investigations. The detailed information, types of aromatic hydrocarbons formed during HDS, in the desulfurization mechanism is limited due to the selective characterization of sulfur aromatics.

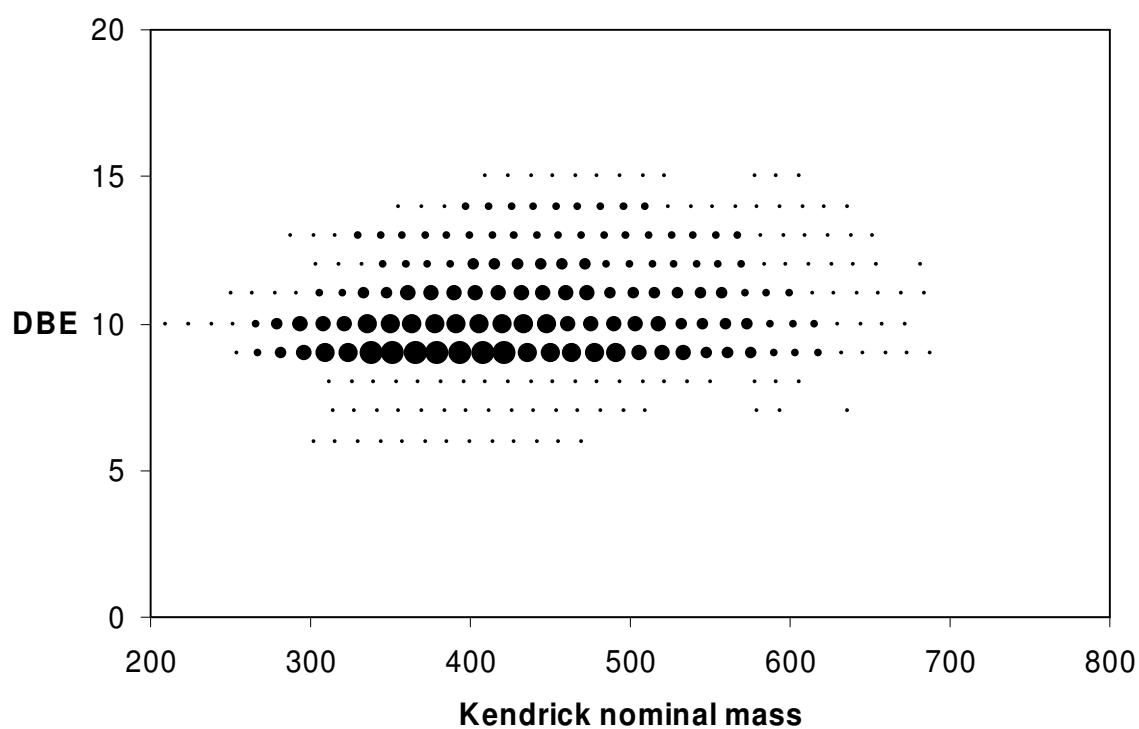
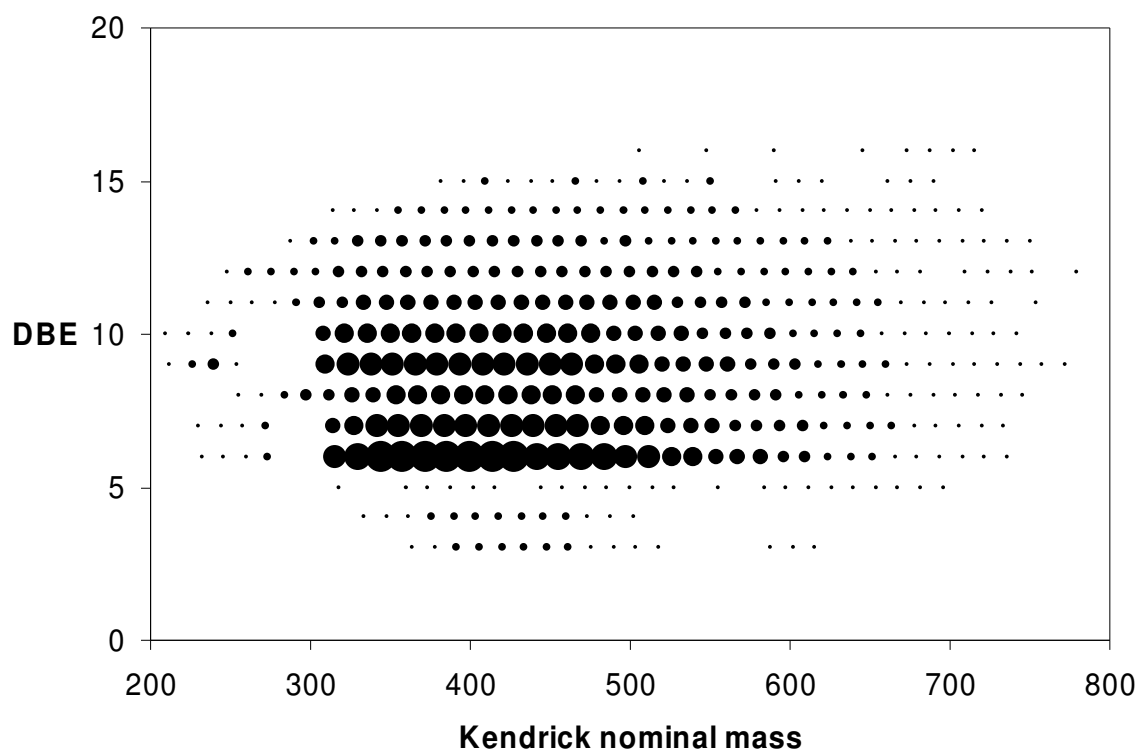


Figure 7.5. Kendrick plots of S1 compounds in Fraction 2 from 'Feed' (top) and 'Effluent' (bottom).

Also, after HDS, a strongly changed pattern for compounds in the second fraction is seen in the Kendrick plot (Figure 7.5). A lower intensity of the highest masses is observable but the most dramatic change is the loss of nearly all compounds with a DBE of 6, 7, and 8 which were among the most prominent ones in the Feed. The dibenzothiophenes are now the most intense PASHs. This result indicates that desulfurization of benzothiophenes in a VGO is easier compared to dibenzothiophenes, which is the case for low-boiling fractions also [17].

Since the Kendrick plot only gives a coarse impression of the quantitative importance of the different parent compounds, we have calculated the sum of the ion intensities for each DBE (Figure 7.6). This graphic presentation gives a clearer picture of the changes in abundance of the parent systems due to the HDS. Benzothiophenes (DBE 6) are the most prominent compounds before the HDS, but are of only minor importance afterwards. Dibenzothiophenes (DBE 9) and naphtheno-substituted dibenzothiophenes (DBE 10) are the major ones after the HDS. It is well-known for lighter PASHs that dibenzothiophenes are among the most refractory compounds, especially those that carry substituents in the 4- and 6-positions [27]. Therefore, their dominance in the Effluent can be explained on the basis of two factors: (a) an inherent slow reactivity due to sterically demanding alkyl groups, and (b) formation of dibenzothiophenes due to hydrogenation of higher DBE compounds such as the benzonaphthothiophenes that would lead to DBE 10 compounds [20]. Phenanthrothiophenes (DBE 11), being of lower reactivity towards the HDS process [20], also accumulate in the desulfurized product.

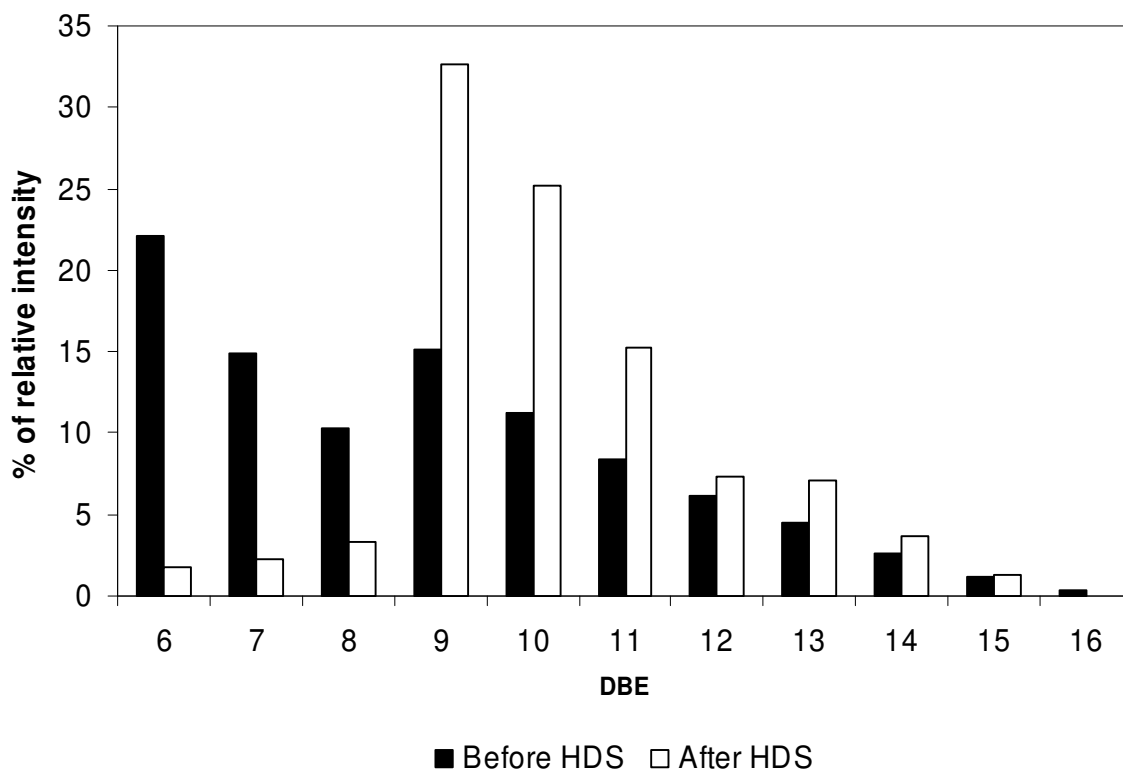


Figure 7.6. Change in distribution patterns of condensed thiophenes at different DBEs during course of hydrodesulfurization.

7.3 Summary

This study shows the power of the FT-ICR MS technique that, in conjunction with chromatographic separations according to well-defined criteria, can aid enormously in the structural characterization of complex mixtures. Still, LC separation, based on a specific mechanism, can possibly narrow down the number of isomers of the parent ring systems in order to get a clear picture of the PASH composition. Comparison between Feed and Effluent of hydrodesulfurized cuts will yield valuable information on the reactivity of these compounds and aid in the development of better catalysts and process conditions.

8. Liquid Chromatography of Sulfur Heterocycles

In recent years, with the introduction of FT-ICR MS, mass spectrometry plays a significant role in characterizing vast number of unknown components in highly complex mixtures such as fossil fuel. No doubt, FT-ICR MS, with its high resolving power and mass accuracy, is able to separate a number of components present beneath a single nominal mass, which was beyond the scope of other mass analyzers until date. This advancement in MS instrumentation helps to identify polycyclic aromatic heterocycles (N, S, and O) in the presence of large amount of polycyclic aromatic hydrocarbons without prior chromatographic separation. Therefore, FT-ICR MS is becoming an ultimate analytical tool for the analysis of highly unresolved complex mixtures. However, even for ultra-high-resolution mass spectrometer, there is an inherent limitation in that isomers cannot be individually detected. This means that there is a lack of ability to give structural insights in detail, which is highly essential for refining processes. It is not feasible to separate isomers of aromatic and naphthenic rings based on exact double bond equivalent information alone as obtained from the mass spectrometer. This illustration can be depicted in the following way. A mass of 296 Da ($C_{20}H_{24}S$) can correspond to either benzothiophene with three naphthenic rings or dibenzothiophene with 8 alkyl carbons present in it. As mass goes up, the probability of finding isomers increases significantly making it more difficult to assign an exact carbon skeleton. Although this problem can be solved with high-resolution gas chromatography using polar stationary phase, low volatility of high molecular weight compounds restricts the analysis of high-boiling petroleum fractions. In order to obtain an optimized condition for the characterization of such isomers, liquid chromatographic separation of components according to size of the aromatic systems (number of pi electrons) and identification with ultra-high-resolution FT-ICR mass spectrometer is indispensable.

In the early period, LC separation of polynuclear aromatic compounds according to the number of condensed aromatic rings in aqueous samples was achieved in the reversed-phase mode [123]. Although it had provided the selectivity required for separation of different condensed aromatic compounds according to their ring numbers, alkyl-substitution interfered the retention properties to a great extent making it more difficult to attain the goal in a desired way. Therefore, polar chemically bonded stationary phases, containing NO_2 , NH_2 , $NH-CH_3$ and CN were used for the group type separation of polycyclic aromatic

hydrocarbons [124]. Out of all the mentioned stationary phases, the aminopropano silica phase (AP) was used frequently [35,125] for the separation of polycyclic aromatic compounds according to the number of aromatic rings in petroleum samples. Also, the same phase was used in studies of PASHs, of interest in the present study, in crude oil [37]. In the same direction, perfluorocarbon modified silica gel was found to be a better option, being less perturbed by alkylation in the aromatic ring-size separation [126]. However, in our study, the selectivity among PASHs of different ring numbers was too low to be used for real-world samples. A different separation mechanism, namely a charge-transfer interaction, is found for the tetrachlorophthalimide-containing (TCP) stationary phase that has been used for PAHs in coal products [38]. Also, a 2,4-dinitroanilinopropano silica phase was tested since it was claimed by previous workers that there is a lower influence of alkyl substituents [127,128], but in our hands this phase only showed a smooth chromatographic envelope without features. Therefore, AP and TCP, together with a chemically bonded β -cyclodextrin phase (β -CD), were investigated in this study for their ability to separate PASHs from a VGO according to the number of aromatic double bonds.

8.1. Experimental Section

8.1.1 Sample

An Iranian Light vacuum gas oil was obtained from the Institut Français du Pétrole, Vernaison, France. Its boiling range was 390 - 460 °C and the sulfur content was 1.69 wt %. The aromatic fraction from about 1 g of vacuum gas oil was isolated as described in the Section 5.1.1. Figure 8.1 outlines the detailed analysis scheme for isolation and identification of PASHs in the vacuum gas oil.

8.1.2 Chemicals and Standard Compounds

Chemicals for synthesis and HPLC grade solvents were from Sigma-Aldrich (Taufkirchen, Germany). Most of the reference compounds except a few were synthesized in our laboratory [129, Appendix].

8.1.3 Ligand Exchange Chromatography

Pd(II)-bonded silica was synthesized with 10 μm LiChrosorb Si 100 (Merck, Darmstadt, Germany) following the literature [109-111]. The ligand exchange chromatography was accomplished as described in the Section 5.1.2.

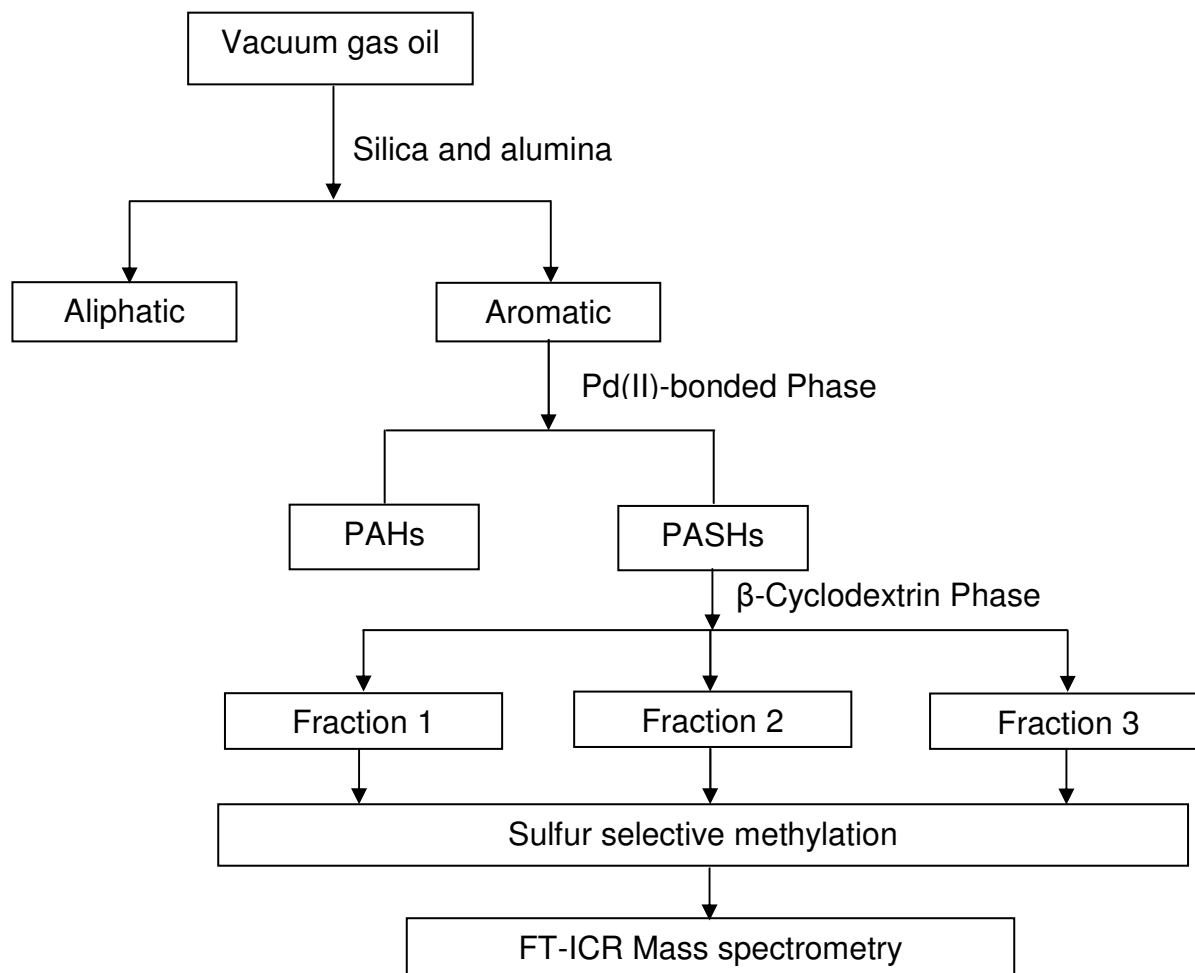


Figure 8.1. Analysis scheme for polycyclic aromatic sulfur heterocycles in the vacuum gas oil.

8.1.4 Comparison of Three Stationary Phases

The AP and TCP phases were synthesized with 10 μm LiChrosorb Si 100 according to the literature [38,110]. β -Cyclodextrin bonded silica phase (5 μm) was commercially available (Merck ChiraDex). About 1.5 g of each modified silica gel was packed into stainless steel columns (150 mm x 4.6 mm) with the slurry method at a pressure of 450 bar using a Knauer pneumatic pump. Methanol was used for both making the slurry and filling the column. The packed columns were washed with methanol, dichloromethane and

cyclohexane successively. The retention factors of model thiophenic compounds were determined using cyclohexane as eluent. In this regard, the first disturbance of the base line when a small amount of dichloromethane was injected was taken as the hold-up time for all the columns.

8.1.5 Sulfur Selective Methylation

Before being characterized by ESI FT-ICR MS, the PASH fractions were selectively methylated at the sulfur atom using methyl iodide and silver tetrafluoroborate [103] as described in the Section 5.1.3.

8.1.6 High-Resolution Mass Spectrometry

Mass spectra were acquired using an APEX III Fourier transform ion cyclotron resonance mass spectrometer (Bruker Daltonics, Bremen, Germany) equipped with a 7 T actively shielded super conducting magnet and an Agilent ESI source. The conditions maintained for measurements are described in the Section 5.1.4.

8.1.7 Data Analysis

All signals obtained as $[M+CH_3]^+$ were converted to neutral masses by subtracting 15.02293 from the measured mass. The IUPAC masses were then converted to the Kendrick mass scale [101] and the Kendrick masses were further sorted according to the procedure described in the Chapter 4.

8.2 Results and Discussion

In the chromatographic simplification of heavy aromatic petroleum fractions, we first performed a fractionation on the Pd(II)-bonded phase that makes two tasks: first, all PAHs are separated into a first fraction and PASHs eluting in the second fraction are free from any hydrocarbons; and second, especially in very heavy fractions like vacuum residues, there is a separation of PASHs into the two fractions depending on how the thiophene ring is connected with other aromatic rings [113]. In the first fraction of this VGO, the amount of PASHs was negligible as evidenced by FT-ICR MS data so that all further studies were done only on the second fraction, which is free of PAHs.

8.2.1 Selection of a Stationary Phase

Ultra-high resolution mass spectrometry of the VGO reveals that compound series possessing twelve double bond equivalents (DBEs) are represented, indicating that there are at least twelve different parent ring systems. In reality, this number will be much higher since different compound classes and isomers, possessing the same DBE, are highly likely to be present. A first chromatographic simplification of such a mixture might be performed according to the size of the aromatic system. Such a separation should, ideally, show a minimal dependence on the alkyl groups and thus only depend on the number of aromatic double bonds. Chemically bonded phases like the aminopropano ligand have frequently been used in the normal-phase mode for such separations since it has been shown that a good separation according to the number of unsaturated carbon atoms is achieved and that methyl groups have a negligible effect on the retention [35].

Unfortunately, many of those studies have only included parent systems and methylated derivatives. It appears that in many normal-phase separations, methyl groups contribute to increased retention times but longer alkyl chains lead to shortened retention times. This could be an adverse property for the separation of the aromatic compounds in our samples since they are known to be highly alkylated, the benzothiophenes containing up to 30 carbon atoms in the side chains. Nevertheless, being a benchmark phase for the present purposes, this phase was included in this study.

Among the many other phases that have been used for the separation of PAHs [130], we also selected one that separates aromatic molecules based on a charge-transfer mechanism. Tetrachlorophthalimide is among the strongest of such phases [131] and shows a linear relationship between the number of pi electrons in the PAH and log k , where k is the retention factor. Methyl groups have an influence on the retention [132] but not much is known for longer-chain alkyl substituents. 1-Butylpyrene has a retention index of 424, 1-methylpyrene 417 and pyrene itself 399 [132] which might indicate that methyl and longer groups affect the retention similarly.

The final phase investigated is a β -cyclodextrin modified silica. Such phases have been employed in the reversed-phase mode for polycyclic aromatic compounds, but only one report on its use in the normal-phase mode seems to have appeared, showing the separation

of alkyl nitrates [133]. Cyclodextrin phases have been extensively used for decades in the separation of enantiomers [134]. Cyclodextrins are cyclic oligoglucoses, the β phase consisting of seven glucose units in a ring with the hydroxy groups pointing outwards. The cavity of the molecule is therefore non-polar. Since the mobile phase in the present application is cyclohexane, we presume that the cavity is filled with mobile phase and that the interaction with the solutes will be through the hydroxyl groups on the outer surface of the cyclodextrin. Thus this phase will have some resemblance to diol phases which have been used for the separation of PAHs [124].

In order to test the separation of polycyclic sulfur heterocycles in a simpler mixture than a VGO, a diesel sample of 18600 ppm sulfur was chromatographed on this phase. The separation into three distinct peaks is shown in Figure 8.2; the fractions indicated in the figure correspond quite well to the compound classes of benzothiophenes, dibenzothiophenes and benzonaphthothiophenes as shown by the retention data in Table 8.1.

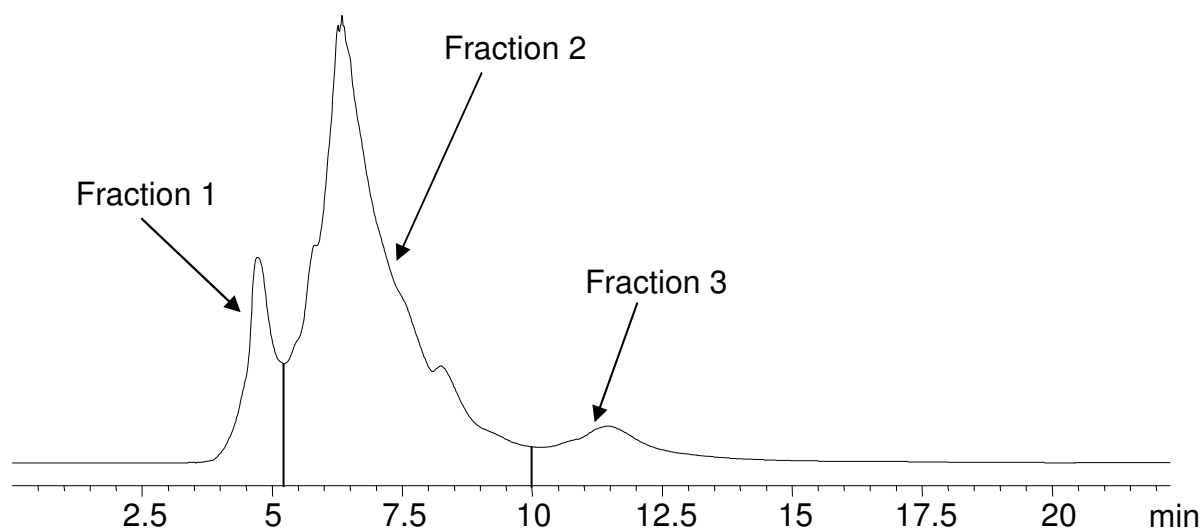


Figure 8.2. HPLC analysis of PASH fraction from a diesel on the β -cyclodextrin column (250 mm x 4.6 mm). Conditions: mobile phase 0.5 % *t*-butyl methyl ether in cyclohexane, oven temperature 30 °C, UV detection at 254 nm.

Table 8.1 Retention factors (*k*) for some polycyclic aromatic sulfur heterocycles on a β -cyclodextrin, an aminopropano and a TCP stationary phase with cyclohexane as an eluent.

	β -CD	AP	TCP
Two aromatic rings			
Benzothiophene	2.08	0.47	0.34
2-Methylbenzothiophene	1.68	0.50	0.60
3-Methylbenzothiophene	3.42	0.49	0.48
5-Methylbenzothiophene	1.60	0.52	0.52
6-Methylbenzothiophene	1.44	0.48	0.72
2,5-Dimethylbenzothiophene	1.49	0.53	0.96
2,6-Dimethylbenzothiophene	1.49	0.56	0.99
1,2,3,4-Tetrahydrodibenzothiophene	1.28	0.42	0.94
2-Dodecylbenzothiophene	0.48	0.27	0.34
Cholestano[2,3- <i>b</i>]-5,6,7,8-tetrahydronaphtho[2,1- <i>d</i>]thiophene	1.00	0.25	0.87
Three aromatic rings			
Dibenzothiophene	3.82	0.89	1.00
2-Methyldibenzothiophene	3.42	0.87	1.76
4-Methyldibenzothiophene	2.98	0.82	2.13
2,4-Dimethyldibenzothiophene	2.38	0.69	3.55
4,6-Dimethyldibenzothiophene	2.88	0.76	4.02
1,3,7-Trimethyldibenzothiophene	3.01	0.81	3.96
1,4,6-Trimethyldibenzothiophene	2.77	0.72	5.36
1,4,7-Trimethyldibenzothiophene	3.07	0.78	5.55
1,4,8-Trimethyldibenzothiophene	3.33	0.78	5.56
2,4,6-Trimethyldibenzothiophene	2.80	0.76	6.19
3,4,7-Trimethyldibenzothiophene	2.76	0.80	3.82
2,4-Dimethyl-6-ethyldibenzothiophene	2.44	0.69	3.97
2,3,4,7-Tetramethyldibenzothiophene	1.62	0.52	3.89
2,3,7,8-Tetramethyldibenzothiophene	3.65	0.90	5.84
2,4,6,8-Tetramethyldibenzothiophene	3.02	0.71	9.99
2-Octyldibenzothiophene	1.58	0.46	1.00
4-Octyldibenzothiophene	1.86	0.61	1.06
Naphtho[2,3- <i>b</i>]thiophene	4.32	1.17	1.76
2-(1-Naphthylethano)thiophene	3.37	1.08	0.55
3-[(4-Butylphenyl)ethano]benzo[<i>b</i>]thiophene	2.59	0.82	0.38
More than three aromatic rings			
Phenanthro[4,5- <i>bcd</i>]thiophene	5.81	1.08	2.39
Benzo[<i>b</i>]naphtho[1,2- <i>d</i>]thiophene	7.01	1.41	3.29
2-(1-Naphthyl)benzothiophenes	4.41	1.15	0.63

For the three stationary phases here, the order of selectivity towards parent aromatic rings (benzothiophene, dibenzothiophene and benzonaphthothiophene) is in the order TCP > β -CD > AP (Figure 8.3 and Table 8.1). This might point to TCP as the more favorable phase, but retention on TCP is more sensitive to the alkylation than the other phases.

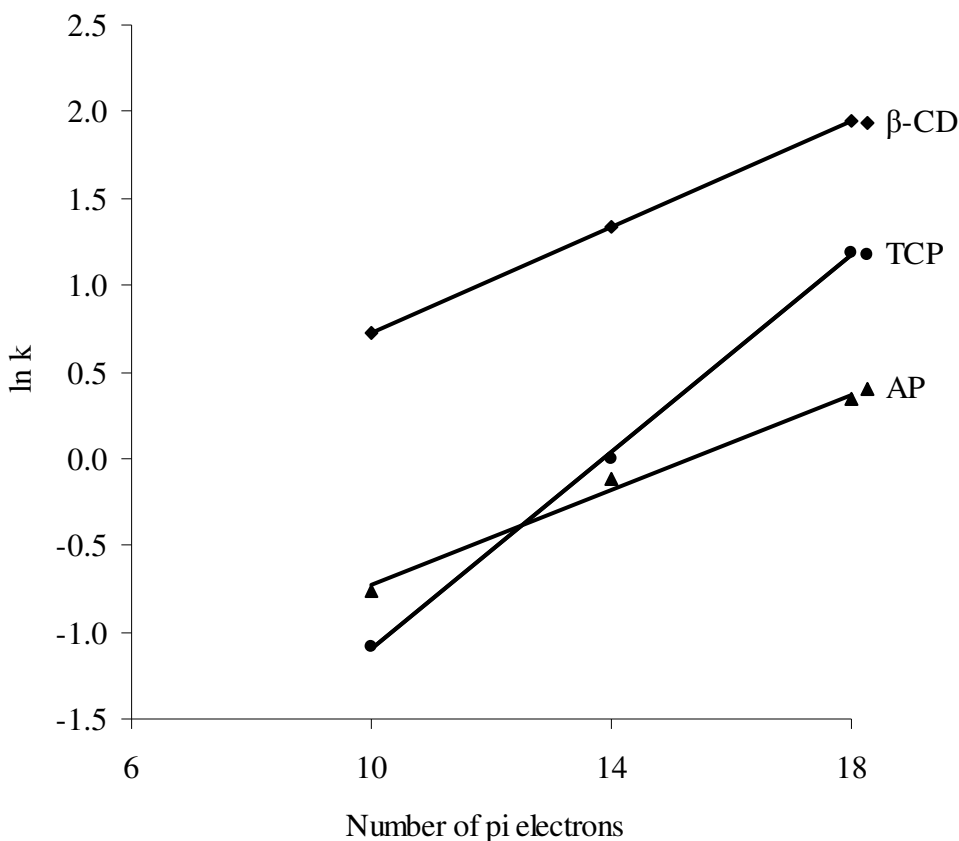


Figure 8.3. Selectivity of stationary phases towards benzothiophene, dibenzothiophene and benzonaphthothiophene.

The retention factors, for the TCP phase, in Table 8.1 increase with the number of methyl substituents so that dimethylbenzothiophenes coelute with dibenzothiophene and dimethyldibenzothiophenes coelute with the four-ring compound benzonaphthothiophene. Thus, this stationary phase cannot be used to separate a mixture according to the number of rings. The chromatogram of the PASHs from the VGO on this phase indeed shows poor selectivity based on the number of aromatic rings (Figure 8.4), i.e. there are no distinct peaks corresponding to the benzothiophenes, the dibenzothiophenes, etc.

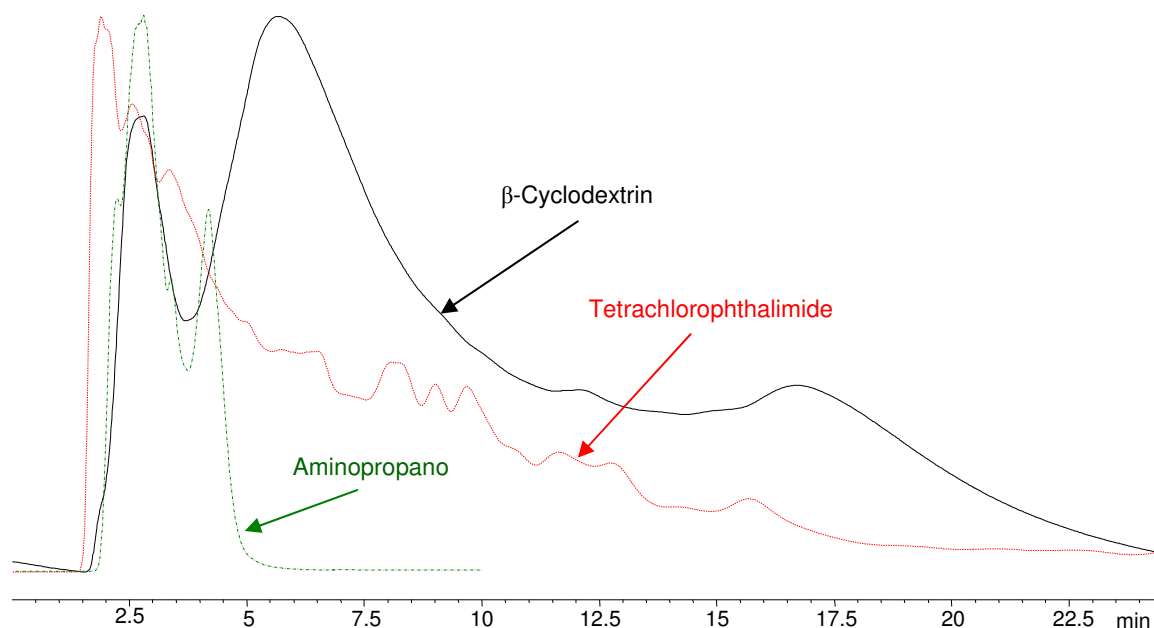


Figure 8.4. HPLC analysis of PASH fraction from VGO on aminopropano, tetrachlorophthalimido and β -cyclodextrin columns. Conditions: mobile phase cyclohexane, flow rate 1 mL/min, oven temperature 30 °C, UV absorption detection at 254 nm.

The aminopropano phase has a demonstrated potential to separate aromatics according to the number of aromatic rings of PASHs in fossil fuels [37,135]. Few data are available in the literature for aromatics substituted with long aliphatic chains. In agreement with published studies we find that there is only a slight dependence of the retention time on the number of methyl groups. However, compounds with long alkyl groups, like octyl and dodecyl, elute much ahead of the parent system. Thus the octyldibenzothiophenes (Table 8.1) elute together with the benzothiophenes which would thwart the intended separation according to aromatic parent system. In agreement with this, the chromatogram of the VGO on this stationary phase (Figure 8.4) confirms the poor resolution between peaks expected to arise from the two-ring and three-ring aromatics.

For the β -cyclodextrin phase we found that most mono- and disubstituted benzothiophenes with few exceptions elute earlier than benzothiophene. Thus, the addition of alkyl groups and a cycloalkano ring to benzothiophene decreases the retention time compared to the parent structure. The same trend applies to the dibenzothiophenes. Of particular interest here is that long alkyl chains (Table 8.1) significantly decrease the retention times compared to the parent compound. Therefore, the distinct peaks corresponding to the substituted benzothiophenes and dibenzothiophenes in the sample

(Figure 8.4) were observed at about half the retention time of the respective parent compounds. Benzonaphthothiophene elutes much later than the three-ring aromatics; we presume that alkylation will have the same effect for this class of compounds.

In Figure 8.4, depicting the PASHs from the VGO, the resolution between the two-ring and the three-ring compounds is much more pronounced than on the AP phase as was predicted from the study with reference compounds. The later part of the chromatogram is also more structured on this phase, indicating natural cutting points for further fractionation. An optimization of the mobile phase and the separation temperature led to the situation shown in Figure 8.5 in which the three fractions collected for mass spectral analysis are also indicated.

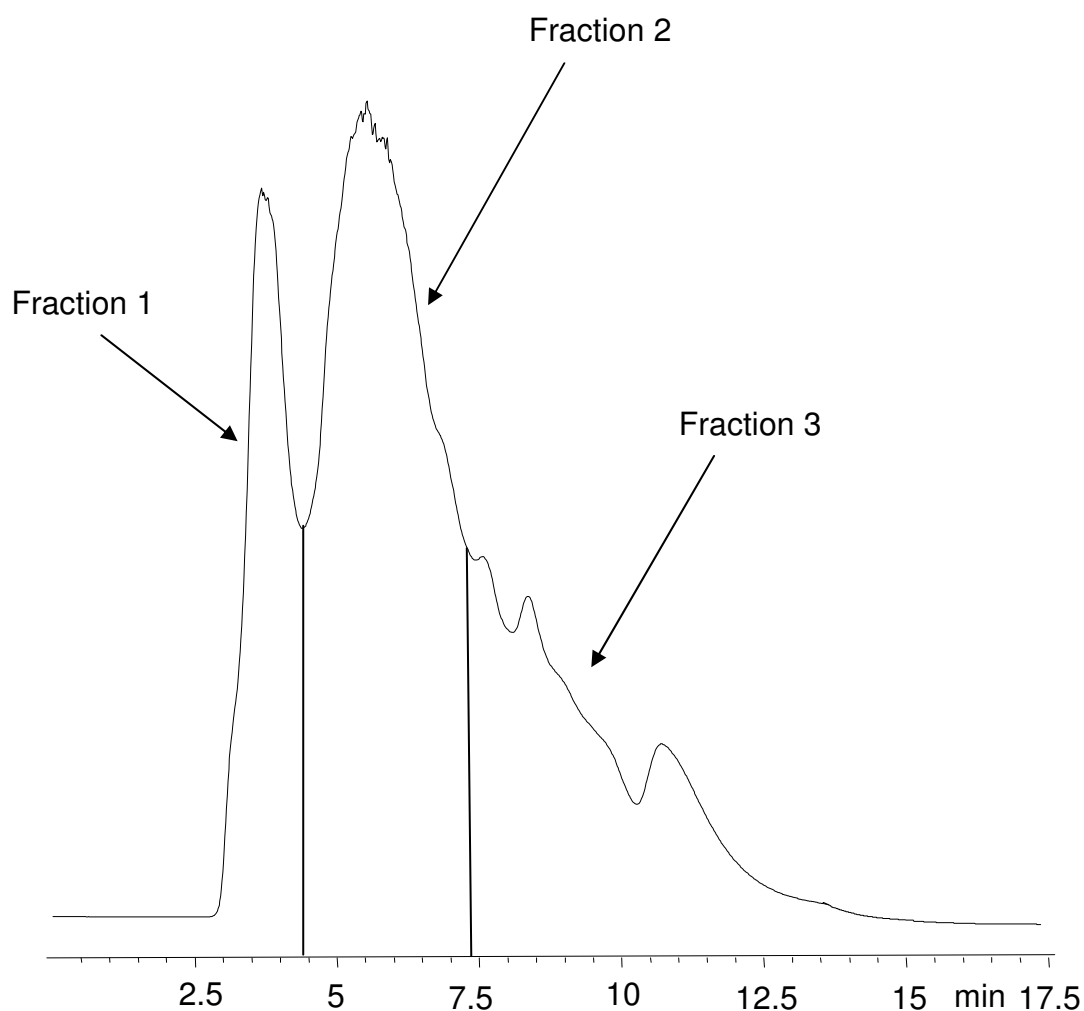


Figure 8.5. HPLC analysis of PASH fraction from VGO on the β -cyclodextrin column. Conditions: mobile phase 0.5 % *t*-butylmethyl ether in cyclohexane, flow rate 1 mL/min, oven temperature 50 °C, two columns (150 x 4.6) mm connected in series, UV absorption detection at 254 nm.

Since a diode array detector was used for monitoring these separations, complete UV spectra were recorded at all retention times. In Figure 8.6 the UV spectra taken at the retention times corresponding to the apexes of the three fractions indicated are reproduced. Included are also the UV spectra of appropriate PASHs that resemble the compounds expected in these fractions. The absorption maxima of the VGO fractions are shifted a few nanometers to longer wavelengths as is expected for compounds with multiple alkyl substitution but otherwise the spectra show a good agreement with those of the reference compounds. The spectrum of the four-ring fraction closely resembles that of benzonaphtho[2,1-*d*]thiophene but not those of the other two isomers of this compound. The UV spectra thus support the conclusions drawn from the study of the chromatographic properties of reference compounds.

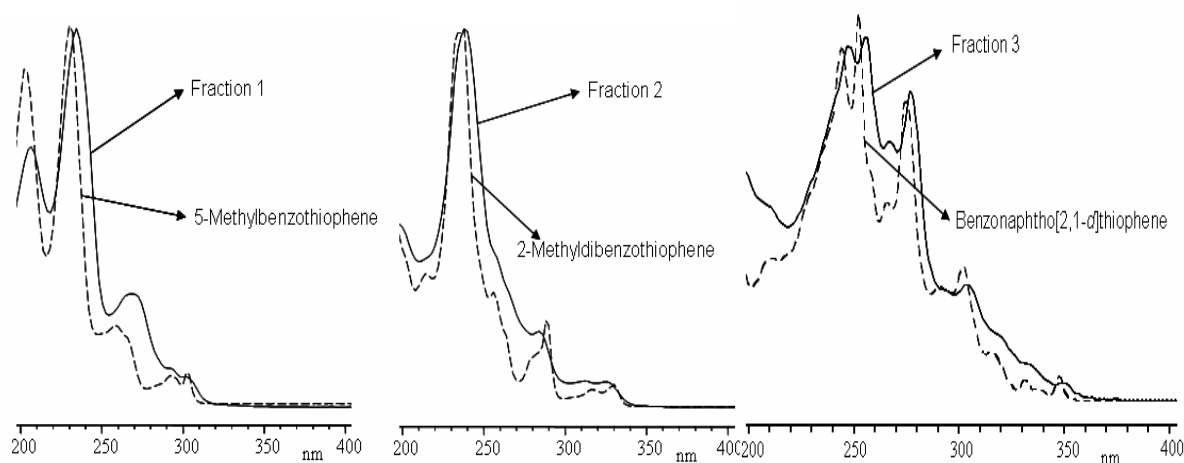


Figure 8.6. UV apex spectra of the three fractions separated on β -cyclodextrin phase with respect to their corresponding aromatic ring systems.

8.2.2 Identification of PASHs with FT-ICR MS

Each of the three fractions collected from β -CD was selectively methylated at the sulfur atom [103] to preform ions for FT-ICR MS analysis. In this study, we have assigned an elemental composition to all aromatics containing one sulfur atom. It is practically impossible to get any information from the mass spectra without further sorting using the Kendrick mass scale. In this scale, different classes (N, S, O) of compounds can be easily identified since they exhibit different Kendrick mass defects. Even within the same class, different types (number of rings plus double bonds) of compounds can be easily identified as described in the Chapter 4.

The complexity of the PASH fraction before fractionation is clearly reflected in its mass spectrum, Figure 8.7. The fractionation on β -CD reduces the complexity to such an extent that a repetitive pattern can be discerned. It is evident that there is a cluster of compounds whose pattern is repeated every 14 mass units. Figure 8.7 depicts three of these clusters. Note that the smaller signals repeat the intensity pattern at one mass unit higher values, indicating that they are derived from the same compounds containing one ^{13}C isotope. The double bond equivalents are indicated for the middle cluster.

To investigate how well the separation of the very complex mixture of PASHs on the cyclodextrin column has succeeded, all the compounds of the S1 class (compounds containing one sulfur atom) in each of the three fractions, together with their KMD value and double bond equivalent (DBE), are given in Figures 8.8, 8.9 and 8.10. The DBE number gives direct information on the different types of compounds in a thiophene series.

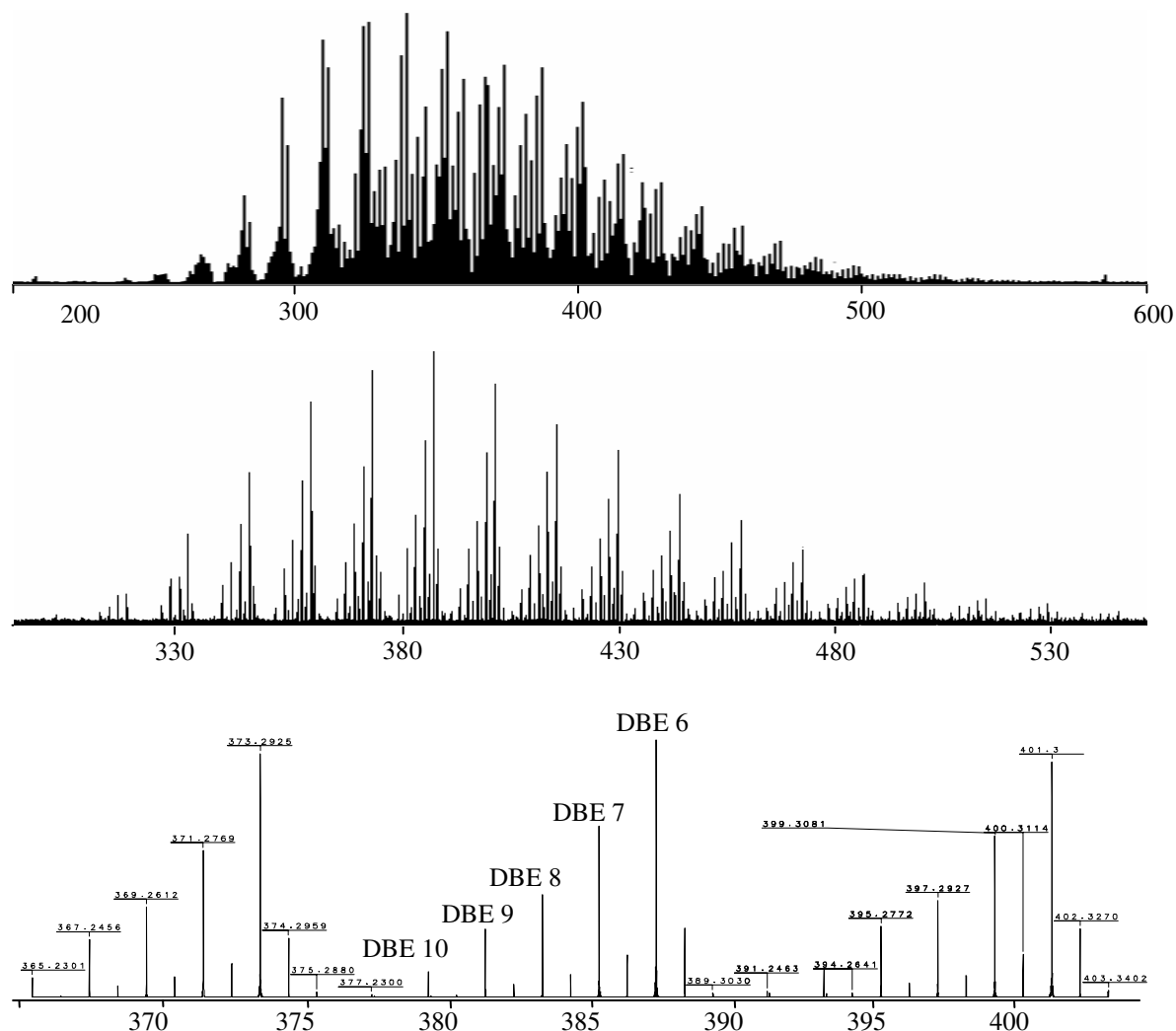


Figure 8.7. High resolution mass spectra of PASH fraction from vacuum gas oil (top), Fraction 1 from the β -cyclodextrin column (middle) and an expanded scale of Fraction 1 (bottom).

8.2.3 Fraction 1

Figure 8.8 shows the absence of open-chain sulfides, tetrahydrothiophenes and dihydrothiophenes (DBE = 0, 1 and 2 resp.) in the first fraction. This is as expected since such compounds should not be found in the polycyclic aromatic fraction and, if present, they should be irreversibly adsorbed on the Pd(II) column [113]. The presence of very low concentrations of alkylated thiophenes (DBE = 3) is indicated. Although earlier studies have shown that most thiophenes appear in the first fraction on the Pd(II) phase, it is not yet clear what structure those thiophenes may have that allows them to appear in the Fraction 2 from Pd(II)-bonded phase. This series contains from C₂₀-thiophene to C₂₈-thiophenes.

Conceivably a tetrasubstituted thiophene ring would be electron rich enough to permit such compounds to complex so strongly with Pd(II) that it appears here.

The next higher series would be naphthenothiophene (C_7H_8S) with a DBE of 4. Here are found C_{17} - to C_{25} -naphthenothiophenes but neither LC nor MS can differentiate between the size of the naphthene ring. The minute amounts can be interpreted as cyclopentenothiophenes or cyclohexenothiophenes with 18 to 24 carbon atoms in addition to the aromatic ring. DBE 6 corresponds to the benzothiophene series. Compounds with 11 to 30 alkyl carbons are strongly represented. The next higher DBE = 7 would correspond to naphthenobenzothiophenes, for instance 1,2,3,4-tetrahydrodibenzothiophenes. In addition to the thiophene ring, there are from 11 to 30 carbon atoms found in the molecules.

Compound classes with DBE = 8 can correspond to indenothiophenes and indanylthiophenes as well as to benzothiophene with two naphthenic rings. Such compounds occur here in the mass range from 284 to 550. DBE = 9 most likely represent alkylated dibenzothiophenes (or benzothiophenes with three naphthenic rings). In this fraction the abundance of those compounds is much lower than in the second fraction. To judge from the less than baseline resolved peaks in Figure 8.5 and from the retention data in Table 8.1, it can be expected that some overlap between compounds with two and three aromatic rings will be found but judging from the complexity of the sample, the two groups of aromatics are well separated.

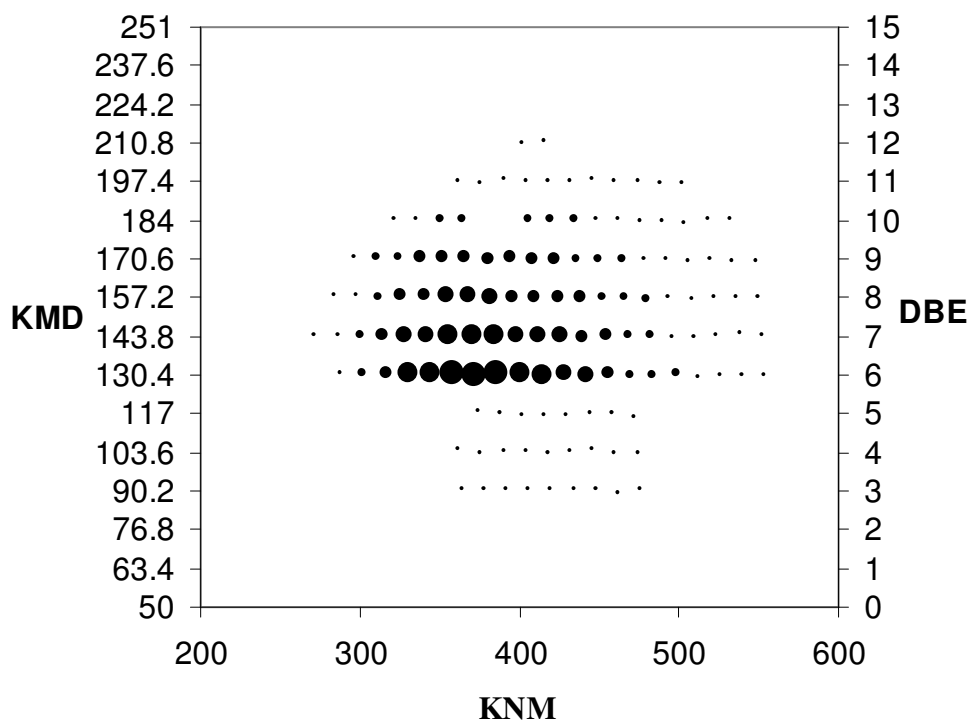


Figure 8.8. Kendrick plot of Fraction 1 from the β -cyclodextrin column.

8.2.4 Fraction 2

In this fraction, plotted in Figure 8.9, no alkylated benzothiophenes (DBE 6) are detected. Compounds of DBE 7 and 8 are almost negligible. This shows that (substituted) benzothiophenes are well separated from the higher aromatic systems and nearly exclusively found in Fraction 1 with insignificant carry-over into the next fraction. The most abundant series of compounds possesses a DBE of 9 and is the dibenzothiophene series. Compounds carrying 5 to 20 alkyl carbons are counted. The next higher series (DBE 10) might consist of the acenaphthenothiophenes ($C_{14}H_{10}S$) or dibenzothiophene with one naphtheno ring or benzothiophenes with a phenyl group as a substituent. The compounds here contain up to 19 alkyl carbons. At higher double bond equivalents, the number of possible ring systems starts rising quite strongly and without further evidence it is questionable how much information speculations as to their identity may reveal. A very low amount of benzonaphthothiophenes or dibenzothiophene with three naphtheno rings is the probable explanation for the presence of compounds of DBE 12.

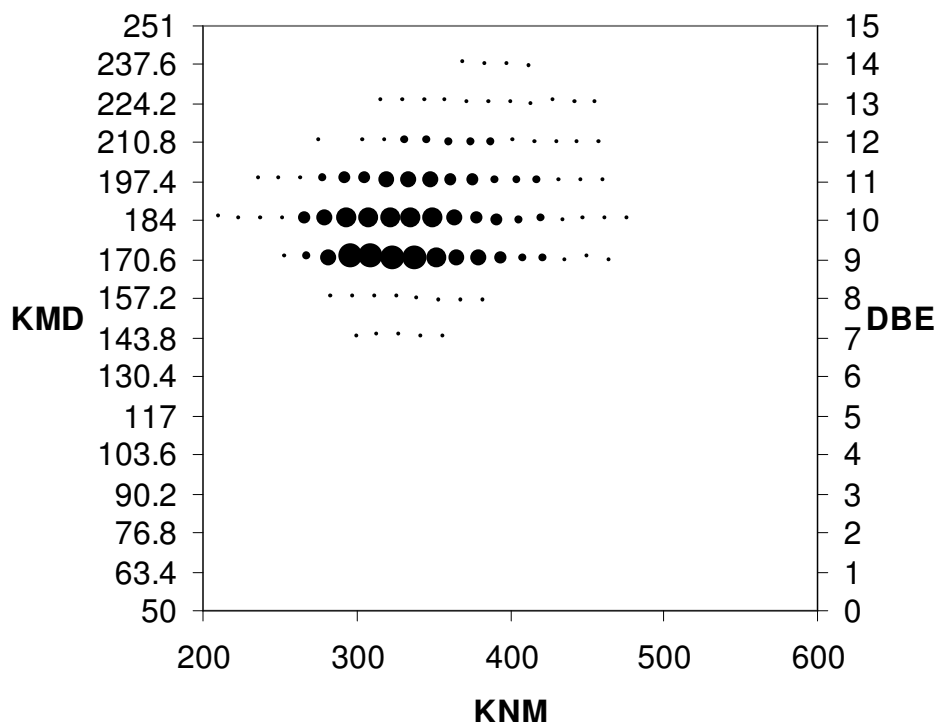


Figure 8.9. Kendrick plot of Fraction 2 from the β -cyclodextrin column.

8.2.5 Fraction 3

This fraction is dominated by compounds of DBE 12 and 13 as can be seen in Figure 8.10. DBE 12 can correspond to the benzonaphthothiophene series which is reasonable since the parent benzonaphthothiophene elutes in this fraction and many substituted benzonaphthothiophenes are known to occur in vacuum gas oils [114]. DBE 13 can represent benzonaphthothiophenes with one naphtheno ring or dibenzothiophenes with one phenyl group as a substituent as well as several other parent systems. Compounds of DBE 9, 10 and 11 were also observed as fairly strong.

The results discussed show that a very useful separation based on the parent aromatic systems on the β -CD phase was possible even from a sample as complex as the VGO. Although two columns were coupled together for enhanced resolution, there is still some overlap between different compound classes as evidenced in the Kendrick plots. A perfectly selective separation into ring classes can certainly not be expected and has also not been achieved on traditional phases like the aminopropano phase even for much simpler real-world samples. The use of reference compounds with a large range of both alkyl group

length and position on the aromatic ring is a prerequisite for studies of this kind but has inherent limitations since one can never know how well the selected reference compounds represent those in a sample of unknown composition.

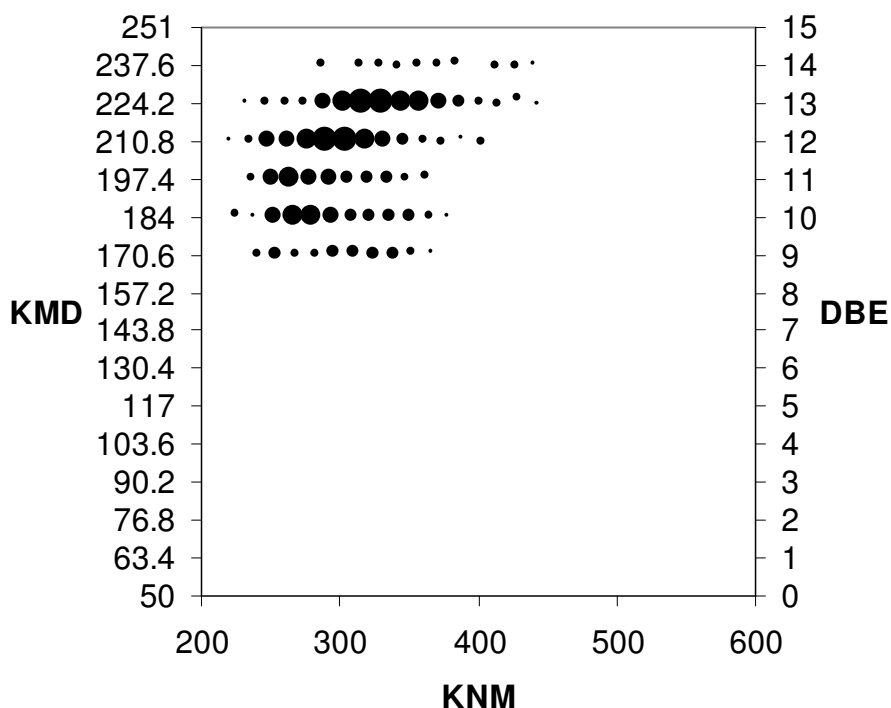


Figure 8.10. Kendrick plot of Fraction 3 from the β -cyclodextrin column.

The use of the Kendrick plots to extract structural information from the mass spectral data is a superior method and is possible because of the ultra-high resolution of the FT-ICR MS technique. This is made obvious through a comparison with traditional techniques. A VGO (boiling range: 340-530 °C) has been examined using GC-MS after a separation of the PASHs on a column containing silica with PdCl_2 . The subsequent liquid chromatographic separation according to the number of aromatic double bonds on silica appears to be inferior to the one reported here on β -CD [114]. In that study, 123 masses were reported for the whole sample and they belonged to only four DBEs in contrast to the twelve that we find here.

It must be recognized that the initial separation of the PAHs and the PASHs on the Pd(II) phase makes the sample considerably easier to investigate than by any HPLC method. The level of sulfur heterocycles is quite high, as is expected for a heavier petroleum fraction. Were an HPLC separation undertaken on the complete polycyclic aromatic fraction, it is

doubtful whether distinct valleys as shown here would appear and a fractionation would be guided by some guesswork.

8.3 Summary

The commercially available chemically bonded β -cyclodextrin stationary phase is introduced here for the separation of polycyclic aromatic compounds according to their number of aromatic double bonds. The efficiency of this phase to separate alkylated polycyclic aromatic sulfur heterocycles was compared with that of traditionally used stationary phases. This phase is highly selective toward the number of aromatic double bonds and is influenced in a fairly uniform manner by the number and length of alkyl groups. However, it is obvious that even so, better phases are still required for an optimal separation of the different classes of aromatics present in these highly complex samples. The difficulty lies in two facts. The first is that the number of parent systems strongly goes up as the distillation temperature increases, as evidenced by the twelve DBEs found in this VGO where each DBE can represent several parent compounds. Each parent system should ideally be completely separated from the others by the HPLC phase. The second complicating factor is the heavy alkylation that is found. Whereas methyl groups seem to increase the retention times in normal-phase LC, probably due to the higher electron density in the aromatic rings, longer alkyl groups, such as those in the aromatic compounds studied here, regularly elute at shorter retention times than their parent systems. The reason is likely to be a combination of their steric effect, making it more difficult for the aromatic rings to interact with the stationary phase, and of the solvation of the alkyl chains by the mobile phase, which is more efficient for longer chains than for methyl groups.

9. Summary

The present demand of energy from petroleum sources and diminishing source of light, sweet crude oils enforces making use of heavy ends of light, sweet crude oils and/or heavy, sour crude oils. Unfortunately, refining of heavy crudes cannot be carried out with presently available technologies, used for light, sweet crudes. Therefore, a heavy amount of expenditure (in the order of billions euro) is expected for the conversion of present technologies to advanced technologies that are suitable for heavy oils. The problem with heavy oils, in refining terms, is the presence of a large number of heterocycles containing N, O and S atoms. Out of them, sulfur, being the most abundant heteroatom in crude oils, poses a major threat, acting as a poison in many catalytic processes involved in secondary refinery processes. Moreover, the stringent limit of sulfur in transportation fuels set by different countries, from an environmental point of view, is continually being lowered. All these combined causes draw attention to the effective sulfur removal from crude oils and its distillates before being used as a source of energy.

In order to remove sulfur effectively from petroleum fractions, it is essential to gain detail structural knowledge of sulfur components in heavy crudes and in the heavy ends of crudes. The isolation and characterization of sulfur compounds in the presence of large number of hydrocarbons always remains a demanding task although many approaches have been attempted for a long time. The analysis of sulfur aromatics in low-boiling fractions, e.g. diesel, is achievable with the presently available analytical protocols. The reason is due to the use of high-resolution gas chromatography, which is not efficient for heavier compounds due to its limitation for non-volatile compounds. Therefore, in the present study, liquid chromatography and high-resolution mass spectrometry have been used for the characterization of the vast number of high molecular weight sulfur heterocycles in fossil fuels.

In the first part, our goal was to separate polycyclic aromatic sulfur heterocycles from polycyclic aromatic hydrocarbons. For the said purpose, a Pd(II)-bonded stationary phase was exploited. However, the Pd(II)-phase was not able to separate all the PASHs from PAHs. Nevertheless, it provided one more dimension in separation among PASHs. With the Pd(II)-bonded phase, PASHs were separated into two fractions depending on the connectivity of aromatic rings to thiophenes. The thiophenes connected with aromatic rings

in a non-condensed fashion are eluted with PAHs whereas the thiophenes connected with aromatic rings in a condensed fashion are eluted separately.

After this first dimension of separation, both the fractions containing sulfur aromatics were characterized by Fourier transform ion cyclotron resonance mass spectrometry, which is a technique that provides ultra-high-resolution and accuracy in mass measurement. However, in MS techniques, an ionization step is necessary to produce ions from any selected group of compounds. In this regard, it is quite essential to consider high molecular weight and non-polar nature of sulfur heterocycles present in heavy oils and in high-boiling fractions. Although there are many soft ionization techniques like electrospray ionization, low-voltage electron ionization and field desorption ionization that have been interfaced with FT-ICR mass spectrometer for the speciation of aromatics in petroleum fractions, none of them has come up as the ultimate tool for the speciation of sulfur heterocycles either due to inefficiency of some techniques or due to limited access of the particular technique. In the present work, two derivatization techniques, namely methylation and phenylation, are introduced for production of charged ions from sulfur compounds selectively without modifying the large numbers of PAHs simultaneously present in the sample. Out of them, methylation, considering all the aspects, was adopted for a variety of samples, namely vacuum gas oils, crude oils and desulfurized vacuum gas oils. After successful methylation, all the samples were characterized by FT-ICR MS. After measurements, the data obtained from mass spectrometry were further sorted with multiple sorting procedures using Kendrick mass scale in order to extract useful information from the complex mass spectrum.

For vacuum gas oil samples, three VGOs having boiling ranges 390-460 °C, 460-520 °C and 520-550 °C, were taken for analysis. Here, separation on the palladium phase and sulfur selective methylation enhance sensitivity to such an extent that it was possible to assign about 900 S1 compounds in the three vacuum gas oils. With increase in boiling temperature, increase in aromaticity and alkylation of sulfur aromatics was observed as reported in the earlier literatures. In addition, the relative abundance of masses at lower double bond equivalents was more pronounced for the low-boiling fraction but the relative abundance shifts towards higher DBEs with increase in boiling temperature.

In case of crude oils, three Saudi Arabian crude oils, namely Arabian Heavy, Arabian Medium, Arabian Light, were included for the investigation. Here it was possible to see a large number of sulfur-containing compounds with respect to both higher mass and larger

aromatic system, which was not possible by earlier studies due to involvement of gas chromatographic technique. The highest DBE was 17 for AH crude oil whereas 14 for both AM and AL. The increase in DBE number indicates presence of large variety of aromatic systems, which are key factors in processing of crude oils. In addition, implementation of liquid chromatographic separation using the Pd(II)-bonded phase aided finding out a number of isomers present in sulfur-enriched crude oil (AH).

In order to understand the fate of sulfur aromatics during the course of hydrodesulfurization, two VGOs, i.e. Feed and Effluent, were studied. In this case, it was clearly observed that the reactivity of different classes of sulfur aromatics towards the HDS process mostly depend on their parent aromatic structures. Benzothiophenes and higher homologous containing one and two naphthenic rings are easily removed in the HDS process whereas dibenzothiophenes and higher homologous are quite recalcitrant and accumulate in the desulfurized product. In the case of non-condensed thiophenes, eluting with PAH from Pd(II)-phase, the trend is different. The compounds having higher DBEs, i.e. more aromatic rings attached to thiophene in a non-condensed way, are easily removed or are saturated to give rise to compounds of lower DBEs initially not present in the sample. In addition, the non-condensed thiophenes found in Effluent fraction may be partially contributed from condensed thiophenes of Feed fraction because of hydrogenation.

However, MS is not able to separate isomers. Therefore, it is quite difficult to deduce the exact carbon skeleton even with most accurate masses obtained from FT-ICR MS. In this regard, three stationary phases, based on different mechanisms, were used for the separation of highly alkylated sulfur heterocycles present in VGO, according to size of their aromatic systems. A large number of reference compounds containing several parent ring systems and different alkylation patterns were first investigated to characterize the retention of polycyclic aromatic compounds likely to occur in high-boiling petroleum samples. A β -cyclodextrin phase was found to be more suitable than chemically bonded aminopropanosilane and tetrachlorophthalimide in normal-phase HPLC with respect to a combination of selectivity towards the number of aromatic double bonds and degree of influence of the alkyl groups of the aromatic compounds. This phase was able to provide a better separation of PASHs into three major fractions corresponding to benzothiophenes, dibenzothiophenes and benzonaphthothiophenes, which were verified by UV spectroscopy and FT-ICR MS,

although there were some overlaps between some classes of compounds due to unresolved base line separation.

10. Zusammenfassung

Der gegenwärtige Energiebedarf aus Erdölquellen und abnehmende Vorkommen leichter, süßer Rohöle erfordert die Nutzung schwerer Fraktionen von leichten, süßen und/oder schweren, sauren Rohölen. Leider kann die Raffination schwerer Rohöle nicht mit den derzeit vorhandenen, für leichte, süße Öle verwendeten Technologien durchgeführt werden. Daher wird ein erheblicher Investitionsaufwand (in der Größenordnung von Milliarden Euros) für die Umrüstung der bestehenden zu weiterentwickelten Technologien, welche für Schweröle geeignet sind betrieben. Die Schwierigkeit bei Schwerölen, im Hinblick auf die Raffinierung, liegt in dem Vorhandensein einer großen Anzahl N-, O- und S-atomhaltiger Heterocyclen. Von diesen stellt Schwefel, das am häufigsten vorkommende Heteroatom in Rohölen, eine bedeutende Gefährdung dar, da es als Gift in vielen katalytischen Prozessen der nachgeschalteten Raffinierung wirkt. Zudem wird der strenge, in verschiedenen Staaten festgelegte Schwefelgrenzwert in Transportkraftstoffen aus umweltpolitischen Gesichtspunkten ständig abgesenkt. Alle diese gemeinsamen Gründe lenken die Aufmerksamkeit auf eine effektive Schwefelentfernung aus Rohölen und seinen Destillaten vor ihrer Nutzung als Energiequelle.

Um Schwefel effektiv aus Erdölfraktionen zu entfernen, ist es notwendig, genaue Strukturkenntnisse über die Schwefelverbindungen in schweren Rohölen und Schwersiedern zu erlangen. Die Isolierung und Charakterisierung der Schwefelverbindungen neben einer großen Anzahl von Kohlenwasserstoffen bleibt immer eine anspruchsvolle Aufgabe, obwohl seit langem viele Methoden versucht worden sind. Die Analyse der Schwefelaromaten in niedrig siedenden Fraktionen wie Diesel ist mit gegenwärtig vorhandenen Analysevorschriften erreichbar. Der Grund ist der Einsatz hochauflösender Gaschromatographie, welche für höhermolekulare Verbindungen aufgrund seiner Beschränkung für nichtflüchtige Verbindungen nicht einsatzfähig ist. Daher ist in der vorliegenden Untersuchung Flüssigchromatographie kombiniert mit Massenspektrometrie für die Charakterisierung zahlreicher hochmolekularer Schwefelaromaten eingesetzt worden.

Im ersten Teil war unser Ziel, die polycyclischen aromatischen Schwefelheterocyclen (PASHs) von den polycyclischen aromatischen Kohlenwasserstoffen (PAHs) zu trennen. Zu diesem Zweck wurde eine Pd(II)-gebundene stationäre Phase ausgenutzt. Dennoch war die Pd(II)-Phase nicht in der Lage, alle PASHs von den PAHs abzutrennen. Trotzdem bietet sie

eine zusätzliche Dimension bei der Auftrennung unter den PASHs. Mit der Pd(II)-gebundenen Phase wurden die PASHs in zwei Fraktionen getrennt, abhängig von der Konnektivität der aromatischen zu den Thiophenringen. Thiophene, welche mit aromatischen Ringen in nicht-kondensierter Weise verbunden sind, eluieren gemeinsam mit den PAHs, während Thiophene mit kondensierten aromatischen Ringen getrennt eluieren.

Nach dieser ersten Trenndimension wurden beide schwefelaromatenhaltige Fraktionen mit Hilfe der Fourier-Transform-Ionencyclotronresonanz-Massenspektrometrie (FT-ICR MS) charakterisiert, welche eine Technik darstellt, die ultrahohe Auflösung und Genauigkeit in der Massenbestimmung liefert. Dennoch ist für MS Techniken ein Ionisierungsschritt notwendig, um Ionen von ausgewählten Verbindungsgruppen zu erzeugen. In dieser Hinsicht ist es unumgänglich, das hohe Molekulargewicht und die Unpolarität der in Schwerölen und hochsiedenden Fraktionen vorhandenen Schwefelheterocyclen zu berücksichtigen. Trotz vieler weicher Ionisierungstechniken wie Elektrospray, Nieder-eV-Elektronenstoß und Felddesorption, welche mit FT-ICR Massenspektrometern für die Speziation von Aromaten in Erdölfraktionen gekoppelt worden sind, konnte sich keines von diesen als an geeignetes Instrument für die Speziation von Schwefelaromaten durchsetzen – sei es aus Leistungsschwäche oder aus mangelnder Verbreitung der Technik. In dieser Doktorarbeit werden zwei Derivatisierungstechniken, nämlich Methylierung und Phenylierung, für die selektive Erzeugung geladener Ionen aus Schwefelverbindungen eingeführt, ohne die große Anzahl an PAHs zu verändern, welche gleichzeitig in der Probe vorhanden sind. Von diesen wurde die Methylierung, unter Berücksichtigung aller Gesichtspunkte, für eine Probenreihe übernommen, und zwar für Vakuumgasöle, Rohöle und entschwefelte Vakuumgasöle. Nach erfolgreicher Methylierung wurden alle Proben mit Hilfe der FT-ICR MS charakterisiert. Die aus den Messungen erhaltenen Rohdaten wurden weiterhin mit Hilfe von multiplen Sortieralgorithmen geordnet, unter Verwendung der Kendrick-Massenskala geordnet, um aus dem komplexen Massenspektrum Informationen zu extrahieren.

Von den Vakuumgasölen (VGO) wurden drei VGOs mit den Siedebereichen 390-460 °C, 460-520 °C und 520-550 °C analysiert. Die Trennung auf der Palladiumphase und die schwefelselektive Methylierung erhöhen die Empfindlichkeit in solchem Ausmaß, dass das Zuordnen von über 900 S1 Verbindungen in den drei Vakuumgasölen möglich ist. Mit Zunahme der Siedetemperatur wurde eine Zunahme in Aromatizität und Alkylierungsgrad bei den Schwefelaromaten beobachtet, wie zuvor in Literaturstellen

berichtet. Des Weiteren war die relative Häufigkeit bei Massen mit niedrigen Doppelbindungsäquivalenten (DBEs) bei der niedrigsiedenden Fraktion stärker ausgeprägt, die relative Häufigkeit verlagert sich jedoch mit dem Anstieg der Siedetemperatur zu höheren DBEs.

Im Fall der Rohöle wurden drei saudi-arabischen Öle für die Untersuchung berücksichtigt, und zwar Arabian Heavy, Arabian Medium und Arabian Light. Hierbei war es möglich, eine große Anzahl schwefelhaltiger Verbindungen hinsichtlich hoher Massen und ausgedehnter aromatischer Systeme zu entdecken, was durch frühere Untersuchungen aufgrund des Einsatzes gaschromatographischer Techniken nicht möglich war. Das höchste Doppelbindungsäquivalent betrug 17 für das Erdöl AH gegenüber 14 für AM und AL. Der Anstieg der DBE-Zahl zeigt die Anwesenheit einer großen Vielzahl aromatischer Systeme, welche Schlüsselfaktoren in der Erdölverarbeitung darstellen. Zusätzlich trägt die Verwendung der flüssigchromatographischen Trennung mit der Pd(II)-gebundenen Phase dazu bei, eine Isomerenanzahl in einem schwefelreichen Rohöl (AH) zu eruieren.

Zum Verstehen des Verbleibs der Schwefelaromaten während des Hydro-entschwefelungsprozesses werden zwei VGOs („Feed“ und „Effluent“) untersucht. In diesem Fall wurde deutlich beobachtet, dass die Reaktivität verschiedener Schwefelaromatenklassen gegenüber dem HDS Prozess am stärksten von ihren aromatischen Grundstrukturen abhängig sind. Benzothiophene und höhere Homologe mit einem und zwei naphthenischen Ringen werden leicht während des HDS Prozesses entfernt, während Dibenzothiophene und höhere Homologe recht resistent sind und sich in dem entschwefelten Produkt anreichern. Im Falle der nichtkondensierten Thiophene, welche gemeinsam mit den PAH von der Pd(II)-Phase eluieren, ist der Trend umgekehrt. Die Verbindungen mit höheren DBEs, das heißt mit mehreren aromatischen, nicht am Thiophen kondensierten Ringen werden leicht entfernt oder werden gesättigt, was zu Verbindungen mit niedrigerem DBE führt, welche ursprünglich nicht in der Probe vorhanden waren. Außerdem könnten solche nichtkondensierte Thiophene in der „Effluent“-Fraktion teilweise von kondensierten Thiophenen aus dem „Feed“ infolge von Hydrierung herrühren.

Dennoch kann die Massenspektrometrie keine Isomere trennen. Daher ist es recht schwierig, das bestimmte Kohlenstoffgerüst herzuleiten, auch mit den höchst exakten Massen aus der FT-ICR MS. In diesem Zusammenhang wurden drei stationäre Phasen mit unterschiedlichen Trennmechanismen für die Trennung hochalkylierter Schwefel-

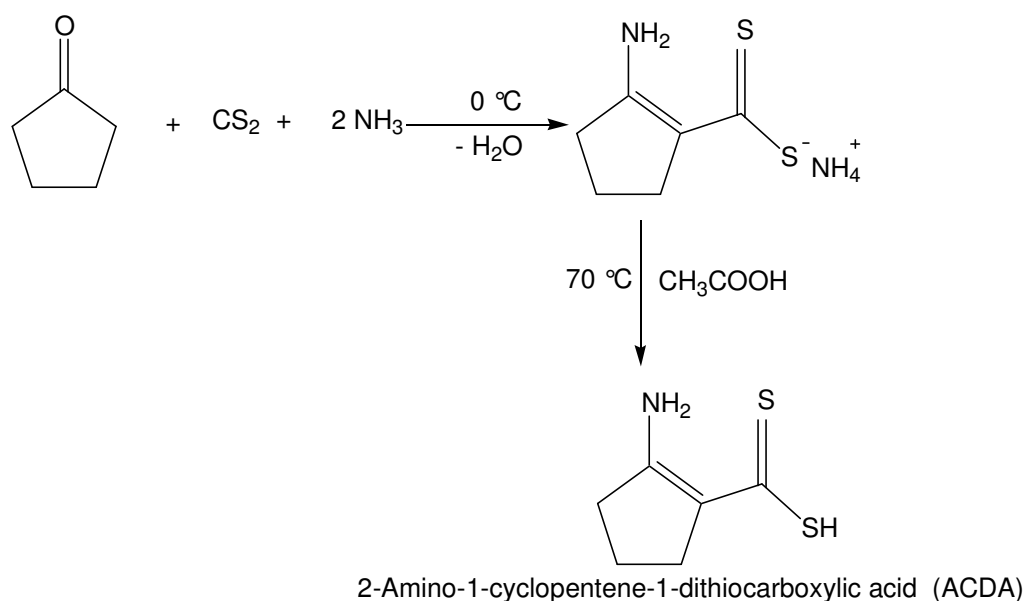
heterocyclen in Vakuumgasöl nach Größe ihrer aromatischen Systeme verwendet. Eine beträchtliche Anzahl an Referenzverbindungen mit mehreren Grundsystemen und verschiedenen Alkylierungsmustern wurden zunächst untersucht, um das Retentionsverhalten von polycyclischen Aromaten zu charakterisieren, welche wahrscheinlich in hochsiedenden Erdölproben vorkommen. Eine β -Cyclodextrinphase stellte sich als geeigneter als chemisch gebundenes Aminopropanosilan und Tetrachlorphthalimid in der Normalphasenflüssigchromatographie heraus, sowohl hinsichtlich der Selektivität zur Zahl aromatischer Doppelbindungen als auch zum Einfluss der Alkylgruppen der aromatischen Verbindungen. Diese Phase ermöglichte eine bessere Trennung der PASH in drei Hauptfraktionen gemäß Benzothiophenen, Dibenzothiophenen und Benzonaphthothiophenen, welche durch UV Spektroskopie und FT-ICR MS bestätigt wurden, obwohl es zu einigen Überschneidungen zwischen einigen Verbindungsklassen aufgrund der Nichtbasislinientrennung kam.

11. Appendix

11.1 Synthesis of Pd(II)-ACDA Silica Gel [109-111]

11.1.1 Synthesis of 2-Amino-1-cyclopentene-dithiocarboxylic Acid (ACDA)

A mixture of cyclopentanone (12.5 g, 150 mmol), carbon disulfide (15 g, 195 mmol), and 150 mL of aqueous ammonia (25 %) was stirred at 0 °C for 8 h. The yellow solid product was collected, washed with ether, and dried. The crude product was recrystallized from ethanol. 5 g of the ammonium salt of ACDA was dissolved in 50 mL of acetic acid at 70 °C. Ammonia gas evolved. The resulting solution was cooled and water was added until the solution became turbid. The yellow solid material which separated from the solution was collected and recrystallized from methanol.



CHNS analyses of ACDA

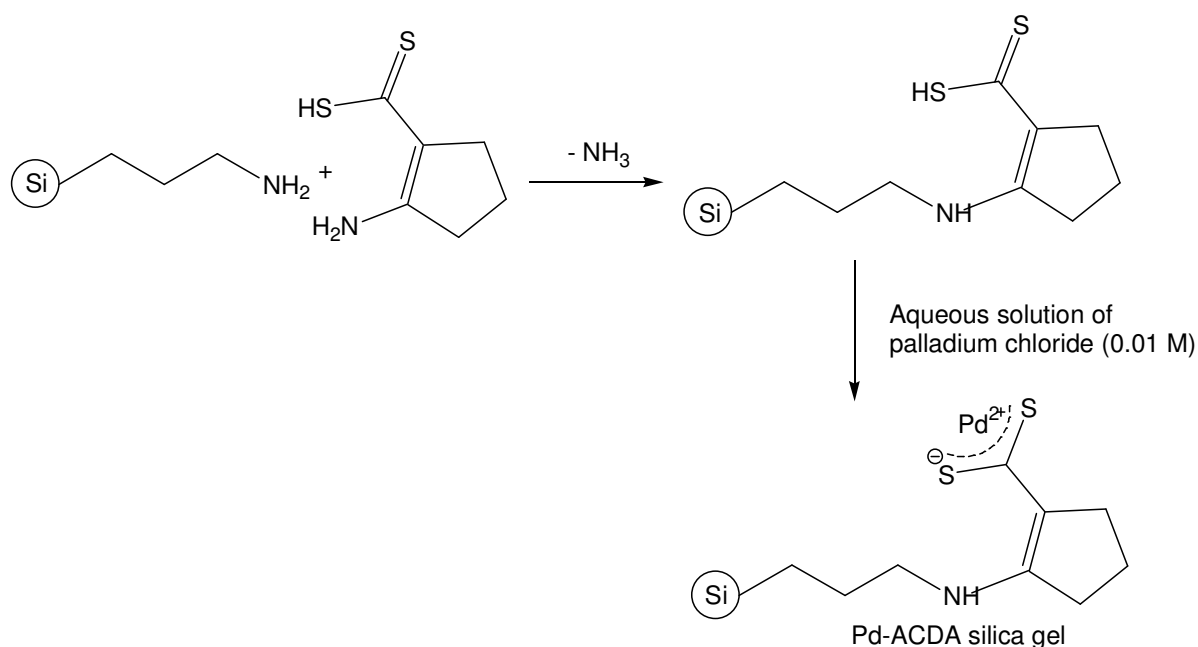
	C (%)	H (%)	N (%)	S (%)
Calculated	45.3	5.7	8.8	40.2
Measurement 1	45.2	5.5	8.7	39.9
Measurement 2	45.0	5.5	8.7	40.2

11.1.2 Synthesis of Aminopropano Silica Gel

10 g of LiChrosorb Si 100 (10 μm , dried at 130 $^{\circ}\text{C}$ for 24 h) was refluxed with 12.5 mL of 3-aminopropanotrimethoxysilane in 50 mL dry toluene. The resulting product was filtered off and washed successively with toluene and methanol. The obtained aminopropano silica gel was dried at 50 $^{\circ}\text{C}$ in an oven.

11.1.3 Synthesis of ACDA-functionalized Silica Gel

10 g of aminopropano silica gel was added to a solution of 1.6 g of ACDA dissolved in 25 mL of methanol and refluxed for 5 h. The apparatus was purged with nitrogen during the reaction. After cooling to room temperature, the ACDA bonded silica was filtered off and washed with methanol.



CHNS analyses of ACDA-functionalized silica gel

Measurement	C (%)	H (%)	N (%)	S (%)
First	6.9	1.4	1.1	1.9
Second	6.9	1.4	1.1	1.9
Third	6.9	1.4	1.1	1.9

2.5 g of ACDA-bonded silica was further treated with 250 mL aqueous solution of palladium chloride (0.01 M) in a 500 mL conical flask in order to obtain Pd(II)-ACDA silica gel.

11.2 Synthesis of Pd(II)-Mercaptopropano Silica Gel [121]

Silica gel (LiChrosorb Si 100, 10 μm) was dried at 130 $^{\circ}\text{C}$ for 24 h. 10 g of dried silica gel was refluxed in a solution of 15 mL 3-mercaptopropanotrimethoxysilane in 50 mL dry toluene for 5 h. The resulting bonded silica gel was filtered off and was washed with toluene and methanol successively. The obtained mercaptopropano silica gel (MPS) was dried at 50 $^{\circ}\text{C}$ in an oven.

CHS analyses of MPS

Measurement	C (%)	H (%)	S (%)
First	3.4	1.3	1.8
Second	3.4	1.3	1.9
Third	3.4	1.3	1.9

2.5 g of MPS was further treated with 250 mL aqueous palladium chloride solution (0.01 M) for 12 h. The palladium bonded silica phase was filtered off, washed successively with water, isopropanol and cyclohexane, and dried in vacuo at room temperature.

11.3 Synthesis of Tetrachlorophthalimide Silica Gel [38]

11.3.1 Synthesis of Tetrachlorophthalicmonoallylamide-allylammonium Salt

7.15 g of tetrachlorophthalic anhydride was added to 11.4 g of allylamine. The reaction was allowed to stand until the exothermic reaction stopped. Then, the reaction mixture was refluxed until all of tetrachlorophthalic anhydride dissolved. After that, the excess of allylamine was removed under vacuum. The white crystalline residue obtained was the allyl ammonium salt.

11.3.2 Synthesis of Tetrachlorophthalicallylimide

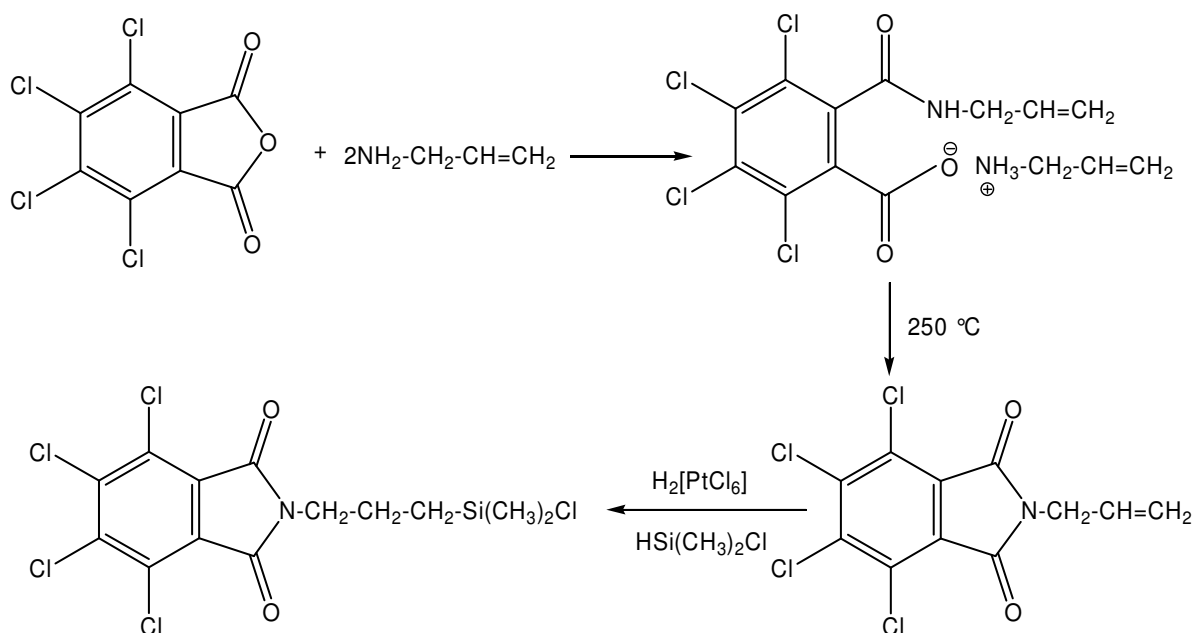
9 g raw allyl ammonium salt was heated at 250 $^{\circ}\text{C}$ in a round bottom flask. After the salt melted, it was heated another 10 minutes. The solid dark brown product was taken for further reaction.

11.3.3 Synthesis of Tetrachlorophthalimidopropanodimethylchlorosilane

7.5 g of tetrachlorophthalicallylimide, 6.65 g of freshly distilled $(\text{CH}_3)_2\text{HSiCl}$ and 22 drops of a 0.1 molar solution of $\text{H}_2[\text{PtCl}_6]$ in isopropanol were dissolved in 75 mL of absolute dichloromethane and refluxed in dry argon atmosphere for 24 h. After that, excess $(\text{CH}_3)_2\text{HSiHCl}$ and solvent were removed under vacuum. The yellow solid residue obtained was washed in the flask with a small amount of dichloromethane. Dichloromethane was decanted and the product was instantly dissolved in fresh 100 mL absolute dichloromethane.

11.3.4 Synthesis of Tetrachlorophthalimidopropanosilica (TCP-silica)

7.5 g of LiChrosorb Si 100 (10 μm) was suspended in the above mentioned solution. To it, 15 mL of absolute quinoline was added and the mixture was refluxed for 48 h in argon atmosphere. After that, all solid particles were removed from the solution by filtering the mixture through a glass filter. The modified silica gel was washed with 50 mL toluene, 50 mL dichloromethane, 50 mL methanol and 50 mL acetone successively and was dried at 80 $^\circ\text{C}$ for 12 h.

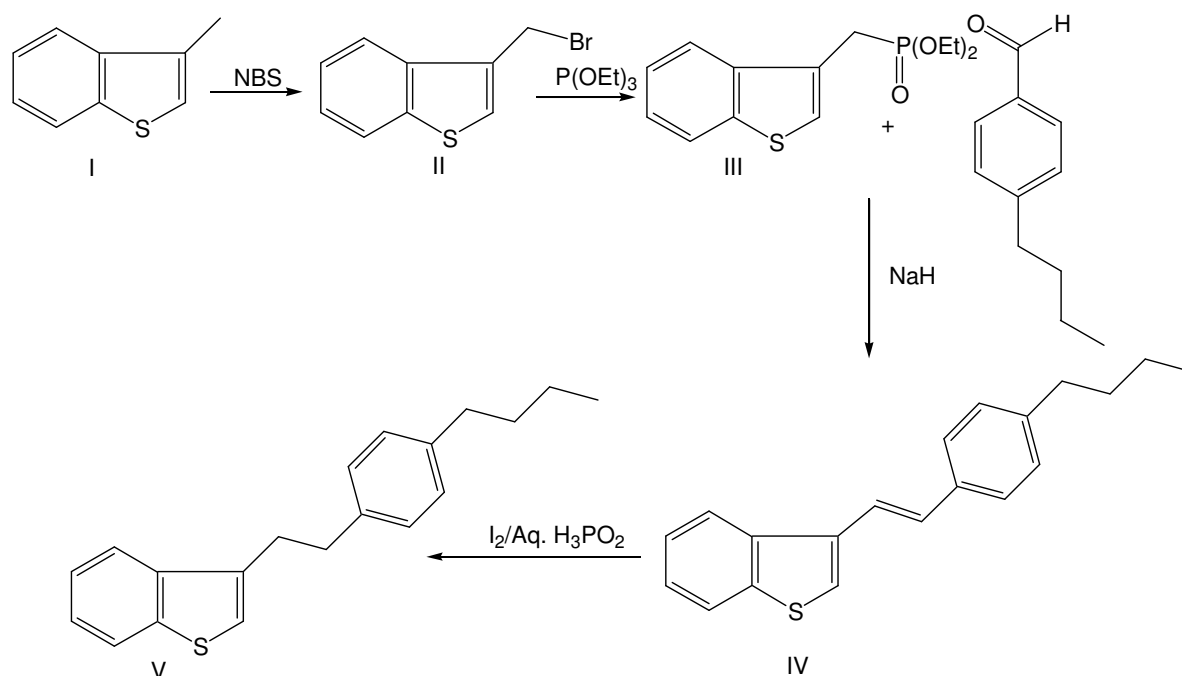


CHN analyses of TCP-silica

Measurement	C (%)	H (%)	N (%)
First	5.4	1.1	0.5
Second	5.5	1.1	0.8
Third	5.4	1.1	0.7

11.4 Synthesis of Model Thiophenic Compounds

11.4.1 Synthesis of 3-[(4-Butylphenyl)ethano]benzo[*b*]thiophene [136-138]



The reaction was continued from intermediate III as it was obtained as a gift. A dry, 25 mL, three-necked flask equipped with magnetic stirrer and condenser was purged with dry nitrogen. About 0.168 g of a 55-65 % dispersion of sodium hydride in mineral oil was added to the flask. The oil was washed with 2 x 2 mL toluene. The mixture was allowed to stir for 5 minutes. Then, about 1 g (3.5 mmol) of the intermediate III was added to it over a 5-10 minute period. During the addition, the reaction was continued at room temperature. After the complete addition, the mixture was stirred for 30 minutes to ensure complete reaction. To this about 0.63 g (3.5 mmol) of 90 % pure 4-butylbenzaldehyde was added using a syringe over a 5-10 minute period. During the addition the temperature was maintained at 20-30 °C by appropriate cooling with an ice bath. Then, the reaction mixture was heated at 60-65 °C

for 15 minutes. The resulting product was cooled to room temperature and the mother liquor was decanted. About 1 g (3.42 mmol) of crude gummy precipitate (IV) was treated with 1 g (3.94 mmol) iodine in 20 mL acetic acid. The reaction apparatus was flushed with nitrogen. Then, 2 mL of hypophosphorous acid (50 % aq.) was added and the reaction mixture was heated under reflux. After 24 h the reaction mixture was quenched with 50 mL water and extracted with toluene. The organic extracts were washed with aq. NaHCO_3 and dried over MgSO_4 .

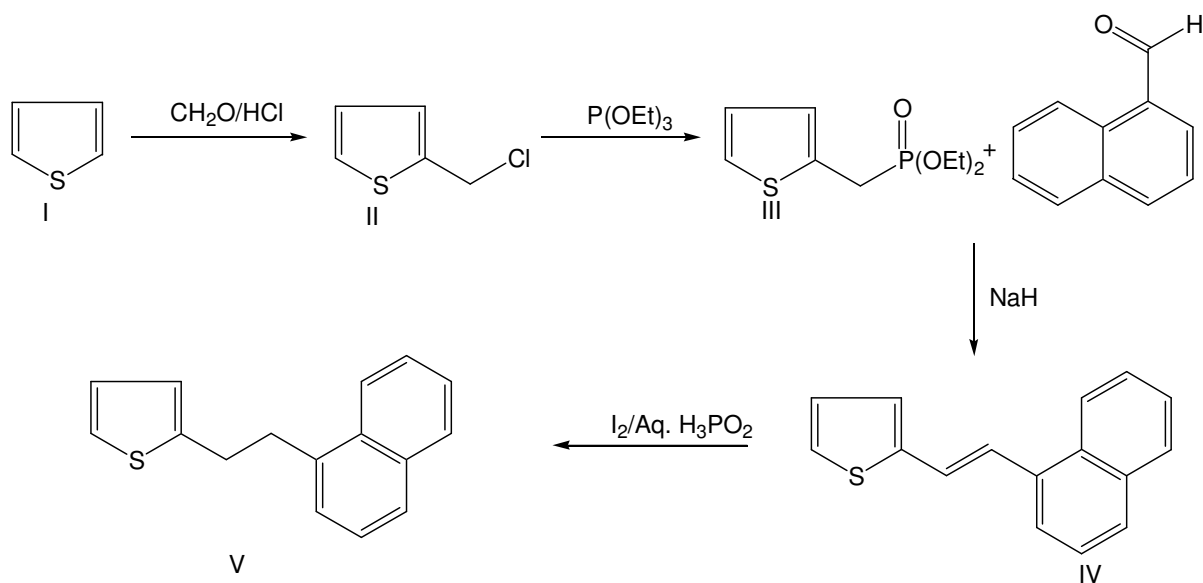
Purity: 90 % (GC)

MS (EI, 70 eV): 294 (40 %, M^+), 147 (100 %, $\text{M}^+ - \text{C}_{11}\text{H}_{15}$)

^1H NMR (200 MHz, CDCl_3) δ = 1.06 (t, J = 7.0 Hz, 3 H; CH_3), 1.47 (septet, J = 7.3 Hz, 2 H; CH_2CH_3), 1.63-1.80 (m, 2 H; $\text{CH}_2\text{CH}_2\text{CH}_3$), 2.72 (t, J = 7.6 Hz, 2 H; $\text{CH}_2\text{CH}_2\text{CH}_2\text{CH}_3$), 3.10-3.18 (m, 2 H; ArCH_2), 3.22-3.21 (m, 2 H; ArCH_2CH_2), 6.89 (s, 1H; SCH), 7.05-8.00 ppm (m, 8 H; Ar)

$^{13}\text{C}\{^1\text{H}\}$ NMR (50 MHz, CDCl_3) δ = 13.98 (CH_2CH_3), 22.37 (CH_2CH_3), 30.62 (ArCH_2CH_2 -), 33.72 ($\text{CH}_2\text{CH}_2\text{CH}_3$), 35.04 ($\text{CH}_2\text{CH}_2\text{CH}_2\text{CH}_3$), 35.23 (ArCH_2CH_2), 121.27 (SCH), 121.58 (SCCH), 122.85 (SCCCH), 123.81 (SCCCHCH), 124.13 (SCCHCH), 128.23 (benzothiophene- $\text{CH}_2\text{CH}_2\text{CCH}$ -), 128.44 (benzothiophene- $\text{CH}_2\text{CH}_2\text{CCHCH}$), 136.28 (SCHC), 138.78 ($\text{CH}_3\text{CH}_2\text{CH}_2\text{CH}_2\text{C}$), 140.40 (benzothiophene- $\text{CH}_2\text{CH}_2\text{C}$), 140.62 (SC), 141.11 ppm (SCC).

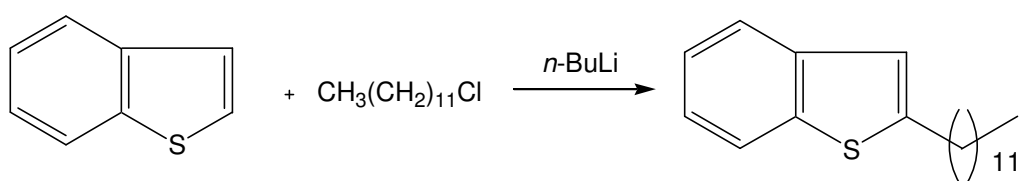
11.4.2 Synthesis of 2-(1-Naphthylethano)thiophene [138-139]



The intermediate IV was obtained as a gift. About 1 g (4.23 mmol) of 2-(1-Naphthylethene)thiophene (IV) was treated with 1 g (3.94 mmol) iodine in 20 mL acetic acid. The reaction apparatus was flushed with nitrogen. Then, 2 mL of hypophosphorous acid (50 % aq.) was added and the reaction mixture was heated under reflux. After 24 h, the reaction mixture was quenched with 50 mL water and extracted with toluene. The organic extracts were washed with aq. NaHCO_3 and dried over MgSO_4 .

MS (EI, 70 eV): 238 (60 %, M^+), 141 (100 %, $\text{M}^+ - \text{C}_5\text{H}_5\text{S}$)

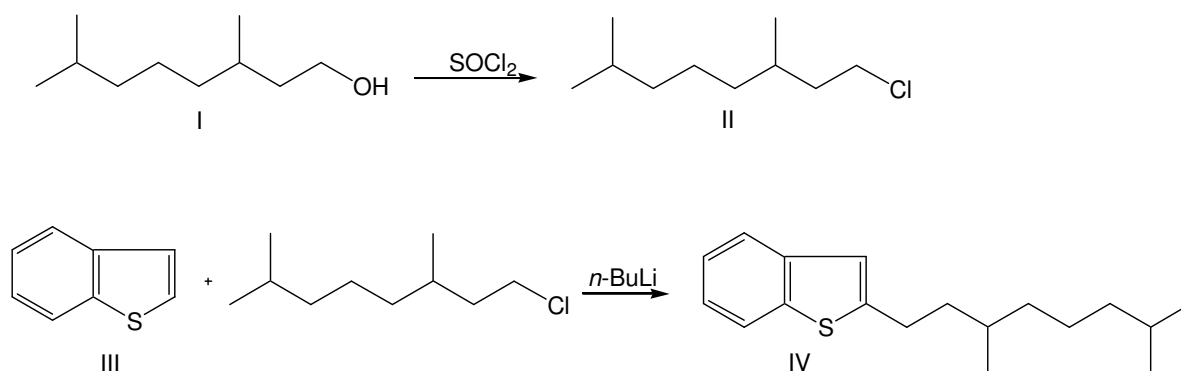
11.4.3 Synthesis of Dodecylbenzothiophene [140,141]



About 1 g (7.46 mmol) of benzothiophene was taken in a dry three-necked flask. Then, 20 mL of dry tetrahydrofuran was added to it. The solution was purged with nitrogen. The temperature was kept at 0 °C. To the solution, 4 mL of 2.5 M *n*-BuLi was added and it was allowed to react for 15 minute. After that, 2.04 g of dodecylchloride was added through a syringe over a period of 10 minute. Then the reaction was quenched with distilled water after 1 h. The product was extracted with 3 x 10 mL of diethylether. The solvent was evaporated and the product was collected.

MS (EI, 70 eV): 302 (50 %, M^+), 148 (100 %, $\text{M}^+ - \text{C}_{11}\text{H}_{22}$)

11.4.4 Synthesis of 2-(3,7-Dimethyloctyl)benzothiophene [140-142]



About 7.9 g (50 mmol) of 3,7-dimethylchlorooctanol was taken in a dry two-necked flask. To it, 3.95 g (50 mmol) of dry pyridine was added. After that, addition of 8.33 g (70 mmol) of thionyl chloride was added over a period of 30 minutes. The mixture was heated at

60-90 ° C for 4 h. The crude product was washed with dilute hydrochloric acid, dried with anhydrous potassium carbonate. The solvent was removed under reduced pressure. About 1 g (7.46 mmol) of benzothiophene was taken in a dry three-necked flask. Then, 20 mL of dry ether was added to it. The solution was purged with nitrogen. The temperature was kept at 0 °C. To the solution, 6 mL of 1.6 M *n*-BuLi was added and it was allowed to react for 15 minutes. After that, 1.5 g of 3,7-dimethylchlorooctane was added through a syringe over a period of 10 minutes. Then the reaction was refluxed for 1 h. After that, the reaction was quenched with distilled water. The product was extracted with 3 x 10 mL of diethylether and dried over MgSO₄.

MS (EI, 70 eV): 274 (20 %, M⁺), 148 (100 %, M⁺ - C₉H₁₈)

11.5 Instrumental Parameters

11.5.1 HPLC Instrumentation

Knauer Wellchrom

Knauer HPLC system consists of an interface box, 4 channel solvent degasser, two Ministar K 501 analytical pumps, a mixing chamber, an electrical injection valve or basic marathon plus autosampler and a variable wavelength detector. Instrument control and data recording were done with Chromgate version 2.8 (Knauer, 14163 Berlin, Germany).

HP 1050

Hewlett-Packard 1050 HPLC system with a quaternary pump, degasser, manual injection valve and a diode array detector set to record the UV spectra from 200 to 500 nm. Instrument control and data recording were done with Chemstation version 9.03 (Agilent, 71034 Böblingen, Germany).

11.5.2 Gas Chromatographs

GC-FID

Gas Chromatograph:	Hewlett-Packard 5890 II
Autosampler:	Gerstel MPS 2L
Injector:	Split/Splitless (60 s)
Injector temperature:	280 °C
Detector temperature:	300 °C
Capillary column:	VF5ms (Varian), 30 m x 0.25 mm x 0.25 µm
Carrier gas:	Hydrogen (4.8)
Temperature program:	60 °C – 2 min – 10 °C/min – 300 °C – 5min
Injection volume:	1 µL

GC-AED

Gas Chromatograph:	Agilent 6890N
Atomic emission detector:	Agilent G2350A
Autosampler:	Gerstel MPS 2L
Injector:	Gerstel cold injection system
Transfer line:	300 °C
Capillary column:	VF5ms, 30 m x 0.25 mm x 0.25 µm
Carrier gas:	Helium
Temperature program:	60 °C – 2 min – 10 °C/min – 300 °C – 5min
Injection volume:	1 µL

GC-MS

Gas Chromatograph:	Finnegan MAT GCQ
Mass spectrometer:	Finnegan MAT GCQ Polaris MS
Autosampler:	CTC A200S Liquid Sampler
Injector:	Split/Splitless (60 s)
Injector temperature:	260 °C
Capillary column:	J&W DB 17ms, 29.5 m x 0.25 mm x 0.25 µm
Transfer line:	275 °C
Carrier gas:	Helium (5.8)
Ionization conditions:	EI, 70 eV, Ion source 200 °C
Modus:	Full scan (50-600 amu)
Temperature program:	60 °C – 2 min – 10 °C/min – 300 °C – 5min
Injection volume:	1 µL

11.5.3 FT-ICR MS

Mass spectra were acquired using an APEX III Fourier transform ion cyclotron resonance mass spectrometer (Bruker Daltonics, Bremen, Germany) equipped with a 7 T actively shielded super conducting magnet and an Agilent ESI source. The samples were introduced in a 1:1 (v/v) solution of dichloromethane/acetonitrile and injected in the infusion mode with a flow rate of 2 $\mu\text{L}/\text{min}$ detecting positive ions. The spray voltage was maintained at 4.5 kV. After ionization, the ions were accumulated for 0.5 s in the octapole before transfer to the cyclotron cell. For a better signal-to-noise ratio, at least 64 scans were accumulated. Internal and external calibrations were done using a mixture of the Agilent electrospray calibration solution of masses 622.02896 and 922.00980 with the addition of indolacrylic acid of masses 397.11589 $[2M+\text{Na}]^+$ and 584.17923 $[3M+\text{Na}]^+$ covering the whole range of masses in the samples. All the measurements by FT-ICR mass spectrometer were performed in collaboration with Max-Planck-Institute of coal research, Mülheim, Germany.

11.5.4 Elemental Analyses or CHNS Analyses

Vario EL III CHNOS elemental analysis system (Service Department in the Institute of Inorganic and Analytical Chemistry)

11.6 Materials

Acetic acid	96 %	Merck
Allyl amine	98 %	Aldrich
Aluminium oxide	for chromatography	Fluka
Aminopropanosilica	for HPLC	in house
Ammonia	25 %	Grüssing
Benzo[<i>b</i>]naphtho[2,1- <i>d</i>]thiophene	98 %	in house
Benzothiophene	95 %	Aldrich
<i>n</i> -Butyllithium	1.6 M in hexane	Merck
<i>tert</i> -Butylmethylether	p.a.	Merck
Carbon disulfide	n.a.	Aldrich
Copper(II)acetate	99 % (anhydrous)	Acros Organics
Cyclohexane	99.8 %	Fluka
Cyclopentanone	99 %	Aldrich
Dibenzothiophene	98 %	Aldrich
Dichloromethane	99.8 %	Riedel de Haen
Diethylether	p.a.	in house
Dimethylchlorosilane	98 %	Janssen Chimica
Diphenyliodoniumtrifluoromethane sulfonate	97 %	Alfa Aesar
Ethanol	p.a.	in house
Helium	5.8	Institute supply
Helium	He GC BiP	Air products
<i>n</i> -Heptane	99 %	Grüssing
Hexachloroplatinic acid	> 99 %	Alpha
Hydrochloric acid	37 %	Grüssing
Hypophosphorous acid	50 %	Aldrich
Isopropanol	99.8 %	Fluka
Magnesium sulfate(water free)	p.a.	in house
Methanol	p.a.	in house
Methyliodide	99 %	Merck
Nitrogen	Purity 4.6	Institute supply
Palladium(II)chloride	59 %	Acros Organics
Polyphosphoric acid	83 %	Fluka
Potassium hydroxide	p.a.	Grüssing
Pyridine	99 %	Aldrich
Quinoline	technical grade	in house
Silica 10 µm 100 Å	for HPLC	Merck
Silicagel 60	for chromatography	Fluka
Silver tetrafluoroborate	98 %	Aldrich
Sodium bicarbonate	p.a.	in house
Sodium carbonate	p.a.	in house
Sodium hydride	55-65 %	Fluka

Sodium hydroxide	p.a.	Merck
Sodium sulfate	p.a.	Merck
Tetrachlorophthalic anhydride	98 %	Acros Organics
Toluene	99.8 %	Fluka
1,2,3,4-Tetrahydrodibenzothiophene	> 98 %	In house
1,2-Dichloroethane	99.5 %	Fluka
2-Methylbenzothiophene	98 %	in house
2-Methyldibenzothiophene	> 98 %	In house
2-Octyldibenzothiophene	n.a.	in house
3-Aminopropyltrimethoxysilane	97 %	Aldrich
3-Mercaptopropyltrimethoxysilane	97 %	Aldrich
4,6-Dimethyldibenzothiophene	> 98 %	In house
4-Butylbenzaldehyde	90 %	Aldrich

11.7 Abbreviations

AED	Atomic emission detector
AH	Arabian heavy
AL	Arabian light
AM	Arabian medium
AP	Aminopropano
APCI	Atmospheric pressure chemical ionization
API	American petroleum institute
APPI	Atmospheric pressure photo ionization
aq.	Aqueous
CI	Chemical ionization
β -CD	β -Cyclodextrin
Da	Dalton
DBE	Double bond equivalent
DBT	Dibenzothiophene
DCE	1,2-Dichloroethane
DRIFT	Diffuse reflectance infrared spectroscopy
EI	Electron impact ionization
ESI	Electrospray ionization
eV	electron Volt
FCC	Fluid catalytic cracking
FD	Field desorption
FI	Field ionization
FT-ICR MS	Fourier transform ion cyclotron resonance mass spectrometry
FWHM	Full width of the peak at half maximum intensity
GC	Gas chromatography
h	Hour(s)
HDS	Hydrodesulfurization
HPLC	High performance liquid chromatography
ICR	Ion cyclotron resonance
IP	Ionization potential
IR	Infrared
IUPAC	International Union of Pure and Applied Chemistry
KE	Kinetic energy
KM	Kendrick mass
KMD	Kendrick mass defect
KNM	Kendrick nominal mass
kV	Kilovolt
LC	Liquid chromatography
LDI	Laser desorption ionization
LEC	Ligand exchange chromatography
MALDI	Matrix assisted laser desorption ionization
mDa	Millidalton
mmol	Millimole
MPS	Mercaptopropanosilica gel
MS	Mass spectrometry
NBS	N-Bromosuccinimide
NMR	Nuclear magnetic resonance

OPEC	Organisation of the Petroleum Exporting Countries
OSC	Organic sulfur compounds
p.a.	Pro analyse
PAC	Polycyclic aromatic compounds
PAHs	Polycyclic aromatic hydrocarbons
PASHs	Polycyclic aromatic sulfur heterocycles
PB	Particle beam
ppb	Parts per billion
ppm	Parts per million
R	Resolution
SARA	Saturates, aromatics, resins and asphaltenes
SEC	Size exclusion chromatography
TCP	Tetrachlophthalimide
TLC	Thin layer chromatography
TOF	Time of flight
UV	Ultraviolet
v/v	Volume per volume
VGO	Vacuum gas oil
XANES	X-ray absorption near edge structure
XPS	X-ray photoelectron spectroscopy

12. References

- [1] <http://www.energy.gov/energysources/oil.htm>, accessed 17 October 2006.
- [2] Marshall, A. G.; Rodgers, R. P., Petroleomics: The next grand challenge for chemical analysis. *Accounts of Chemical Research* **2004**, 37, 53-59.
- [3] Czogalla, C. D.; Boberg, F., Sulfur compounds in fossil fuels. I. Annulated thiophenes in crude oils, oil shales, tar sands, syncrudes, and extracts from coals. *Sulfur Reports* **1983**, 3, 121-167.
- [4] Janssen, A. J. H.; Keizer, A. D.; Kleinjan, W. E., *Elemental sulfur and sulfur-rich compounds I*. Springer Berlin / Heidelberg: Berlin, 2003; Vol. 230, p 167-188.
- [5] Cyr, T. D.; Payzant, J. D.; Montgomery, D. S.; Strausz, O. P., A homologous series of novel hopane sulfides in petroleum. *Organic Geochemistry* **1986**, 9, 139-143.
- [6] Payzant, J. D.; Montgomery, D. S.; Strausz, O. P., Novel terpenoid sulfoxides and sulfides in petroleum. *Tetrahedron Letters* **1983**, 24, 651-654.
- [7] Payzant, J. D.; Cyr, T. D.; Montgomery, D. S.; Strausz, O. P., The synthesis of 1-beta-(H), 6-beta-(Me)-2,2,6-trimethyl-8-ethylbicyclo-[4,3,0]-7-thianonane and the structure of the isomeric bicyclic-terpenoid sulfides occurring in petroleum. *Tetrahedron Letters* **1985**, 26, 4175-4178.
- [8] Brassell, S. C.; Lewis, C. A.; De Leeuw, J. W.; Delange, F.; Damste Sinninghe, J. S., Isoprenoid thiophenes - novel products of sediment diagenesis. *Nature* **1986**, 320, 160-162.
- [9] Sinninghe Damste, J. S.; Ten Haven, H. L.; De Leeuw, J. W.; Schenck, P. A., Organic geochemical studies of a Messinian evaporitic basin, northern Apennines (Italy)-II. Isoprenoid and n-alkyl thiophenes and thiolanes. *Organic Geochemistry* **1986**, 10, 791-805.
- [10] Sinninghe Damste, J. S.; De Leeuw, J. W.; Kock-Van Dalen, A. C.; De Zeeuw, M.; De Lange, F.; Rijpstra, W. I. C.; Schenck, P. A., The occurrence and identification of series of organic sulfur compounds in oils and sediment extracts. I. A study of Rozel Point Oil (U.S.A.). *Geochimica et Cosmochimica Acta* **1987**, 51, (9), 2369-91.
- [11] Sinninghe Damste, J. S.; Rijpstra, W. I. C.; De Leeuw, J. W.; Schenck, P. A., The occurrence and identification of series of organic sulfur compounds in oils and sediment extracts: II. Their presence in samples from hypersaline and non-hypersaline palaeoenvironments and possible application as source, palaeoenvironmental and maturity indicators. *Geochimica et Cosmochimica Acta* **1989**, 53, 1323-1341.
- [12] Schmid, J. C.; Connan, J.; Albrecht, P., Occurrence and geochemical significance of long-chain dialkylthiacyclopentanes. *Nature* **1987**, 329, 54-56.
- [13] Sinninghe Damste, J. S.; De Leeuw, J. W., The origin and fate of isoprenoid C₂₀ and C₁₅ sulfur compounds in sediments and oils. *International Journal of Environmental Analytical Chemistry* **1987**, 28, 1-19.
- [14] Sinninghe Damste, J. S.; Rijpstra, W. I. C.; De Leeuw, J. W.; Schenck, P. A., Origin of organic sulfur compounds and sulfur-containing high-molecular-weight substances in sediments and immature crude oils. *Organic Geochemistry* **1988**, 13, 593-606.
- [15] http://www.chevron.com/products/prodserv/fuels/bulletin/motorgas/3_refining-testing/pg2.asp, accessed 17 October 2006.
- [16] Babich, I. V.; Moulijn, J. A., Science and technology of novel processes for deep desulfurization of oil refinery streams: A review. *Fuel* **2003**, 82, 607-631.

- [17] Whitehurst, D. D.; Isoda, T.; Mochida, I., Present state of the art and future challenges in the hydrodesulfurization of polyaromatic sulfur compounds. *Advances in Catalysis* **1998**, 42, 345-471.
- [18] Shafi, R.; Hutchings, G. J., Hydrodesulfurization of hindered dibenzothiophenes: an overview. *Catalysis Today* **2000**, 59, 423-442.
- [19] Nag, N. K.; Sapre, A. V.; Broderick, D. H.; Gates, B. C., Hydrodesulfurization of polycyclic aromatics catalyzed by sulfided CoO-MoO₃/γ-Al₂O₃: The relative reactivities. *Journal of Catalysis* **1979**, 57, 509-512.
- [20] Choudhary, T. V.; Malandra, J.; Green, J.; Parrott, S.; Johnson, B., Towards clean fuels: Molecular-level sulfur reactivity in heavy oils. *Angewandte Chemie-International Edition* **2006**, 45, 3299-3303.
- [21] Satterfield, C. N.; Modell, M.; Wilkens, J. A., Simultaneous catalytic hydrodenitrogenation of pyridine and hydrodesulfurization of thiophene. *Industrial & Engineering Chemistry Process Design and Development* **1980**, 19, 154-160.
- [22] Desikan, P.; Amberg, C. H., Catalytic hydrodesulfurization of thiophane. IV. The methylthiophenes. *Canadian Journal of Chemistry* **1963**, 41, 1966-1971.
- [23] Kilanowski, D. R.; Gates, B. C., Kinetics of hydrodesulfurization of benzothiophene catalyzed by sulfided Co-Mo-Al₂O₃. *Journal of Catalysis* **1980**, 62, 70-78.
- [24] Van Parijs, I. A.; Froment, G. F., Kinetics of hydrodesulfurization on a CoMo/Gamma-Al₂O₃ catalyst.1. Kinetics of the hydrogenolysis of thiophene. *Industrial & Engineering Chemistry Product Research and Development* **1986**, 25, 431-436.
- [25] Van Parijs, I. A.; Hosten, L. H.; Froment, G. F., Kinetics of hydrodesulfurization on a CoMo/Gamma-Al₂O₃ Catalyst.2. Kinetics of the hydrogenolysis of benzothiophene. *Industrial & Engineering Chemistry Product Research and Development* **1986**, 25, 437-443.
- [26] Geneste, P.; Amblard, P.; Bonnet, M.; Graffin, P., Hydrodesulfurization of oxidized sulfur-compounds in benzothiophene, methylbenzothiophene, and dibenzothiophene series over CoO-MoO₃-Al₂O₃ catalyst. *Journal of Catalysis* **1980**, 61, 115-127.
- [27] Ma, X. L.; Sakanishi, K. Y.; Mochida, I., Hydrodesulfurization reactivities of various sulfur-compounds in diesel fuel. *Industrial & Engineering Chemistry Research* **1994**, 33, 218-222.
- [28] Schade, T.; Roberz, B.; Andersson, J. T., Polycyclic aromatic sulfur heterocycles in desulfurized diesel fuels and their separation on a novel palladium(II)-complex stationary phase. *Polycyclic Aromatic Compounds* **2002**, 22, 311-320.
- [29] Bej, S. K.; Maity, S. K.; Turaga, U. T., Search for an efficient 4,6-DMDBT hydrodesulfurization catalyst: A review of recent studies. *Energy & Fuels* **2004**, 18, 1227-1237.
- [30] Schade, T.; Andersson, J. T., Speciation of alkylated dibenzothiophenes in a deeply desulfurized diesel fuel. *Energy & Fuels* **2006**, 20, 1614-1620.
- [31] Moza, P. N.; Hustert, K.; Leoff, S., Photochemical-transformations of selected organic-chemicals in 2 phase system. *Toxicological and Environmental Chemistry* **1991**, 31-32, 103-106.
- [32] Hirai, T.; Ogawa, K.; Komasaawa, I., Desulfurization process for dibenzothiophenes from light oil by photochemical reaction and liquid-liquid extraction. *Industrial & Engineering Chemistry Research* **1996**, 35, 586-589.
- [33] Gray, K. A.; Pogrebinsky, O. S.; Mrachko, G. T.; Xi, L.; Monticello, D. J.; Squires, C. H., Molecular mechanisms of biocatalytic desulfurization of fossil fuels. *Nature Biotechnology* **1996**, 14, 1705-1709.
- [34] Setti, L.; Lanzarini, G.; Pifferi, P. G., Dibenzothiophene biodegradation by a Pseudomonas Sp in model solutions. *Process Biochemistry* **1995**, 30, 721-728.

- [35] Wise, S. A.; Chesler, S. N.; Hertz, H. S.; Hilpert, L. R.; May, W. E., Chemically-bonded aminosilane stationary phase for high-performance liquid-chromatographic separation of polynuclear aromatic-compounds. *Analytical Chemistry* **1977**, 49, 2306-2310.
- [36] Davies, I. L.; Bartle, K. D.; Andrews, G. E.; Williams, P. T., Automated chemical class characterization of kerosene and diesel fuels by online coupled microbore HPLC/capillary GC. *Journal of Chromatographic Science* **1988**, 26, 125-130.
- [37] Mössner, S. G.; Wise, S. A., Determination of polycyclic aromatic sulfur heterocycles in fossil fuel-related samples. *Analytical Chemistry* **1999**, 71, 58-69.
- [38] Holstein, W., Donor-acceptor complex chromatography. Tetrachlorophthalimidopropyl silica, a new chemically bonded phase for separation of coal liquefaction products and other industrial aromatic mixtures by HPLC. *Chromatographia* **1981**, 14, 468-477.
- [39] Diack, M.; Gruber, R.; Cagniant, D.; Charcosset, H.; Bacaud, R., Analysis of coal hydroliquefaction products (semiaromatic compounds) on a picric acid column by charge-transfer chromatography. *Fuel Processing Technology* **1990**, 24, 151-156.
- [40] Felix, G.; Bertrand, C., HPLC on 3,5-dinitrobenzamidopropyl silica-gel. *Journal of High Resolution Chromatography & Chromatography Communications* **1984**, 7, 160-161.
- [41] Kershaw, J. R.; Black, K. J. T., Structural characterization of coal-tar and petroleum pitches. *Energy & Fuels* **1993**, 7, 420-425.
- [42] Zander, M., On the nitrogen containing constituents of coal-tar pitch. *Fuel* **1991**, 70, 563-565.
- [43] Nondek, L.; Malek, J., Liquid-chromatography of aromatic-hydrocarbons on a chemically bonded stationary phase of charge-transfer type. *Journal of Chromatography* **1978**, 155, 187-190.
- [44] Wise, S. A.; Sander, L. C.; May, W. E., Determination of polycyclic aromatic-hydrocarbons by liquid-chromatography. *Journal of Chromatography* **1993**, 642, 329-349.
- [45] Sander, L. C.; Pursch, M.; Wise, S. A., Shape selectivity for constrained solutes in reversed-phase liquid chromatography. *Analytical Chemistry* **1999**, 71, 4821-4830.
- [46] Fetzer, J. C.; Biggs, W. R., Identification of a new eight-ring condensed polycyclic aromatic hydrocarbon. *Polycyclic Aromatic Compounds* **1994**, 5, 193-199.
- [47] Barman, B. N., Hydrocarbon-type analysis of base oils and other heavy distillates by thin-layer chromatography with flame-ionization detection and by the clay-gel method. *Journal of Chromatographic Science* **1996**, 34, 219-225.
- [48] Vela, J.; Cebolla, V. L.; Membrado, L.; Andres, J. M., Quantitative hydrocarbon group type analysis of petroleum hydroconversion products using an improved TLC-FID system. *Journal of Chromatographic Science* **1995**, 33, 417-425.
- [49] Artok, L.; Su, Y.; Hirose, Y.; Hosokawa, M.; Murata, S.; Nomura, M., Structure and reactivity of petroleum-derived asphaltene. *Energy & Fuels* **1999**, 13, 287-296.
- [50] Artok, L.; Su, Y.; Hirose, Y.; Murata, S.; Nomura, M., Structural characterization of asphaltene fraction from vacuum residue of Arabian crude mixture by spectroscopic and pyrolytic methods. *Sekiyu Gakkaishi-Journal of the Japan Petroleum Institute* **1999**, 42, 206-214.
- [51] Herod, A. A.; Zhang, S. F.; Johnson, B. R.; Bartle, K. D.; Kandiyoti, R., Solubility limitations in the determination of molecular mass distributions of coal liquefaction and hydrocracking products: 1-methyl-2-pyrrolidinone as mobile phase in size exclusion chromatography. *Energy & Fuels* **1996**, 10, 743-750.

- [52] Müller, H.; Andersson, J. T., Gel permeation chromatography of sulfur-containing aromatics in vacuum residues. *Polycyclic Aromatic Compounds* **2004**, 24, 299-308.
- [53] Ralston, C. Y.; MitraKirtley, S.; Mullins, O. C., Small population of one to three fused-aromatic ring moieties in asphaltenes. *Energy & Fuels* **1996**, 10, 623-630.
- [54] Guillen, M. D.; Iglesias, M. J.; Dominguez, A.; Blanco, C. G., Fourier-transform infrared study of coal-tar pitches. *Fuel* **1995**, 74, 1595-1598.
- [55] Machnikowski, J.; Krzton, A.; Weber, J. V.; Zimmy, T.; Petryniak, J.; Wiecek, I., *Coal Science and Technology*. Elsevier: 1995; Vol. 1, p 1097-1100.
- [56] Shao, D. K.; Hutchinson, E. J.; Heidbrink, J.; Pan, W. P.; Chou, C. L., Behavior of sulfur during coal pyrolysis. *Journal of Analytical and Applied Pyrolysis* **1994**, 30, 91-100.
- [57] Kottenstette, R. J.; Schneider, D. A.; Loy, D. A., Absolute hydrogen determination in coal-derived heavy distillate samples. *Abstracts of Papers of the American Chemical Society, Division of Fuel Chemistry* **1994**, 64, 208.
- [58] Tokarska, A., Investigations on the processing of oil vacuum residue and its mixtures with coal and coal tars.2. Hydrogenative upgrading of the liquid products. *Fuel* **1996**, 75, 1206-1212.
- [59] Kapur, G. S.; Berger, S., Unambiguous resolution of alpha-methyl and alpha-methylene protons in H-1 NMR spectra of heavy petroleum fractions. *Energy & Fuels* **2005**, 19, 508-511.
- [60] Bai, S.; Pugmire, R. J.; Mayne, C. L.; Grant, D. M., C-13 NMR determination of protonated and nonprotonated carbons in model compounds, mixtures, and coal-derived liquid samples. *Analytical Chemistry* **1995**, 67, 3433-3440.
- [61] Mansfield, C. T.; Barman, B. N.; Thomas, J. V.; Mehrotra, A. K.; Philp, R. P., Petroleum and coal. *Analytical Chemistry* **1997**, 69, R59-R93.
- [62] Kelemen, S. R.; George, G. N.; Gorbaty, M. L., Direct determination and quantification of sulfur forms in heavy petroleum and coals.1. The X-Ray photoelectron-spectroscopy (XPS) approach. *Fuel* **1990**, 69, 939-944.
- [63] Gorbaty, M. L.; George, G. N.; Kelemen, S. R., Direct determination and quantification of sulfur forms in heavy petroleum and coals.2. The sulfur-K edge X-ray absorption-spectroscopy approach. *Fuel* **1990**, 69, 945-949.
- [64] George, G. N.; Gorbaty, M. L.; Kelemen, S. R.; Sansone, M., Direct determination and quantification of sulfur forms in coals from the argonne premium sample program. *Energy & Fuels* **1991**, 5, 93-97.
- [65] Sheu, E. Y.; Mullins O. C., *In Asphaltenes: Fundamentals and Applications*. Plenum: New York, 1995; p 53-96.
- [66] Boduszynski, M. M., Composition of heavy petroleum.2. Molecular characterization. *Energy & Fuels* **1988**, 2, 597-613.
- [67] Larsen, B. S.; Fenselau, C. C.; Whitehurst, D. D.; Angelini, M. M., Evaluations of heavy constituents in fractions of petroleum residues using gel-permeation and field desorption mass-spectrometry. *Analytical Chemistry* **1986**, 58, 1088-1091.
- [68] Hsu, C. S.; Qian, K., High-boiling aromatic-hydrocarbons characterized by liquid-chromatography thermospray mass-spectrometry. *Energy & Fuels* **1993**, 7, 268-272.
- [69] Pace, C. M.; Betowski, L. D., Measurement of high-molecular-weight polycyclic aromatic-hydrocarbons in soils by particle-beam high-performance liquid-chromatography mass. *Journal of the American Society for Mass Spectrometry* **1995**, 6, 597-607.

- [70] Anacleto, J. F.; Ramaley, L.; Benoit, F. M.; Boyd, R. K.; Quilliam, M. A., Comparison of liquid-chromatography mass-spectrometry interfaces for the analysis of polycyclic aromatic-compounds. *Analytical Chemistry* **1995**, 67, 4145-4154.
- [71] Lafleur, A. L.; Taghizadeh, K.; Howard, J. B.; Anacleto, J. F.; Quilliam, M. A., Characterization of flame-generated C-10 to C-160 polycyclic aromatic hydrocarbons by atmospheric-pressure chemical ionization mass spectrometry with liquid introduction via heated nebulizer interface. *Journal of the American Society for Mass Spectrometry* **1996**, 7, 276-286.
- [72] Roussis, S. G.; Proulx, R., Molecular weight distributions of heavy aromatic petroleum fractions by Ag⁺ electrospray ionization mass spectrometry. *Analytical Chemistry* **2002**, 74, 1408-1414.
- [73] Vanberkel, G. J.; Asano, K. G., Chemical derivatization for electrospray-ionization mass-spectrometry.2. Aromatic and highly conjugated molecules. *Analytical Chemistry* **1994**, 66, 2096-2102.
- [74] Rudzinski, W. E.; Zhang, Y.; Luo, X., Mass spectrometry of polyaromatic sulfur compounds in the presence of palladium(II). *Journal of Mass Spectrometry* **2003**, 38, 167-173.
- [75] Marshall, A. G.; Hendrickson, C. L.; Jackson, G. S., Fourier transform ion cyclotron resonance mass spectrometry: A primer. *Mass Spectrometry Reviews* **1998**, 17, 1-35.
- [76] Rodgers, R. P.; Schaub, T. M.; Marshall, A. G., Petroleomics: MS returns to its roots. *Analytical Chemistry* **2005**, 77, 20A-27A.
- [77] Fu, J. M.; Kim, S.; Rodgers, R. P.; Hendrickson, C. L.; Marshall, A. G.; Qian, K. N., Nonpolar compositional analysis of vacuum gas oil distillation fractions by electron ionization Fourier transform ion cyclotron resonance mass spectrometry. *Energy & Fuels* **2006**, 20, 661-667.
- [78] Schaub, T. M.; Hendrickson, C. L.; Qian, K. N.; Quinn, J. P.; Marshall, A. G., High-resolution field desorption/ionization Fourier transform ion cyclotron resonance mass analysis of nonpolar molecules. *Analytical Chemistry* **2003**, 75, 2172-2176.
- [79] Schaub, T. M.; Hendrickson, C. L.; Quinn, J. P.; Rodgers, R. P.; Marshall, A. G., Instrumentation and method for ultrahigh resolution field desorption ionization Fourier transform ion cyclotron resonance mass spectrometry of nonpolar species. *Analytical Chemistry* **2005**, 77, 1317-1324.
- [80] Purcell, J. M.; Hendrickson, C. L.; Rodgers, R. P.; Marshall, A. G., Atmospheric pressure photoionization Fourier transform ion cyclotron resonance mass spectrometry for complex mixture analysis. *Analytical Chemistry* **2006**, 78, 5906-5912.
- [81] Qian, K.; Rodgers, R. P.; Hendrickson, C. L.; Emmett, M. R.; Marshall, A. G., Reading chemical fine print: Resolution and identification of 3000 nitrogen-containing aromatic compounds from a single electrospray ionization Fourier transform ion cyclotron resonance mass spectrum of heavy petroleum crude oil. *Energy & Fuels* **2001**, 15, 492-498.
- [82] Qian, K. N.; Robbins, W. K.; Hughey, C. A.; Cooper, H. J.; Rodgers, R. P.; Marshall, A. G., Resolution and identification of elemental compositions for more than 3000 crude acids in heavy petroleum by negative-ion microelectrospray high-field Fourier transform ion cyclotron resonance mass spectrometry. *Energy & Fuels* **2001**, 15, 1505-1511.
- [83] Hughey, C. A.; Rodgers, R. P.; Marshall, A. G., Resolution of 11,000 compositionally distinct components in a single electrospray ionization Fourier transform ion cyclotron resonance mass spectrum of crude oil. *Analytical Chemistry* **2002**, 74, 4145-4149.
- [84] Friedman, L.; Fishel, D. L.; Shechter, H., Oxidation of alkylarenes with aqueous sodium dichromate. A useful method for preparing mono- and polyaromatic carboxylic acids. *Journal of Organic Chemistry* **1965**, 30, 1453-1457.
- [85] Barakat, A. O.; Rullkotter, J., Product distribution from oxidative degradation of sulphur-rich kerogens from the Nordlinger Ries (southern Germany). *Fuel* **1998**, 77, 85-94.

- [86] Kasai, M.; Ziffer, H., Ruthenium tetroxide catalyzed oxidations of aromatic and heteroaromatic rings. *Journal of Organic Chemistry* **1983**, 48, 2346-2349.
- [87] Carlsen, P. H. J.; Katsuki, T.; Martin, V. S.; Sharpless, K. B., A greatly improved procedure for ruthenium tetroxide catalyzed oxidations of organic-compounds. *Journal of Organic Chemistry* **1981**, 46, 3936-3938.
- [88] Warton, B.; Alexander, R.; Kagi, R. I., Characterisation of the ruthenium tetroxide oxidation products from the aromatic unresolved complex mixture of a biodegraded crude oil. *Organic Geochemistry* **1999**, 30, 1255-1272.
- [89] Adam, P.; Schaeffer, P.; Albrecht, P., C-40 monoaromatic lycopane derivatives as indicators of the contribution of the alga *Botryococcus braunii* race L to the organic matter of Messel oil shale (Eocene, Germany). *Organic Geochemistry* **2006**, 37, 584-596.
- [90] Kim, S.; Rodgers, R. P.; Marshall, A. G., Truly "exact" mass: Elemental composition can be determined uniquely from molecular mass measurement at approx. 0.1 mDa accuracy for molecules up to approx. 500 Da. *International Journal of Mass Spectrometry* **2006**, 251, 260-265.
- [91] Dole, M.; Mack, L. L.; Hines, R. L.; Mobley, R. C.; Ferguson, L. D.; Alice, M. B., Molecular beams of macroions. *Journal of Chemical Physics* **1968**, 49, 2240-2249.
- [92] Yamashita, M.; Fenn, J. B., Negative-ion production with the electrospray ion-source. *Journal of Physical Chemistry* **1984**, 88, 4671-4675.
- [93] Yamashita, M.; Fenn, J. B., Electrospray ion-source - Another variation on the free-jet theme. *Journal of Physical Chemistry* **1984**, 88, 4451-4459.
- [94] Tanaka, K.; Waki, H.; Ido, Y.; Akita, S.; Yoshida, Y.; Yohida, T., Protein and polymer analyses up to m/z 100,000 by laser ionization time-of-flight mass spectrometry. *Rapid Communications in Mass Spectrometry* **1988**, 2, 151-153.
- [95] Karas, M.; Bachmann, D.; Bahr, U.; Hillenkamp, F., Matrix-assisted ultraviolet-laser desorption of nonvolatile compounds. *International Journal of Mass Spectrometry and Ion Processes* **1987**, 78, 53-68.
- [96] Robb, D. B.; Covey, T. R.; Bruins, A. P., Atmospheric pressure photoionisation: An ionization method for liquid chromatography-mass spectrometry. *Analytical Chemistry* **2000**, 72, 3653-3659.
- [97] Comisarow, M. B.; Marshall, A. G., Fourier-transform ion-cyclotron resonance spectroscopy. *Chemical Physics Letters* **1974**, 25, 282-283.
- [98] Guan, S. H.; Marshall, A. G.; Scheppele, S. E., Resolution and chemical formula identification of aromatic hydrocarbons and aromatic compounds containing sulfur, nitrogen, or oxygen in petroleum distillates and refinery streams. *Analytical Chemistry* **1996**, 68, 46-71.
- [99] Hsu, C. S.; Qian, K. N.; Chen, Y. N. C., An innovative approach to data-analysis in hydrocarbon characterization by online liquid-chromatography mass-spectrometry. *Analytica Chimica Acta* **1992**, 264, 79-89.
- [100] Scheppele, S. E.; Chung, K. C.; Hwang, C. S., Computer processing of mass-spectral data. I. Assignment of formulas to experimental masses; chemical and mathematical principles. *International Journal of Mass Spectrometry and Ion Physics* **1983**, 49, 143-78.
- [101] Kendrick, E., Mass scale based on CH₂ = 14.0000 for high-resolution mass spectrometry of organic compounds. *Analytical Chemistry* **1963**, 35, 2146-2154.
- [102] Wu, Z.; Jernstroem, S.; Hughey, C. A.; Rodgers, R. P.; Marshall, A. G., Resolution of 10 000 compositionally distinct components in polar coal extracts by negative-ion electrospray ionization Fourier transform ion cyclotron resonance mass spectrometry. *Energy & Fuels* **2003**, 17, 946-953.

- [103] Müller, H.; Andersson, J. T.; Schrader, W., Characterization of high-molecular-weight sulfur-containing aromatics in vacuum residues using Fourier transform ion cyclotron resonance mass spectrometry. *Analytical Chemistry* **2005**, *77*, 2536-2543.
- [104] Acheson, R. M.; Harrison, D. R., The synthesis, spectra, and reactions of some S-alkylthiophenium salts. *Journal of the Chemical Society C: Organic* **1970**, *13*, 1764-1780.
- [105] Kitamura, T.; Yamane, M.; Zhang, B. X.; Fujiwara, Y., 1-phenyl-1-benzothiophenium triflates by a direct S-phenylation with diphenyliodonium triflate. *Bulletin of the Chemical Society of Japan* **1998**, *71*, 1215-1219.
- [106] Schulz, H.; Ousmanov, F.; Waller, P.; Böhringer, W., Refractory sulfur compounds in gas oils. *Fuel processing Technology* **1999**, *61*, 5-41.
- [107] Ma, X. L.; Sakanishi, K.; Mochida, I., Hydrodesulfurization reactivities of various sulfur compounds in vacuum gas oil. *Industrial & Engineering Chemistry Research* **1996**, *35*, 2487-2494.
- [108] Bacaud, R.; Cebolla, V. L.; Membrado, L.; Matt, M.; Pessayre, S.; Galvez, E. M., Evolution of sulfur compounds and hydrocarbons classes in diesel fuels during hydrodesulfurization. Combined use of thin-layer chromatography and GC-sulfur-selective chemiluminescence detection. *Industrial & Engineering Chemistry Research* **2002**, *41*, 6005-6014.
- [109] Takeshim.T; Yokoyama, M.; Imamoto, T.; Akano, M.; Asaba, H., Reaction of active methylene compounds with carbon disulfide in presence of ammonia. III. Reaction of cyclopentanone and cycloheptanone. *Journal of Organic Chemistry* **1969**, *34*, 730-732.
- [110] Pyell, U.; Stork, G., Preparation and properties of an 8-Hydroxyquinoline silica-gel, synthesized via Mannich reaction. *Fresenius Journal of Analytical Chemistry* **1992**, *342*, 281-286.
- [111] Seshadri, T.; Kettrup, A., Synthesis and characterization of silica-gel ion-exchanger bearing 2-amino-1-cyclopentene-1-dithio-carboxylic acid (ACDA) as chelating compound. *Fresenius Zeitschrift Für Analytische Chemie* **1982**, *310*, 1-5.
- [112] Schaub, T. M.; Rodgers, R. P.; Marshall, A. G.; Qian, K.; Green, L. A.; Olmstead, W. N., Speciation of aromatic compounds in petroleum refinery streams by continuous flow field desorption ionization FT-ICR mass spectrometry. *Energy & Fuels* **2005**, *19*, 1566-1573.
- [113] Sripada, K.; Andersson, J. T., Liquid chromatographic properties of aromatic sulfur heterocycles on a Pd(II)-containing stationary phase for petroleum analysis. *Analytical and Bioanalytical Chemistry* **2005**, *382*, 735-741.
- [114] Ma, X. L.; Sakanishi, K.; Isoda, T.; Mochida, I., Determination of sulfur compounds in non-polar fraction of vacuum gas oil. *Fuel* **1997**, *76*, 329-339.
- [115] Fenn, J. B.; Mann, M.; Meng, C. K.; Wong, S. F.; Whitehouse, C. M., Electrospray ionization-Principles and practice. *Mass Spectrometry Reviews* **1990**, *9*, 37-70.
- [116] Panda, S. K.; Schrader, W.; Andersson, J. T., β -Cyclodextrin as a stationary phase for the group separation of polycyclic aromatic compounds in normal-phase liquid chromatography. *Journal of Chromatography A* **2006**, *1122*, 88-96.
- [117] Sugimoto, Y.; Tannukij, K.; Miki, Y.; Yamadaya, S., Characterization of compound-class fractions of vacuum gas oil by using capillary GC and GCMS. *Sekiyu Gakkaishi* **1992**, *35*, 339-48.
- [118] Yang, R. T.; Hernandez-Maldonado, A. J.; Yang, F. H., Desulfurization of transportation fuels with zeolites under ambient conditions. *Science* **2003**, *301*, 79-81.
- [119] Ma, X. L.; Sun, L.; Song, C. S., A new approach to deep desulfurization of gasoline, diesel fuel and jet fuel by selective adsorption for ultra-clean fuels and for fuel cell applications. *Catalysis Today* **2002**, *77*, 107-116.

- [120] Gupta, N.; Roychoudhury, P. K.; Deb, J. K., Biotechnology of desulfurization of diesel: Prospects and challenges. *Applied Microbiology and Biotechnology* **2005**, 66, 356-366.
- [121] Sripada, K. Metal ion containing liquid chromatographic stationary phases for the analysis of polycyclic aromatic sulfur heterocycles in fossil fuels. Ph.D Thesis, **2005**, University of Münster, Germany.
- [122] Knudsen, K. G.; Cooper, B. H.; Topsoe, H., Catalyst and process technologies for ultra low sulfur diesel. *Applied Catalysis A: General* **1999**, 189, 205-215.
- [123] Ogan, K.; Katz, E.; Slavin, W., Determination of polycyclic aromatic-hydrocarbons in aqueous samples by reversed-phase liquid-chromatography. *Analytical Chemistry* **1979**, 51, 1315-1320.
- [124] Chmielowiec, J.; George, A. E., Polar bonded-phase sorbents for high-performance liquid-chromatographic separations of polycyclic aromatic-hydrocarbons. *Analytical Chemistry* **1980**, 52, 1154-1157.
- [125] Davies, I. L.; Bartle, K. D.; Williams, P. T.; Andrews, G. E., Online fractionation and identification of diesel fuel polycyclic aromatic-compounds by two-dimensional microbore high-performance Liquid-chromatography capillary gas-chromatography. *Analytical Chemistry* **1988**, 60, 204-209.
- [126] Ecknig, W.; Trung, B.; Radeaglia, R.; Gross, U., Group separation of alkyl-substituted aromatic-hydrocarbons by high-performance liquid-chromatography using perfluorocarbon modified silica-Gel. *Chromatographia* **1982**, 16, 178-182.
- [127] Grizzle, P. L.; Thomson, J. S., Liquid-chromatographic separation of aromatic-hydrocarbons with chemically bonded (2,4-dinitroanilinopropyl)silica. *Analytical Chemistry* **1982**, 54, 1071-1078.
- [128] Welch, K. J.; Hoffman, N. E., Physicochemical properties of electron-acceptor stationary phases in liquid-chromatography. *Journal of Chromatography* **1992**, 591, 75-88.
- [129] www.pash-standards.de, accessed 17 October 2006.
- [130] Ballschmiter, K.; Wöbner, M., Recent developments in adsorption liquid chromatography (NP-HPLC) - A review. *Fresenius Journal of Analytical Chemistry* **1998**, 361, 743-755.
- [131] Felix, G.; Thienpont, A.; Dentraygues, P., Synthesis of acceptor bonded phases for donor-acceptor liquid-chromatography. *Chromatographia* **1992**, 34, 177-181.
- [132] Cleon, P.; Foucheres, M. C.; Cagniant, D.; Severin, D.; Holstein, W., Donor-acceptor complex chromatography - Application to analysis of coal-liquefaction products by HPLC. *Chromatographia* **1985**, 20, 543-554.
- [133] Wöbner, M.; Ballschmiter, K., New stationary phase based on beta-cyclodextrin for normal-phase HPLC group-separation of organic nitrates. *Fresenius journal of analytical chemistry* **2000**, 366, 346-350.
- [134] Mitchell, C. R.; Armstrong, D. W., Cyclodextrin-based chiral stationary phases for liquid chromatography: A twenty-year overview. *Methods in Molecular Biology (Totowa, NJ, United States)* **2004**, 243, (Chiral Separations), 61-112.
- [135] Rudzinski, W. E.; Rai, V., Detection of polyaromatic sulfur heterocycles in crude oil using postcolumn addition of tropylium and tandem mass spectrometry. *Energy & Fuels* **2005**, 19, 1611-1618.
- [136] Blicke, F. F.; Sheets, D. G., Derivatives of Thianaphthene.1. *Journal of the American Chemical Society* **1948**, 70, 3768-3770.
- [137] Wadsworth, W. S.; Emmons, W. D., Ethyl cyclohexylidene acetate. *Organic Synthesis* **1965**, 45, 44-46.
- [138] Fry, A. J.; Allukian, M.; Williams, A. D., Reduction of diaryl alkenes by hypophosphorous acid-iodine in acetic acid. *Tetrahedron* **2002**, 58, 4411-4415.

- [139] Wiberg, K. B.; McShane, H. F., 2-Chloromethylthiophene. *Organic Synthesis* **1949**, 29, 31-33.
- [140] Shirley, D. A.; Cameron, M. D., Metalation of thianaphthene by normal-butyllithium. *Journal of the American Chemical Society* **1950**, 72, 2788-2789.
- [141] Shirley, D. A.; Cameron, M. D., Some 2-substituted thianaphthenes derived from 2-thianaphthenyllithium. *Journal of the American Chemical Society* **1952**, 74, 664-665.
- [142] Whitmore, F. C.; Karnatz, F. A., Alkyl chlorides obtained from 2-ethylbutanol. *Journal of the American Chemical Society* **1938**, 60, 2533-2536

Lebenslauf

Name: Saroj Kumar Panda
Geboren: am 14.07.1977 in Orissa (Indien)
Familienstand: ledig

Eltern: Laxmimani Panda (Mutter)
Harihar Panda (Vater)

Schulbildung: U. P. School, Jageswarpada, Indien (1982-1987)
M. E. School, Jageswarpada, Indien (1987-1989)
High School, Gopalpur, Indien (1989-1992)

Studium: M.P.C. College, Baripada, Indien (1992-1994)
Chemie an der Utkal University,
Indien (1994-1999)
Chemie am Indian Institute of Technology Delhi,
Indien (1999-2000)

Prüfungen: Bachelor in Fach Chemie an der Utkal University, Indien
Master im Fach Chemie an der Utkal University, Indien
Master im Fach Analytische Chemie am Indian Institute
of Technology Delhi, Indien

Promotionsstudiengang: Chemie in der „NRW-Graduate School of Chemistry“ an
der Universität Münster am Institut für Anorganische und
Analytische Chemie. (2003-2006)

Tätigkeiten: Dozent für Chemie am PIE Education systems &
solutions Ltd., New Delhi, India (Dezember 2002-August
2003)
Wissenschaftlicher Mitarbeiter am Institut für
Analytische Chemie der TU Dresden, Germany (Oktober
2001-August 2002)
Research Executive Trainee in der Abteilung für
analytische Forschung & Entwicklung bei Orchid
Chemicals & Pharmaceutical Ltd., Chennai , India (Marz
2001-August 2001)

Beginn der Dissertation: Im Oktober 2003 in der NRW Graduate School of
Chemistry am Institut für Anorganische und Analytische
Chemie unter Betreuung von Prof. Dr. Jan T. Andersson

Acknowledgement

First and foremost I would like to thank my principal mentor Prof. Jan T. Andersson for his invaluable guidance and continuous support during my entire Ph.D. tenure. The successful completion of my research work was only possible by his informative suggestion and stimulatory discussion. In addition, his amicable nature and conducive attitude made my stay pleasant here.

I would like to thank Prof. E.–U. Würthwein and Prof. H.–U. Humpf being my mentors for the dissertation committee.

In addition, my sincere thanks to Prof. Uwe Karst for his consent to be one of my thesis supervisors.

However, this project was smoothly accomplished with the coordination of Dr. Wolfgang Schrader from Max Planck Institute, Mülheim. I am highly obliged for the remarkable collaboration in FT-ICR mass measurement.

I would like to thank NRW Graduate School of Chemistry, Münster (GSC-MS) for providing the financial assistance to carry out this work. Also, I would like to thank all the members of GSC-MS, in particular Dr. Hubert Koller, Dr. Stefan Elbers, Uta Bröcker and Christina Bäumer for their help to make the bureaucracy procedures easier during my stay in Germany.

I thank my colleagues, who really provided me a pleasant working environment in a foreign country. Although it is difficult to enumerate all their support during the last three years, an attempt is made. Frau Marianne Lüttmann, Frau Karin Weißenhorn, Dr. Hendrik Müller for his kind effort to introduce me into the project in initial days, Dr. Kishore Sripada for his incredible support both in scientific and personal matters, Dr. Thomas Schade, Markus Penassa, Ansgar Japes for their critical comments in the improvement of my thesis, and other members Dr. Frank Wasinski, Dr. Benedikte Roberz, Dr. Abd El-Rahman Hegazi, Nina Kolbe (introduction to Power fitness), Eiman Fathalla, Claudia Sill, Magdalena Ulman, Michael Scherges, Peni Handayani and Daniel Plothe for their kind coordination to finish my project at the scheduled time.

With the labmates, I want to thank certain people in the department of Analytical Chemistry. First of all, I thank Mr. Jens Kühnmeyer being a close friend to me during this period. Also, it is further extended to Nils, Bettina, Wiebke, Stefan, Andy, Tobias, Björn, Torsten, Carsten, Sascha, Suze, Dr. Wolfgang Buscher and Dr. Martin Vogel for their kind interaction.

In addition, I would like to convey my special thanks to Dnyaneshwar Gawas, Geo Paul, Sebastian Peter, Surajit Jana, and Rajeshwari Marikkannu for their continual support and coordination during my doctoral work.

My Dresden friends Pradeep Pareek, Shankar Venkataraman, Biswajeet Pradhan and Mahesh Babu Madishetti are acknowledged for their friendship during my first visit in Germany.

Acknowledgement

Also, the Indian colleagues in Münster, Deepak, Nitin, Ravi, Sreeraj, Sanjeev, Devidas, Rudra, Ajay, Joyram, Arijit, Sudhi and all the sub-juniors, especially Chandan and Barun are thanked for their cordial invitation for dinner and providing a friendly environment.

My sincere thanks to Sarat Barik, Kailash Barik, Tapas Barik, Kshamasagar Barik, Parsuram Barik and Shantanu Nayak for their kind efforts to make me comfortable during my career, and Meenaketan Ojha being an intimate friend from my school days.

In addition, friends Sandesh, Hrushikesh, Jagajit, Raja Babu, Manas, Noopur, Varun, Tapas, Naveen, Sudhir, and Samir are thanked for their support in due course of my study.

Also, my friends are not limited to only labs and Indian colleagues. It extends to Frederik (Luxembourg), Olexy (Ukraine), Swantje (Germany), Nuno (Portugal), Nacho (Spain), Natascha (Germany), Corine (The Netherlands), Christine (Germany), Britta (Germany), Wahida (Lithuania) and Franz (Germany) for introducing me to “night-life” at Münster.

However, the present achievement could not be attained without the strength, love and continuous support from all my brothers, sisters, sisters-in-law, brothers-in-law, nephews Papu, Bapu, Milu, Babua, Omkar, Pinku, Chiku, Shiva and niece Riki, Rimi, Mili, Pooja.